Université du Québec
INRS-ETE

VISUALISATION DES MÉCANISMES DE RÉCUPÉRATION DU TCE PAR DES SOLUTIONS MICELLAIRES ET POLYMÈRES DANS UN MODÈLE PHYSIQUE 2D HÉTÉROGÈNE

Par
Thomas Robert

Mémoire présenté
pour l'obtention
du grade de Maître ès sciences (M.Sc.)

Jury d'évaluation

Examinateur externe	John Molson, Ph.D. Département des génies civil, Géologique et Minier École Polytechnique
Examinateur interne	Pierre J. Gélinas, Ph.D. Département de géologie et de génie géologique Université Laval
Directeur de recherche	Richard Martel, Ph.D. INRS-ETE Université du Québec
Codirecteur de recherche	René Lefebvre, Ph.D. INRS-ETE Université du Québec

13 Janvier 2004

RÉSUMÉ

L'injection dans le sol de solutions de lavage composées d'alcools et/ou de tensioactifs est une méthode prometteuse pour la réhabilitation des aquifères contaminés aux solvants chlorés. La première partie de cette recherche est basée sur les résultats provenant d'essais en colonne réalisés précédemment par St-Pierre (2001). Des mesures complémentaires ont permis de mieux comprendre les procédés de récupération du TCE dans un milieu homogène, où le TCE était distribué uniformément et à saturation résiduelle. Les mécanismes observés de récupération du TCE, soit la mobilisation et la solubilisation, de même que l'efficacité de récupération du TCE, ont été mis en relation avec les tensions interfaciales, la viscosité et la densité des phases aqueuses et organiques, mesurées en laboratoire, sur des mélanges préparés en vrac et représentatifs des phases observées lors des essais antérieurs. Par la suite, un procédé de récupération du TCE par solubilisation a été élaboré puis testé dans un bac de sable présentant les caractéristiques d'un aquifère hétérogène, à l'intérieur duquel le TCE se trouvait autant à saturation résiduelle qu'en accumulation locale. Une solution de lavage performante, composée de deux surfactants, identifiée et caractérisée lors des mesures complémentaires, a été utilisée. Un gradient de concentration en matière active a été employé pendant l'expérience pour minimiser les conditions favorisant la remobilisation du TCE. Un polymère rhéo-fluidifiant a été ajouté à la solution pour augmenter son efficacité de balayage dans le milieu hétérogène et pour atténuer les effets d'hétérogénéité sur le patron d'écoulement. La visualisation des procédés s'est avérée être la source d'information la plus révélatrice liée à l'utilisation combinée des polymères et des tensioactifs. Ce type d'expérience a permis l'observation directe de processus difficiles à caractériser à partir de l'analyse chimique des effluents. Le procédé testé doit être optimisé pour des applications futures. Entre autres choses, des mesures nécessaires à la fermeture du bilan de masse devraient être prises, ce qui permettrait la quantification du processus de solubilisation.

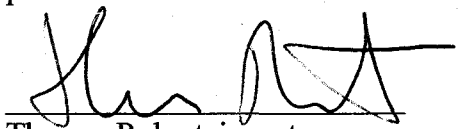

Thomas Robert, ing. stag.
Étudiant à la maîtrise

Richard Martel, ing, Ph.D.
Directeur de recherche

REMERCIEMENTS

Dans un premier temps, je tiens sincèrement à remercier Uta Gabriel pour l'aide précieuse qu'elle m'a rendue à tous les niveaux de ce projet de recherche. Je tiens à remercier également mes directeur et codirecteur Richard Martel et René Lefebvre, pour le support autant scientifique que personnel qu'ils m'ont apporté. Je les remercie spécialement pour la liberté qu'ils m'ont accordé dans l'élaboration et l'exécution de ce projet. Je souhaite également remercier Steve Conrad et William Peplinski, des Laboratoires Sandia au Nouveau-Mexique, pour leur accueil sympathique et leur contribution essentielle à ce projet. Je tiens ensuite à remercier Chantal St-Pierre, pour l'aide qu'elle m'a apportée dans le démarrage du projet, et aussi Pierre Gélinas, pour l'intérêt qu'il a porté à cette étude. Cette recherche a été rendue possible grâce à la contribution financière du CRSNG et du FCAR.

Plus personnellement, je remercie ma famille et mes ami(e)s pour tout l'aide et le support rendus. Enfin, je tiens à remercier du fond de mon cœur Priscilla Desgagnés, source intarissable de bonheur et de motivation.

TABLE DES MATIÈRES

LISTE DES TABLEAUX

LISTE DES FIGURES

LISTE DES APPENDICES

CHAPITRE 1

INTRODUCTION GÉNÉRALE

1.1 INTRODUCTION

1.1.1 La contamination des aquifères aux liquides immiscibles denses

Le trichloroéthène (TCE) est un solvant chloré qui fait partie de la grande classe des contaminants organiques pouvant former des liquides immiscibles denses (LIDs) (ou *Dense Non-Aqueous Phase Liquids - DNAPLs*). Ce composé lourd est le produit de la substitution d'atomes d'hydrogène par des atomes de chlore sur des molécules d'éthène (Cohen et Mercer, 1993). Depuis les années 40, le TCE a été largement utilisé comme dégraissant et nettoyant par les industries et les entreprises de nettoyage à sec. Encore en 1986, les États-Unis ont produit 75 millions de tonnes de TCE. Une mauvaise gestion des déchets liés à son utilisation est responsable aujourd'hui de la contamination du sol et de l'eau souterraine sur un très grand nombre de sites (Pankow et Cherry, 1996). Le TCE est d'ailleurs le composé organique le plus souvent détecté dans l'eau souterraine lors d'évaluation de sites contaminés aux États-Unis. Ici au Québec, des municipalités sont aux prises avec des problèmes liés au TCE dissous dans l'eau qui est pompée par leurs puits d'approvisionnement en eau potable. Le tableau 1.1 présente les propriétés du TCE.

Suite à une fuite d'un réservoir ou à un déversement sur le sol, les LIDs migrent en profondeur dans le sol (Figure 1.1 (a)). Dans la zone saturée du sol, trois forces contrôlent

le déplacement des LIDs dans le milieu poreux (Figure 1.1(b)): la force gravitationnelle, la force capillaire et la force visqueuse (Martel *et al.*, 1998b) (le TCE est employé ici à titre d'exemple de LID) :

La force gravitationnelle ΔP_G est de nature hydrostatique et dépend de la hauteur h de la gouttelette de TCE, de la constante gravitationnelle g et de la différence de densité $\Delta\rho$ entre le TCE et l'eau souterraine. Sous l'influence de cette force, le TCE a tendance à migrer en profondeur dans la zone saturée du sol:

$$\Delta P_G = \Delta\rho\, g\, h$$

La force capillaire P_C dépend de la tension interfaciale σ_{ow} entre le TCE et l'eau souterraine, de l'angle de contact θ_{wr} entre la gouttelette de TCE et la fraction solide du sol, et du rayon r du pore dans lequel se retrouve la gouttelette (donc indirectement de la granulométrie des couches composant l'aquifère). L'angle de contact dépend de la mouillabilité du milieu. Dans le cas des sables de silice, le milieu est hydrophile et c'est l'eau qui a tendance à mouiller les parois des pores. Le TCE occupe alors exclusivement le centre des plus gros pores. La force capillaire résiste à la mobilisation du TCE en profondeur:

$$P_C = (2\ \sigma_{ow} \cos\theta_{wr}) / r$$

Finalement, la force visqueuse ΔP_v (non illustrée dans la figure 1.1) s'applique dans le cas où un fluide circule autour d'une gouttelette de TCE. Cette force dépend de la vitesse de Darcy V et de la viscosité dynamique μ du fluide en question, de la longueur de la gouttelette L de TCE qui est exposée, et de la perméabilité intrinsèque du milieu k:

$$\Delta P_v = VL\mu / k$$

En général, lorsque les forces gravitationnelle et visqueuse sont plus importantes que la force capillaire, le TCE migre dans la zone saturée du sol. Lorsqu'un équilibre est atteint entre les forces, le TCE est piégé dans le milieu poreux. Selon la quantité initiale de TCE déversée et les conditions rencontrées dans le milieu, le volume des pores occupé par le TCE peut varier entre saturation résiduelle (le TCE occupe exclusivement les plus gros pores du milieu) et accumulation locale (le TCE occupe une plus grande partie du volume des pores, et à la limite seule une saturation résiduelle en eau persiste dans la zone). Les zones à saturation résiduelle de même que les accumulations locales forment des zones sources à partir desquelles le TCE est dissous et se disperse dans l'eau souterraine. Ces phénomènes entraînent la création de panaches d'eau souterraine contaminée qui s'étendent par advection et selon le patron d'écoulement dans la région, bien au-delà de la zone d'origine de la contamination (Mackay *et al.,* 1989). La solubilité dans l'eau du TCE est très faible, mais suffisante pour que l'eau souterraine ayant été mise en contact avec des zones à saturation résiduelle ou des accumulations locales se retrouve très souvent contaminée au-delà des critères de potabilité. La faible solubilité du TCE dans l'eau fait également en sorte que les zones sources, et plus particulièrement les accumulations locales, sont très persistantes dans les sols, et peuvent alimenter des panaches d'eau contaminée pendant des années, voire des décennies (Brandes et Farley, 1993). Aussi, le TCE est difficilement biodégradable, et le produit de sa dégradation naturelle, le chlorure de vinyle, est stable et encore plus toxique que le TCE (Mackay *et al.,* 1989).

Les conditions présentées ci-haut rendent les techniques courantes de restauration d'aquifère contaminé lentes et inefficaces. La faible solubilité dans l'eau du TCE et des LIDs en général, de même que leur tendance à se retrouver en accumulation locale dans le milieu (rapport surface/volume très faible), restreint la technique du pompage et traitement à une action passive permettant le contrôle du problème, sans toutefois entraîner son élimination (Ramsburg et Pennell, 2001). La nature des LIDs fait en sorte qu'ils se retrouvent souvent à de grandes profondeurs, ce qui exclut l'excavation des sols contaminés comme solution réaliste. Aussi, suite à une fuite dans des réservoirs, les LIDs

peuvent se retrouver dans des endroits difficiles d'accès comme sous des bâtiments. De plus, la forte toxicité de ces composés rend les techniques de bio-rémédiation inefficaces.

1.1.2 Le lavage de sol aux solutions micellaires

Le lavage de sol est une technique prometteuse développée pour accélérer la restauration des aquifères contaminés par des LIDs, particulièrement les zones sources (Ramsburg et Pennell, 2001; Roeder *et al.,* 2001; Sabatini *et al.,* 2001; Taylor *et al.,* 2001; Boving et Brusseau, 2000; Oostrom *et al.*, 1999; Falta, 1998; Kostarelos *et al.,* 1998; Martel *et al.,* 1998a, 1998b, 1998c, 1993; Walker *et al.*, 1998; Fountain *et al.*, 1996; Shiau *et al.,* 1996, 1994; Farley *et al.*, 1993). Elle consiste à injecter dans la zone saturée des sols des solutions de lavage qui ont pour but de mobiliser les LIDs ou augmenter leur solubilité dans la phase aqueuse. Les solutions et les contaminants sont ensuite récupérés par des puits de pompage. Les solutions micellaires peuvent récupérer le TCE présent dans les sols selon trois procédés différents : la solubilisation, la mobilisation ou la microémulsion.

Les solutions de lavage sont composées d'eau, de tensioactifs et/ou d'alcool. Les tensioactifs sont des molécules ayant une extrémité polaire et soluble dans l'eau et une autre non-polaire et soluble dans la phase organique (LIDs). Les tensioactifs s'accumulent donc aux interfaces eau/contaminant, ce qui a pour effet de réduire les tensions interfaciales. Au delà d'une certaine concentration, appelée concentration micellaire critique (CMC), les monomères de tensioactifs s'agglomèrent et forment des micelles (sphères). Pour les tensioactifs solubles dans l'eau, ces micelles ont la capacité d'emprisonner les composés organiques en leur centre, alors que le tout reste soluble dans la phase aqueuse. Ceci a pour effet d'augmenter la solubilité apparente des LIDs dans la phase aqueuse. Dans ces conditions, le système est solubilisant, il y a réduction de la saturation en LIDs et déplacement miscible de la phase organique. Lorsqu'un autre type de tensioactif est employé, que les conditions de salinités changent, ou que les concentrations en tensioactifs sont augmentées, il peut y avoir formation de micelles inverses, et c'est la phase aqueuse qui est solubilisée au centre des micelles, et le tout

devient soluble dans la phase organique. Ceci a pour effet de gonfler le volume de LIDs. Il y a donc augmentation de la saturation en LIDs, et augmentation de la perméabilité relative à la phase organique. Cette augmentation, accompagnée d'une réduction de tension interfaciale, provoque à l'intérieur des zones contaminées par une saturation résiduelle la formation d'un banc de phase libre de LIDs au devant du front d'injection des solutions. Le système est mobilisant, et il y a déplacement immiscible de la phase organique. Le troisième procédé, la microémulsion, est basé sur la mobilisation des LIDs suite à des réductions extrêmes des tensions interfaciales. Cette technique ne fait pas l'objet de recherche dans le cadre de ce projet, mais est traitée en détail dans les travaux de Kostarelos *et al.* (1998) et Shiau *et al.* (1996, 1994).

Plusieurs facteurs posent de sérieux défis quant à l'application du lavage de sol aux solutions micellaires à des cas réels de terrain. Ces défis sont présentés au Tableau 1 du Chapitre 3. Entre autres, les solutions micellaires réduisent les tensions interfaciales et donc les forces capillaires responsables du piégeage du TCE dans le milieu poreux. Elles ont donc le potentiel de déplacer les contaminants dans le milieu poreux, ce qui peut présenter un danger. Dans le cas des systèmes mobilisants, la remobilisation des LIDs risque d'entraîner leur migration plus en profondeur, et potentiellement en dehors du rayon d'influence des puits d'extraction. Et avec des tensions interfaciales donc des forces capillaires réduites, il y a un risque de pénétration des LIDs dans des couches précédemment non-contaminées, généralement de granulométrie plus fines.

Dans le cas des systèmes solubilisants, la formation d'une phase organique libre ou mobile est moins favorisée parce qu'il n'y a pas de transfert de tensioactif vers cette phase, et donc pas de gonflement. Cependant, les tensions interfaciales sont toujours réduites, et une réduction trop importante peut aussi entraîner la migration des LIDs plus en profondeur. Aussi, la densité de la phase aqueuse peut être augmentée par les composés des LIDs qui y sont dissous. Si cette augmentation est importante, la phase aqueuse peut avoir tendance à migrer vers le bas et en dehors de la zone d'influence des puits d'extraction, et peut entraîner le panache d'eau contaminée plus en profondeur (Oostrom *et al.*, 1999).

Dans les milieux hétérogènes, plusieurs facteurs contrôlent l'écoulement des solutions de lavage dans le sol. Dans un sable homogène, la vitesse d'écoulement est contrôlée par la vitesse d'injection dans le sol, la conductivité hydraulique du milieu et le gradient hydraulique. Le patron d'écoulement est contrôlé par la densité et la viscosité des solutions. La densité détermine la tendance des solutions à «flotter » ou « couler » (*overriding, underriding*) par rapport à l'eau souterraine ou aux zones contaminées, et la viscosité détermine la stabilité du front d'écoulement des solutions. Dans le cas d'un aquifère hétérogène, l'écoulement des solutions sera particulièrement influencé par les contrastes de conductivité hydraulique entre les différentes couches de matériel. En effet, les solutions auront tendance à s'écouler préférentiellement par les chemins où les conductivités hydrauliques sont plus grandes. Les zones de granulométrie plus fine seront en grande partie contournées, et les LIDs qui sont compris dans ces zones ne pourront être récupérés, ou ne le seront qu'après l'injection de grandes quantités de solutions de lavage.

Lors de l'élaboration de solutions performantes ne posant pas de risques de remobilisation verticale, il est essentiel de bien comprendre le comportement des solutions et des contaminants lors du lavage des sols autant en milieu homogène qu'en milieu hétérogène. Et la compréhension des mécanismes de récupération passe par la mise au point des solutions en laboratoire et l'analyse des propriétés physiques et chimiques des systèmes.

1.2 TRAVAUX ANTÉRIEURS

1.2.1 Identification de solutions de lavage performantes

Cette recherche fait suite aux travaux de recherche de St-Pierre (2001). Ces travaux ont conduit à l'identification de solutions de lavage performantes tant pour solubiliser que mobiliser du TCE piégé à saturation résiduelle dans des colonnes de sables. Deux méthodes de sélection ont été employées pour démarquer les solutions intéressantes des autres: les diagrammes de phase et les essais en colonne.

Les diagrammes de phase (Figure 2) sont de bons outils permettant de déterminer si le système de lavage sera performant et s'il sera mobilisant ou solubilisant (Martel *et al.*, 1993). Une courbe de miscibilité sur les diagrammes de phases est obtenue par titration. Plus la courbe de miscibilité est basse, plus le système sera performant. Pour un mélange dont la composition globale se trouve sous cette courbe, il y aura division en deux phases distinctes, et les compositions respectives sont données par deux points sur la courbe de miscibilité. La ligne reliant ces deux points est appelée courbe de distribution. Les tensions interfaciales entre les phases co-existantes sont constantes le long de ces lignes. Un système qui présente des courbes de distribution dont les pentes sont négatives indique la préférence du mélange tensioactif/alcool pour la phase aqueuse, il est donc solubilisant. Un système qui présente des courbes de distribution dont les pentes sont positives indique la préférence du mélange tensioactif/alcool pour la phase organique, il est donc mobilisant.

Les essais en colonnes permettent d'évaluer le type et la performance des mécanismes de récupération dans un environnement dynamique. Une colonne de sable saturé en eau est contaminée avec une saturation résiduelle en LID. Une solution de lavage y est alors injectée et l'effluent est récupéré. L'analyse visuelle et chimique de l'effluent permet d'identifier les phases dissoutes et les phases mobilisées tout au long de l'essai (St-Pierre, 2001). Les essais en colonne ont permis à St-Pierre de valider les prédictions faites à partir des diagrammes de phase.

Ces deux méthodes ont permis à St-Pierre (2001) de classer différents systèmes solution tensioactive/eau/TCE selon le mécanisme de récupération et la performance dans un milieu homogène où le TCE se trouvait initialement à saturation résiduelle. Un tableau des résultats est présenté au Chapitre 2. Les systèmes solubilisants sont performants, et n'entraînent pas de remobilisation de TCE en profondeur. Les systèmes mobilisants sont encore plus performants, donc récupèrent le TCE avec un volume moins important de solution de lavage, mais provoquent la création d'une phase organique mobile (composée de TCE et de matière active ayant transféré dans le TCE).

1.2.2 Contrôle de la mobilité des solutions de lavages

Dans la littérature se rapportant à la récupération assistée du pétrole, l'efficacité de balayage est définie comme étant le rapport entre le volume de phase organique présent dans un réservoir et qui est mis en contact avec un agent mobilisateur, sur le volume total de phase organique en place dans tout le réservoir (Lake, 1989; Mungan, 1982). Dans le cadre environnemental, il est primordial que les solutions de lavage soient mises en contact avec l'ensemble de la zone source de la contamination, pour que les phénomènes de solubilisation, par exemple, puissent être efficaces. Dans les milieux hétérogènes, le patron d'écoulement de l'eau souterraine est contrôlé par les différences de perméabilité entre les différentes couches de matériel, et les zones moins perméables (argile, silt) se retrouvent moins accessibles que les plus perméables (sable, gravier).

Les polymères, en plus d'éliminer les instabilités causées par les force visqueuses (plus de détails sur les rapports de mobilité sont donnés au Chapitre 3), peuvent jouer un rôle important dans le contrôle de la mobilité des fluides et dans l'optimisation de l'efficacité de balayage des solutions dans un milieu hétérogène (Martel, K.E. *et al.,* 1998). En effet, certains polymères ont un comportement rhéofluidifiant, ce qui signifie que leur viscosité dépend des contraintes de cisaillement dans le milieu. Ce comportement est lié aux molécules de polymères qui se déroulent et se déploient sous des contraintes élevées, permettant au fluide de s'écouler plus facilement (Chen et Sheppard, 1980). Donc, dans un horizon fin, où les contraintes de cisaillement sont plus élevées, les solutions auront plus de facilité à s'écouler que dans un horizon plus grossier, où les contraintes sont plus faibles. Ce comportement a pour effet d'uniformiser le front d'écoulement et de permettre un balayage optimisé de la zone contaminée.

Les travaux de recherche de Martel, K. E. *et al.* (1998) ont permis d'identifier des moyens d'augmenter l'efficacité de balayage des solutions micellaires dans un milieu présentant des hétérogénéités. Des essais en bac présentant des couches de sable de granulométrie variable ont permis d'observer le comportement rhéofluidifiant de la gomme de xanthane,

un polymère de la famille des polysaccharides, laissant ainsi présager des applications intéressantes pour d'éventuelles utilisations de solutions de lavage en milieu hétérogène.

1.3 PROBLÉMATIQUE

Les travaux de St-Pierre (2001) ont permis de faire le lien entre les propriétés des systèmes eau/matière-active/TCE et le comportement observé des solutions de lavage et du TCE lors d'essais en colonne (efficacité et mécanisme récupération). Ces liens ont été faits dans un environnement en une dimension, présentant un milieu homogène, et à l'intérieur duquel le TCE se trouvait uniformément distribué et à saturation résiduelle, et l'écoulement des fluides se faisait du haut vers le bas. De plus, les tensions interfaciales des systèmes et la viscosité des fluides n'ont pas été mesurées pendant ces expériences. Aussi, bien que les travaux de Martel, K. E. *et al.* (1998) aient permis d'identifier un moyen efficace d'optimiser le balayage de milieux hétérogènes, aucun contaminant ne fut utilisé lors des expériences, et la dynamique de la récupération du TCE par des solutions de lavage en milieu hétérogène n'a pas été abordée.

Les conditions rencontrées sur le terrain imposent d'autres considérations dans l'évaluation de la performance et des mécanismes de récupération du TCE. En effet, dans un milieu hétérogène, le TCE risque de se retrouver selon une distribution bi-modale : en plus des zones contaminées par une saturation résiduelle de TCE (gouttelettes), d'autres peuvent l'être par des accumulation locales de TCE. La présence d'hétérogénéités et d'accumulations locales dans le milieu poreux ont plusieurs conséquences (Conrad *et al.*, 2001). Premièrement, le TCE présent en accumulation locale est plus difficile d'accès pour les solutions de lavage, puisque la surface de contact TCE/solution de lavage est réduite par rapport aux gouttelettes individuelles retrouvées dans les zones de saturation résiduelle. Deuxièmement, la dynamique du déplacement du TCE dans le milieu poreux est beaucoup plus problématique, et ce pour quatre raisons : (1) Les forces gravitationnelles, qui dépendent de la hauteur des gouttelettes (saturation résiduelle) ou des accumulations locales, sont variables à l'intérieur des accumulations, et plus

importantes que dans le cas des gouttelettes, (2) la variation de la granulométrie à l'intérieur du milieu poreux, donc la variation du volume des pores, fait en sorte que les forces capillaires sont variables d'une couche de matériel à une autre, (3) la réduction des tensions interfaciales, et donc des forces capillaires, entraînée par le contact avec les tensioactifs, ne se fait pas instantanément comme c'est le cas avec les gouttelettes, mais se fait graduellement, de l'extérieur de l'accumulation vers l'intérieur, ce qui fait en sorte que les tensions interfaciales peuvent être variables à l'intérieur d'une même accumulation, et (4) les forces visqueuses deviennent plus significatives lorsque les fluides circulés dans le milieu ont à contourner les accumulations. Finalement, l'écoulement horizontal des solutions d'un puits d'injection vers un puits d'extraction imposent la considération des effets de densité, responsables des phénomènes tels que le sur-chevauchement (*overriding*) ou le sous-chevauchement (*underriding*) des solutions par rapport aux zones contaminées.

1.4 OBJECTIFS

Les objectifs de cette recherche ont été fixés dans le but de poursuivre les travaux de recherche présentés plus haut, et en abordant les points présentés dans la problématique, dans le but d'élaborer un procédé de lavage de sol aux solutions micellaires qui soit applicable à d'éventuels cas de terrain. Dans un premier temps, l'objectif de cette recherche est donc de compléter la compréhension des mécanismes de récupération du TCE observés lors de la réalisation de diagrammes de phase et d'essais en colonne de sable, par la mesure des tensions interfaciales, des angles de contacts, des densités et des viscosités. Dans un deuxième temps, l'objectif est de développer puis d'optimiser un procédé de récupération du TCE par solubilisation dans un milieu hétérogène, à l'intérieur duquel le TCE se retrouve autant à saturation résiduelle que dans des accumulations locales. Il s'agit donc de combiner l'ensemble des connaissances acquises sur les mécanismes de récupération lors des diagrammes de phase, des essais en colonne, et des mesures complémentaires, avec les essais de contrôle de mobilité des solutions en bac de sable. Les résultats de recherche de Glass *et al.* (2000) et Conrad *et al.* (2001),

portant sur la migration du TCE et sur des essais en bac de lavage de sols contaminés au TCE dans un milieu hétérogène, ont également été considérés dans l'élaboration du procédé. Des objectifs spécifiques à chacun des points énumérés dans cette section sont présentés dans les Chapitres 2 et 3.

1.5 METHODOLOGIE

Les mécanismes de récupération du TCE, de même que l'efficacité de récupération des systèmes eau/tensioactifs/TCE, ont été mis en relation avec les propriétés physiques des phases aqueuses et organiques résultantes. Les tensions interfaciales, la densité et la viscosité des phases liquides ont été mesurées sur des mélanges préparés en vrac, dont la composition se rapprochait de celle des fluides retrouvés à l'intérieur des colonnes de sable lors des expériences antérieures. Ensuite, l'approche du nombre capillaire et du nombre de Bond a été employée pour mettre en relation les propriétés mesurées avec les résultats des essais en colonne. Ces nombres, présentés dans la recherche sur le lavage de sol aux solutions micellaires par Pennell *et al.* (1996; 1994), permettent de comparer les effets des forces capillaires, gravitationnelles et visqueuses, puis de prédire les conditions favorables à la mobilisation du TCE lors d'essais de lavage de sol. Plus de détails sur ces applications, de même que les résultats des essais, sont présentés au Chapitre 2. L'étudiant a réalisé l'ensemble des mesures complémentaires, de même que leur interprétation. Il a également rédigé l'article présenté au Chapitre 2, sous la supervision de ses directeurs qui l'ont révisé. Les données expérimentales se rapportant à ces mesures sont présentées à l'Appendice A du mémoire.

En marge de ces travaux, et dans le but d'identifier d'autres solutions de lavage intéressantes, des diagrammes de phases supplémentaires ont été réalisés. Des mélanges d'isopropanol ou d'amines, avec une série de tensioactifs déjà identifiés par St-Pierre (2001), et du TCE, ont été caractérisés par des diagrammes de phase. Les courbes de miscibilité ont été tracées pour chacun des systèmes selon la méthode de titration décrite par Martel *et al.* (1993). Dans le but d'optimiser les systèmes, différents rapports

tensioactif/co-solvant (alcool, amines) ont été essayés. Ces travaux sont présentés à l'Appendice B du mémoire. Les systèmes présentant les courbes de miscibilité les plus basses sont considérées comme étant les plus intéressants, et devraient faire l'objet d'essais en colonne.

Suite à cette caractérisation complémentaire, un essai en bac de sable, présentant un milieu hétérogène 2D saturé en eau à l'intérieur duquel le TCE se retrouvait initialement autant dans des zones contaminées à saturation résiduelle que dans des accumulations locales, a été réalisé. Les essais en bac de sable sont intéressants parce qu'ils permettent de recréer les conditions rencontrées sur le terrain, tout en conservant un contrôle sur l'expérience que permettent les essais en laboratoire (Conrad *et al.*, 2001). Une solution de lavage a été élaborée à partir des résultats de la caractérisation complémentaire. Le meilleur système solubilisant a été sélectionné. De plus, un polymère, identifié lors des travaux antérieurs de Martel, K. E. *et al.* (1998), a été ajouté au mélange pour l'optimisation du balayage du milieu hétérogène. L'expérience a été réalisée en collaboration avec le laboratoire de visualisation d'hydrogéologie des Laboratoires Sandia (Nouveau-Mexique), qui ont fourni l'équipement et le support pour la réalisation de l'expérience. L'expérience est présentée dans le Chapitre 3 de ce mémoire. L'étudiant a élaboré l'expérience, collaboré à sa réalisation et en a interprété les résultats. Il a également rédigé l'article présenté au Chapitre 3, sous la supervision du Dr. Stephen H. Conrad, des Laboratoires Sandia, et de ses directeurs de recherche, qui l'ont révisé. Des données expérimentales supplémentaires sont présentées à l'Appendice C du mémoire. Les résultats d'un essai de traceur réalisé avant le début de l'expérience de lavage de sol, les propriétés de la solution micellaire utilisée et les résultats de l'expérience y sont présentés.

Tableau 1.1 - Propriétés du TCE (Mercer et Cohen, 1990)

Densité	Viscosité Absolue	Tension Interfaciale[1]	Solubilité	Concentration Maximale Acceptable[2]
(Kg/m^3)	(mPa.s)	(mN/m)	(mg/l)	(mg/l)
1464	0.57	35	1100	0,005

[1]avec l'eau

[2]selon la norme en vigueur de l'EPA, la norme canadienne est 10 fois plus élevée

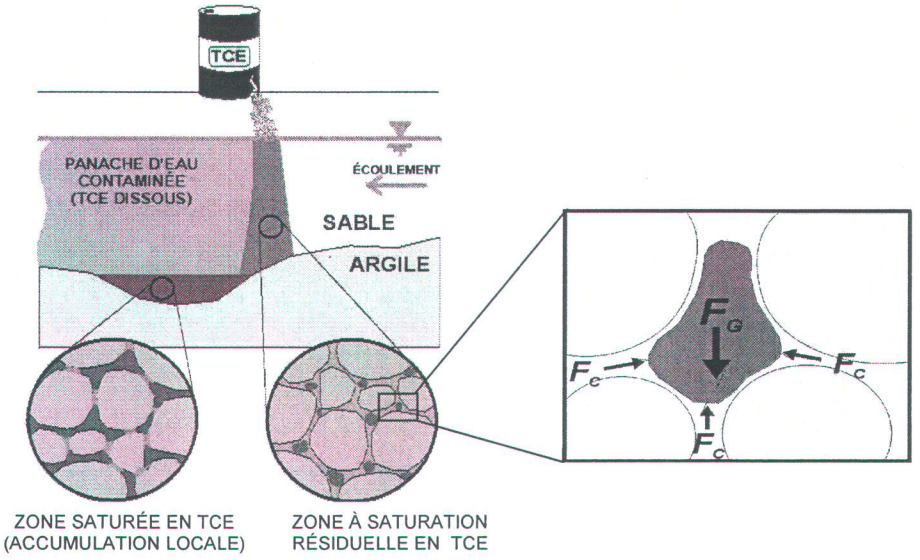

FIGURE 1.1 – Migration du TCE dans le milieu poreux.
(a) Saturation résiduelle et accumulation locale (piscine).
(b) Forces gravitationnelles (F_G) et forces capillaires (F_C) agissant sur une gouttelette de TCE piégée dans le milieu poreux saturé en eau.

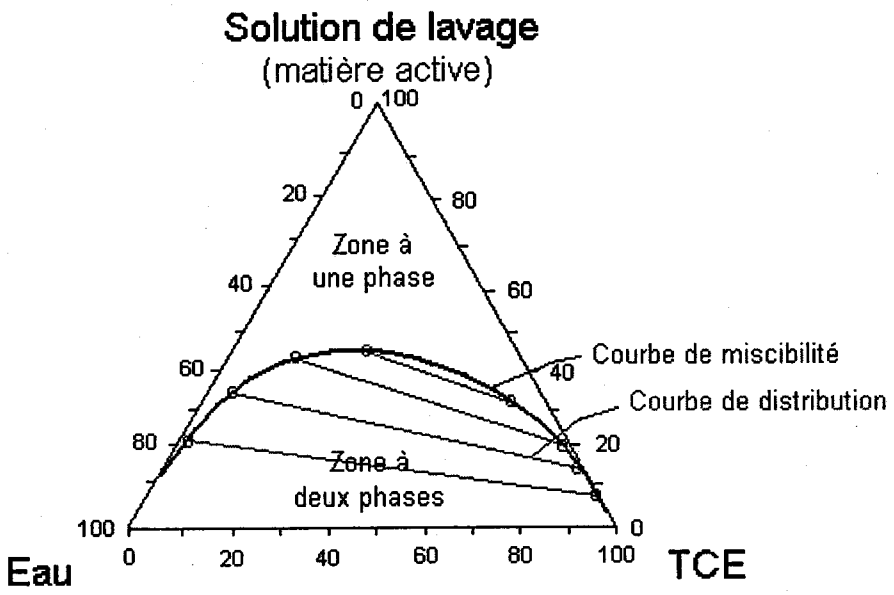

FIGURE 1.2 - Diagramme de phase. Les pôles représentent 100% du composé.

CHAPITRE 2

TCE RECOVERY DURING IN SITU FLUSHING: EXPERIMENTAL STUDY OF THE CONTROLLING PARAMETERS

RÉSUMÉ

L'injection dans le sol de solutions de lavage composées d'alcools et/ou de tensioactifs est une méthode prometteuse pour la réhabilitation des aquifères contaminés aux solvants chlorés. La mobilisation et la solubilisation sont les deux principaux mécanismes de récupération des contaminants avec des solutions de lavage. La solubilisation est cependant considérée comme l'approche la plus favorable et la plus généralement applicable pour les cas de terrain. Ce travail est basé sur les résultats provenant d'essais en colonne réalisés précédemment par St-Pierre (2001), où les deux mécanismes de récupération ont été observés. Ces mécanismes, de même que les saturations en TCE résultantes du lavage, ont été mis en relation avec la viscosité et la densité des phases liquides et les tensions interfaciales. Ces propriétés physiques des systèmes de lavage ont été mesurées durant la présente étude. Pour les systèmes mobilisants, le principal facteur responsable de la récupération du TCE est le gonflement de la phase organique. Pour les systèmes solubilisants, une valeur critique de nombre capillaire de 2×10^{-5} a été déterminée au delà de laquelle il peut y avoir mobilisation du TCE dans le sable d'Ottawa. L'augmentation de la densité des solutions de lavage résultant de la solubilisation du TCE s'est avérée être un problème potentiel pour les deux systèmes solubilisants les plus performants. Cette information devrait permettre d'ajouter de

nouveaux critères de sélection pour l'évaluation de solutions de lavage prometteuses, et permettre ainsi l'élaboration de stratégies de réhabilitation efficaces et sécuritaires.

ABSTRACT

In situ flushing using alcohol and/or surfactant solutions is a promising method for the remediation of DNAPL-contaminated aquifers. Mobilization and solubilization are the two main DNAPL recovery mechanisms with these washing solutions. Solubilization is considered as a generally more applicable and suitable remediation approach. Our work is based on the previous column experiments of St-Pierre (2001) where both mobilization and solubilization were observed. In this study, measured liquid phase viscosities, densities and interfacial tensions are used to interpret recovery mechanisms and TCE saturations. For mobilizing systems, organic phase swelling was found to be the controlling recovery mechanism. For solubilizing systems, a critical capillary number was found around 2×10^{-5} over which TCE mobilization occurs in Ottawa sand. The density increase of washing solutions due to TCE solubilization was found to be a potential problem for two well-performing solubilizing systems. These results will provide new guidelines for the selection of potential washing solutions and for the elaboration of safe and effective remediation schemes.

2.1 INTRODUCTION

2.1.1 Washing solutions

In the past, DNAPL-forming organic products such as chlorinated solvents, were extensively used for degreasing and other cleaning purposes, and disposed of without consideration of their potential impact on groundwater quality (Pankow and Cherry, 1996). For example, in the past, the general practice recommended by solvent manufacturers to eliminate TCE was to dispose the used solvent on land for evaporation.

Because of their high densities and low viscosities, DNAPL tends to migrate downward in the ground, and potentially through aquifers (Cohen and Mercer, 1993). In saturated zones, high interfacial tension with the surrounding water causes trapping of part of the DNAPL in the pore network, resulting in high residual saturations. At this concentration, the trapped DNAPL dissolves slowly in the surrounding groundwater, not enough to readily disappear, but enough to contaminate the flowing water above acceptable levels for years.

In situ flushing using alcohol and/or surfactant solutions is a promising method for remediation of DNAPL-contaminated source zones (Falta, 1998; Shiau *et al.*, 1994; Baran *et al.*, 1994; Martel *et al.*, 1993; Brandes and Farley, 1993). Surfactants have the ability to accumulate at the interfaces between the aqueous and trapped organic phase, reducing interfacial tensions. Once they reach a specific concentration in water (critical micelle concentration), the surfactant molecules aggregate and form micelles. Soluble in water, these micelles trap DNAPL and enhance the apparent water solubility of the DNAPL. Alcohols can also reduce interfacial tensions and change phase compositions (Quirion and Desnoyers, 1984). When more soluble in the aqueous phase, alcohols promote DNAPL solubilization, whereas when they are more soluble in the organic phase, they cause swelling and promote DNAPL mobilization.

Alcohols and surfactants work best when used in combination (Martel *et al.*, 1993). Surfactants enhance the water solubility of some alcohols, while alcohols decrease the concentration of surfactants at which micelles are formed. Alcohols also reduce the surfactant solution's viscosity and their adsorption on sand particles(Martel *et al.*, 1996). A combination of anionic and nonionic surfactants is also efficient (St-Pierre, 2001).

2.1.2 Mobilization process

In order to displace the DNAPL during flushing, viscous and buoyancy forces have to overcome the capillary forces, governed by interfacial tensions and responsible for

DNAPL trapping (Mercer and Cohen, 1990). With interfacial tensions reduced to ultra-low values by surfactants and alcohols, the trapped droplets of DNAPL have the ability to distort more easily and be mobile again. This results in an accumulation of a continuous organic phase ahead of the washing solution (mobilization). Swelling of the organic phase by alcohol transfer also contributes to a rise in organic phase saturation and relative permeability to the organic phase, favoring its immiscible displacement (Falta, 1998).

Although considered fast and economic because only a few pore volumes are necessary for near complete DNAPL removal, mobilization of a free-phase DNAPL may result in downward migration of the DNAPL, possibly beyond the zone of influence of extraction wells. Also, with interfacial tensions reduced, mobilized DNAPL can penetrate finer layers previously uncontaminated.

Several authors have studied the mobilization process for potential aquifer remediation while considering the dangers associated with free-phase downward DNAPL migration. One common option is to use this approach only when a continuous impermeable layer (clay or aquitard of compact glacial till) is located under the contaminated zone (St-Pierre, 2001; Pennell *et al.*, 1996; Brandes *et al.*, 1993). Therefore, in order to safely recover mobilized DNAPL, the integrity of the underlying impermeable layer has to be proven by an extensive site characterization. Another option is to reduce the density contrast between the DNAPL and the surrounding water. This can be done by turning the DNAPL into a LNAPL by alcohol transfer during a pre-flush, and by increasing the ground water density with the addition of sugars (Roeder *et al.*, 2001; Lunn and Kueper, 1999a; 1999b). In this case, the exact quantity and distribution of the DNAPL needs to be well understood, and the pre-flush solutions need to be prepared and distributed throughout the contaminated zone accordingly. Other strategies were developed to recover the mobilized DNAPL in the same well used for injection of the mobilizing solution (Knox *et al.*, 1997; Sabatini *et al.*, 1997). With such requirements, costs saved on remediation may go to more intense site characterization and monitoring. Moreover, because of the generally poor understanding of pooled TCE behavior and effects of site heterogeneities, the

dangers of DNAPL downward migration is still of great concern. With this in mind, we see solubilization as a more generally field-applicable remediation approach.

2.1.3 Solubilization process

Designing a solubilizing remediation flood is quite a challenge because a compromise has to be made between the governing factors: solubilization power, interfacial tension and density (Ramsburg and Pennell, 2001; Taylor *et al.*, 2001; Sabatini *et al.*, 2000; Boving and Brusseau, 2000; Kostarelos *et al.*, 1998; Pennell *et al.*, 1996; Pennell *et al.*, 1994).

The ability of the washing solution to solubilize a DNAPL is primarily based on the nature of the solution components (alcohols and/or surfactants), and their concentration in the solution (active matter concentration). For example, with surfactants, once the critical micelle concentration is reached, the more surfactant is added in the solution, the more micelles form and apparent DNAPL solubility increases (Shiau *et al.*, 1994). Also, Pope and Wade (1995) demonstrated through the Chun-Huh relationship that the solubilization potential is inversely proportional to the square root of the interfacial tension. Therefore, best solubilization is achieved with high active matter concentration, which is in turn inducing the lowest interfacial tensions. However, in the field or in sand column experiments, high enough interfacial tensions have to be maintained to avoid immiscible displacement of the DNAPL and formation of a free organic phase ahead of the washing solution. Therefore, a compromise has to be found between solubilizing power and reduction in interfacial tension.

The capillary number (N_C) and the bond number (N_B) are good criteria to evaluate the potential of the trapped organic phase for mobilization (Pennell *et al.*, 1996). They represent respectively the ratio of the viscous forces and buoyancy forces to the capillary forces. N_C is defined as follows:

$$N_C = \frac{q_w \mu_w}{\sigma_{ow} \cos\theta} \quad (1)$$

where: q_w = velocity (m/s); μ_w = washing solution viscosity (Pa•s); σ_{ow}= interfacial tension (N/m); θ = contact angle. The bond number represents the ratio of the buoyancy forces to the capillary forces. The following relationship defines N_B:

$$N_B = \frac{\Delta\rho \, g \, k \, k_w}{\sigma_{ow} \cos\theta} \quad (2)$$

where: $\Delta\rho$ = density difference between aqueous and organic phases (kg/m^3); g = constant of gravity (m/s^2); k = intrinsic permeability of the media (m^2); k_w = relative permeability to water; σ_{ow}= interfacial tension (mN/m); θ = contact angle (°). For vertical flow, these numbers can be summed using the following total trapping number (N_T) expression:

$$N_T = | N_C + N_B | \quad (3)$$

In these relationships, q_w was obtained from previous column experiments (St. Pierre, 2001), μ_w was obtained from earlier batch studies (St. Pierre, 2001), and σ_{ow}, θ and $\Delta\rho$ were obtained from the batch studies performed for this research. Generally, greater interfacial tension reductions will yield higher N_T values. Results from several column or sand box experiments presenting different conditions (grain size, flow rate, washing solution density, viscosity and interfacial tension with the DNAPL), can point out a critical N_T value. In systems where N_T is greater than this critical value, the capillary forces are overcome by the viscous and buoyancy forces, and DNAPL mobilization is observed. In systems where N_T is smaller than this critical value, the capillary forces remain high enough to prevent DNAPL mobilization. Ramsburg and Pennell (2001) observed uncontrolled PCE mobilisation into a silica sand (F-70 Ottawa sand) lens using a 8% Aerosol MA surfactant/isopropanol (MA/IPA) solution providing a N_T value of

1.3×10^{-3}, and observed no mobilization with a 4% Tween 80 surfactant solution providing a N_T value of 6.1×10^{-5}. Taylor *et al.* (2001) saw no PCE mobilization in sand box experiments with two different systems yielding N_T values of 2.48×10^{-6} and 5.80×10^{-7} in two Ottawa sands (20-30 mesh and F-70). Boving and Brusseau (2000) compared several solubilizing surfactants, humic acid (all at 5 % active matter concentration) and ethanol (50% mass) in columns filled with Borden aquifer material, and the critical N_T value for the onset of TCE immiscible displacement in this material was close to 10^{-5}. Pennell *et al.* (1994) compared the efficiency of three combinations of surfactants in dissolving PCE in four column experiments using various Ottawa sands (20-30, 40-120 and 40-270 mesh), and found a critical N_T value of 10^{-5} over which mobilization occurred.

In downward flow column experiments where buoyancy forces were negligible in comparison with viscous forces, Sabatini *et al.* (2000) optimized the compromise between the super-solubilization power of middle-phase-microemulsions and interfacial tensions. They achieved good results in keeping this compromise optimal by applying a IFT reduction following a gradient approach. Desaturation curves (S_o/S_{or} vs. N_c) were drawn to identify a critical capillary number N_C value of 5×10^{-6} over which mobilization of residual PCE occurs in the Dover AFB aquifer sand. Similar curves were previously drawn by Pennell *et al.* (1996) for PCE recovery in four size fractions of Ottawa sand (20-30, 60-80, 100-120 and 40-270 mesh). Those curves illustrated a critical N_T value around 2×10^{-5}.

The density of the washing solution, initially and during DNAPL solubilization, is also an important factor. A washing solution containing a high concentration of alcohol has an initial density lower than water, and the potential for overriding the zone to be swept becomes a concern. Moreover, when solubilizing high density DNAPL, the risk of downward migration of the washing solution is also of concern. Taylor *et al.* (2001) proposed to minimize the density effects with a high flow rate. Oostrom *et al.* (1999) observed plume sinking related to a TCE-saturated surfactant solution with a density of 1,0045 kg/m^3. Kostarelos *et al.* (1998) proposed the use of a neutrally buoyant microemulsion adding iso-propanol to the solution while insuring good sweep efficiency

with a polymer. They observed no downward migration for a 1,003 kg/m^3 microemulsion, and dramatic downward migration for a 1,028 kg/m^3 microemulsion. Pennell *et al.* (1996) also observed plume sinking with 1,005 to 1,027 kg/m^3 solutions.

2.1.4 Previous studies

The present work is based on the results of St-Pierre (2001). During her experiments with trichloroethene (TCE), using phase diagrams, several alcohol and surfactant combinations were compared at different active matter concentrations and ratios, and the dominant recovery mechanism was anticipated based on the phase behavior. The most promising washing solutions were then tested in column experiments (Ottawa sand with d_{50}=0.33 mm). Table 2.1 presents a summary of her results for the eleven washing solutions tested. The recovery mechanism was determined from the nature of the phases at the outlet of the column, and TCE concentrations were measured. Almost all experiments showed both mobilization and solubilization processes.

2.1.5 Objectives

The main objective of the present study is to relate and explain the observed recovery mechanisms (solubilization vs. mobilization) and final TCE saturations to liquid phase densities, washing solution viscosity and resulting interfacial tensions between the washing solution and TCE. Contact angles will also be measured for best interpretation. A critical total trapping number (N_T) over which immiscible displacement of TCE is initiated will be identified with desaturation curves. Also, the increase in density of washing solutions as they solubilize TCE will be evaluated. This information should provide new guidelines for the selection of washing solutions and for the elaboration of safe and effective remediation schemes. Gabriel *et al.* (2001) present a more detailed interpretation of the phase behavior based on the experimental data presented here.

2.2 EXPERIMENTAL METHODS

2.2.1 Sample selection and preparation

To study the phase behavior during the washing experiments, new samples representing the solutions as they were inside the sand columns were made, since actual experiment effluents were no longer available. The known parameters were initial composition of the washing solution, initial and final TCE saturation in the column, and TCE concentrations in the column effluents, measured separately in the aqueous and in the organic phase.

Phase diagrams were used for the elaboration of representative samples. Phase diagrams are ternary diagrams used to illustrate the total composition of a three-component system (Martel *et al.*, 1993). Each pole represents respectively 100% of water, TCE and active matter (alcohol and/or surfactant) (Figure 2.1 (a)). Above the miscibility curve, the three components are miscible. Below the curve, the components are not miscible and separate in two liquid phases, aqueous and organic, with the composition of each phase lying on the miscibility curve. A tie-line links the two phases in equilibrium, and interfacial tensions are constant along this line. The plait point is located where the interfacial tension is zero. The critical tie-line is the line tangent to the plait point. For a solubilizing system, active matter partitions preferentially in the aqueous phase, and tie-lines have negative slopes (Falta, 1998) (Figure 2.1 (c)). The overall composition of the aqueous phase as it dissolves TCE will move from its initial position on the water-active matter line towards the TCE corner. For a predominantly solubilizing system, this line will be somewhat parallel to the tie-lines and interfacial tensions (IFT) should remain constant as the solution solubilizes TCE. Therefore, one sample for each solubilizing experiment was chosen for IFT measurements. For mobilizing systems, active matter partitions preferentially in the organic phase, and tie-lines have positive slopes (Figure 2.1 (b)). Since interfacial tensions should not remain constant as TCE is mobilized, three samples lying on different tie-lines were chosen for IFT measurements to obtain a more complete phase behavior characterization.

TCE was added to washing solutions in 60 ml vials, samples were shaken manually and were shelved for 48 hours in a refrigerator. In some cases, the interface between the aqueous and organic phase remained cloudy. After centrifugation, the cloud reappears if samples are moved around. Since fluids are in motion inside the column during the experiments, no centrifugation was done on the samples for best representation.

2.2.2 Density

The density of the equilibrated phases was measured with a hand-held Anton Paar densimeter model DMA 35N which has a ±10 kg/m^3 precision. Each phase was sampled directly in the 60-ml vials with a 3 ml syringe. Densities were measured until three consecutive values fell within a range of ±5 kg/m^3, the highest value being retained, because of possible TCE losses during storage and measurements. Samples were measured in order of increasing density (estimated by TCE content). Temperature was maintained at 10 °C ± 2 °C because of equipment constraints.

2.2.3 Interfacial tensions

Interfacial tensions between the organic and aqueous phases were measured with a FTA 200 Dynamic Contact Angle Analyser from First Ten Angstroms which uses the pendant drop technique. Interfacial tension (IFT) is determined by fitting the shape of the drop (in a captured video image) to the Young-Laplace equation which relates IFT to drop shape. Drops need to be large enough to be distorted by gravity as interfacial tension tries to balance this distortion. Best results were obtained when the drop of equilibrated organic phase was dispensed by a 50 µl glass syringe (Teflon tipped piston), with a 0.305 mm OD flat ended needle. A computer-activated pump controls the syringe. Organic fluid was dispensed inside a glass cell filled with the aqueous phase. The captured video image was calibrated with previously measured phase densities, and with the size of the needle tip. Temperature of the cell was maintained at 10 °C ± 2 °C.

The ±10 kg/m^3 uncertainty related to the density measurement did not affect significantly the measured IFT values (maximum variation related to density measurements is ± 0.5 %). The overall uncertainty of IFT measured values is less than ± 1.5 % for values over 1 mN/m, and less than ± 4 % for lower values. In the case of very low IFT values, organic phase drops could not be kept stable on the tip of the needle. IFT was measured on several drops in motion. IFT values are therefore influenced by the inertia of the moving fluid and less distorted by gravity.

2.2.4 Contact angles

Contact angles were measured using the same instrument as for interfacial tension. A larger glass cell was used where drops were manually placed on a polished quartz crystal cut perpendicular to the c axis, immersed in equilibrated aqueous phase. Angles were manually measured on a captured video image. Uncertainty of measurements is ± 3°.

2.3 RESULTS AND DISCUSSION

In all the previous column experiments carried out by St-Pierre (2001), eleven are considered here for the batch studies. Table 2.2 summarizes the experimental results. Kinematic viscosity and initial washing solution density values are from St-Pierre (2001), and densities at equilibrium of both aqueous and organic phases, as well as interfacial tensions and contact angles, are from this batch study. Depending on the dominant recovery process predicted by phase diagrams, the washing solutions were divided into three categories: first, the mainly solubilizing systems, presenting negative tie-lines on phase diagrams, and with an initial active matter concentration falling under the critical tie-line; secondly, systems with negative tie-lines but with initial active matter concentration over the critical tie-line, known to be mainly mobilizing systems from observation of column experiment effluents (St-Pierre, 2001); and finally, the mainly mobilizing systems presenting positive tie-lines on phase diagrams.

2.3.1 Mobilizing systems

Mobilizing systems promote active matter partitioning into the organic phase. Swelling caused by active matter transfer into the organic phase leads to an increase in organic phase saturation and relative permeability, and favors immiscible TCE displacement. This translates into positive tie-lines on phase diagrams (Figure 2.1 (b)). During this process, interfacial tension and capillary forces are reduced, which also promotes immiscible TCE displacement. The i-BuOH 85, n-PrOH 50 and n-PrOH 20 column experiments showed that 94 to 96 % of the total TCE recovered was from immiscible displacement (Table 2.1).

The batch study results presented in Table 2.2 help in understanding how active matter concentration, interfacial tension and contact angle affect the mobilization efficiency of the three mobilizing systems. Phase densities measured in batch studies provide a means of quantifying the swelling and the solubilization depending on different interfacial tension reductions. Figure 2.2 shows this relationship for the same mobilizing system, n-PrOH, at two initial active matter concentrations, 20 and 50%.

It is possible to observe that solubilization is very limited as the aqueous phase density is only slightly increased. And for this system, interfacial tension reduction does not significantly increase the solubilization. For the organic phase swelling, as interfacial tensions are reduced (going from sample 6 to sample 1 on the phase diagram), the slope of the tie-lines is increased, which means that more swelling takes place. The resulting organic phase density gets closer to the aqueous phase density as it approaches the plait point, where interfacial tensions are zero and the two phases are miscible.

The results also show that interfacial tension is not a controlling parameter in the recovery efficiency of one system. Indeed, the n-PrOH 20 system recovered four times less than the

i-BuOH 85 system with the same number of pore volume circulated (Table 2.1), and those two systems presented very similar interfacial tension values (Table 2.2). From these observations, it seems that the organic phase swelling is the controlling parameter in TCE recovery through immiscible displacement. Organic phase swelling is related to the active matter concentration and to the active matter type and can be relatively quantified with batch studies (density measurements) and phase diagrams.

2.3.2 Solubilizing systems

Solubilizing systems promote the formation of aqueous-soluble micelles, enhancing TCE solubility in the washing solution (Figure 2.1 (c)). The active matter remains in the aqueous phase, and only a very small amount partitions into the organic phase. With the use of alcohols and surfactants, interfacial tensions between the aqueous and the organic phase are reduced, and the extent of this reduction is based on two factors: the initial concentration of active matter in the washing solution, and the type of alcohol and/or surfactant.

For each solubilizing system, Table 2.1 gives the overall recovery and the percentage of solubilized vs. mobilized TCE observed during the previous column experiments (St-Pierre, 2001). In three of the five systems (W2722/SAS=2/1, i-BuOH/SAS=2/1 and EtOH 20), only solubilization was observed and TCE was recovered as a miscible phase. In the other two systems (EtOH: 50 and EtOH/SAS=2/1: 20), a certain amount of TCE was recovered as an immiscible organic phase, indicating that some mobilization did occur. This mobilization means that sometimes during the column experiment, capillary forces responsible for TCE trapping were overcome by viscous and buoyancy forces, thus promoting immiscible TCE displacement. The conditions favoring this situation can be analyzed and quantified through the interpretation of the batch study results presented in Figure 2.2.

Liquid phase properties are used to quantify these forces acting in the media. This is done through the calculation of the capillary, bond and total trapping numbers (Pennell *et al.*, 1996). One system with negative tie-lines on the phase diagram but with an initial active matter concentration falling over the critical tie-line is analyzed with the other solubilizing solutions even though TCE was mainly recovered through mobilization of an immiscible organic phase. Indeed, the EtOH/SAS=2/1 system was considered because active matter did not partition into the organic phase (deducted from the high organic phase density at equilibrium), and the TCE immiscible displacement was initiated by the interaction between viscous, buoyancy and capillary forces. The other two systems from the same category were not considered since there was swelling of the organic phase, in which case TCE immiscible displacement is not due to force interaction and not expressed in the capillary, bond and total trapping numbers. The EtOH: 50 system was not included in this analysis since it produced a strange organic phase whose composition could not be explained with phase diagrams.

With N_T values (Table 2.2), there are two ways we can identify the point where capillary forces are overcome by viscous and buoyancy forces. First, since the column experiments were performed prior to this analysis, we can simply link N_T values to column experiment observations. The two experiments where TCE immiscible displacement has been observed have N_T values of 4.05×10^{-4} and 7.29×10^{-4}. The other experiments have N_T values of 6.56×10^{-6}, 2.28×10^{-7} and 3.76×10^{-6}. This analysis suggests that for systems with N_T values larger than somewhere around 10^{-5}, the viscous forces acting in the media overcome to some extent the capillary forces and immiscible TCE displacement occurs as it was observed during the column experiments.

A more precise way to use the N_T values to identify the threshold of immiscible displacement is through the analysis of desaturation curves, where the reduction of TCE saturation in the column through only the mobilization of an immiscible organic phase is plotted against the N_T values (Sabatini *et al.*, 2000; Pennell *et al.*, 1996). This curve is presented in Figure 2.3.

The initial residual saturation S_{or} represents the saturation of TCE obtained after application of a hydraulic gradient in the column prior to the injection of washing solutions, and is related to organic phase properties as well as porous media properties. S_o is the TCE saturation remaining in the column after the circulation of washing solutions, and is related to the action of the washing fluid. Although contact angles were measured (Table 2.2), they were not included in this interpretation for the sake of comparison with results from other authors who all assumed a zero value for this parameter. Even if it were considered, contact angles of 20° to 25° represent a $cos\theta$ value of 0.9 and greater, and have only little influence on N_c values. Therefore, assuming a contact angle of zero ($cos(0)=1$) is a reasonable hypothesis.

The critical N_T value is given by the sudden drop of S_o/S_{or} values on Figure 2.3. These data provide a minimum critical N_T value around 2×10^{-5} over which TCE mobilization occurs in the Ottawa sand used for our experiment. There is some uncertainty on the actual value since N_T goes from 2×10^{-5} to 2×10^{-4} in experiments respectively without and with mobilization. This resulting curve in Figure 2.3 is in good agreement with results from our column experiments, and with results reported elsewhere (Sabatini *et al.*, 2000; Boving and Brusseau, 2000; Pennell *et al.*, 1996).

Figure 2.3 also shows that conditions favoring TCE immiscible displacement are not mainly governed by interfacial tension values, but other factors such as flow rates and washing solution viscosity have to be accounted for as well. This observation supports the use of the capillary, bond, and total trapping numbers approach, rather than IFT alone. Furthermore, one low IFT system performed poorly (i-BuOH/SAS=2/1, IFT=0.7, 10% overall TCE recovery), compared with a higher IFT system (W2722/SAS=2/1, IFT=3.30, 96% overall TCE recovery), which means that solubilization power may not be solely governed by IFT reduction, but also by other factors such as the ones mentioned above, and possibly by a rate-limited reaction.

The commonly used approach illustrated by Figure 2.3 could give a wrong indication of the critical N_T value for our systems. Solubilization is almost always observed in combination with mobilization. Therefore, the amount of TCE available for immiscible displacement is more or less reduced (depends on the solubilization power of each solution), and relative permeability is improved. This might not affect the systems for which mobilization dominates, but for other mainly solubilizing systems, the resulting S_o can become less representative. Experiments using equilibrated washing solution would provide more accurate N_T values. Also, once mobilized inside the column, the free organic phase in motion enriches itself with trapped TCE until it reaches the outlet. There, its composition is not representative anymore of the situation at first contact ahead of the washing solution. More mobilization can then be attributed to the effect of the interfacial tension reduction between the washing solution and the trapped TCE, and critical values can be overestimated (Gabriel *et al.*, 2001). The behavior of TCE throughout the column experiment can be better understood with the interpretation of the phase diagrams and critical parameters can then be estimated more representatively.

In the case of pooled TCE, at any scale, the factors controlling remobilization are not well represented by the capillary, bond and total trapping numbers, and another approach should be undertaken for the identification of the conditions favoring pooled TCE immiscible displacement (Conrad *et al.*, 2001).

2.3.3 Density effects

With the solubilization of TCE whose density is high (1,464 kg/m^3), the resulting aqueous phase can become denser than groundwater, and downward migration of the solution can occur (plume sinking). Figure 2.4 presents the initial (prior to injection) and equilibrium (saturated with solubilized TCE) density of the samples representing the five solubilizing systems. Two systems (W2722/SAS=2, 20% active matter and EtOH/SAS=2/1, 20% active matter) seem to pose a threat of plume sinking as equilibrium densities, respectively 1,409 kg/m^3 and 1,113 kg/m^3, are over the density of surrounding

groundwater (about 1,000 kg/m^3). These significant density increases are not surprising as these two solutions were the most successful in the overall TCE recovery through solubilization (respectively 95.8% and 73.8%). EtOH 20% and 50% may, with low initial densities, cause potential overriding during flushing, and they show only a minor density increase (as did i-BuOH/SAS=2/1 5% active matter), but this is not a serious concern since those solutions performed poorly during column experiments and do not deserve further study.

Oostrom *et al.* (1999) observed plume sinking related to a TCE-saturated surfactant solution with a density of 1,0045 kg/m^3. Kostarelos *et al.* (1998) observed no downward migration for a 1,003 kg/m^3 microemulsion, and dramatic downward migration for a 1,028 kg/m^3 microemulsion. Pennell *et al.* (1996) also observed sinking with 1,005 to 1,027 kg/m^3 solutions. Although this phenomenon could not be observed during our downward flow column experiment, the W2722/SAS=2 (20% active matter) should not be considered for field application unless mitigating actions are considered, such as decreasing active matter concentration, adding a light alcohol in the solution, increasing the ambient groundwater density with sugars, or playing with the extraction wells set-up.

For the mainly mobilizing systems, it can be seen that all resulting organic phases have a density much higher than groundwater (Table 2.2), and downward migration of mobilized phase could be a serious problem.

2.4 CONCLUSIONS

Recovery mechanisms and TCE final saturations observed during previous column experiments were further characterized with measurements of viscosity, density and interfacial tension. For this purpose, representative samples were elaborated with the guidance of phase diagrams, and fluid properties were measured. Results were compared with literature data. The controlling parameters influencing TCE recovery were identified

for both mobilizing and solubilizing systems studied, and the following conclusions were drawn:

- For mainly mobilizing systems, solubilization is not important and does not significantly increase with interfacial tension reductions;
- For mainly mobilizing systems, organic phase swelling is the main TCE recovery mechanism, and depends on active matter concentration and type.
- For mainly solubilizing systems, immiscible displacement of TCE is not only due to interfacial tension reduction but also to other factors such as flow rates and washing solution viscosities, and conditions favoring immiscible displacement of TCE can be predicted by the capillary, bond, and total trapping number approach. Lower IFT values do not necessarily mean better solubilization;
- In our case, a minimum critical N_T value was found around 2×10^{-5} over which TCE mobilization occurs in Ottawa sand (d_{50}=0.33 mm);
- The density increase of washing solutions due to TCE solubilization was found to be a potential problem for two solubilizing systems, and the active matter concentration will have to be reduced in order to consider their use in field experiments.

These results provide new guidelines for the optimization of washing solutions for TCE recovery. However, prior to field application, more laboratory experiments are needed for further investigation. Among other things, the behavior of the recovery mechanisms needs to be better understood in the presence of pooled TCE.

2.5 ACKNOWLEDGEMENTS

Research grants from NSERC and FCAR supported this work. Experiments were done with the laboratory facilities of the Hydrogeology Laboratory at the Quebec Geoscience Center, and of the Geology and Geological Engineering Department at Laval University.

Table 2.1 - Summary of sand column experiments (from St-Pierre, 2001)

Washing Solution	Active Matter	Total TCE recovery	Sol. vs. Mob.*	PV**	IFT****
	% weight	%	%		$x10^{-3}$ N/m
*Negative slope tie-lines, a.m.*** concentration below critical tie-line*					
W2722/SAS=2/1	20	95.8	**100** : 0	4	3.30
EtOH/SAS=2/1	20	73.8	**88** : 12	4.2	0.06
EtOH	50	52	**81** : 19	4.6	1.31
EtOH	20	0.6	**100** : 0	5.7	13.58
i-BuOH/SAS=2/1	5	9.8	**100** : 0	4.7	0.70
Negative slope tie-lines, a.m. concentration above critical tie-line					
EtOH/SAS=2/1	50	99.8	34 : **66**	4.2	0.05
EtOH	80	87.8	10 : **90**	4.7	0.11
i-BuOH/SAS=2/1	20	93.4	27 : **73**	4.2	0.09
Positive slope tie-lines (3 samples/system)					
i-BuOH	85	88.8	4 : **96**	4.7	2.93-8.60
n-PrOH	50	88.6	6 : **94**	4.8	0.29-3.05
n-PrOH	20	22.6	4 : **96**	5.5	3.98-7.67

*Percentage of TCE solubilized vs. mobilized (dominant mechanism is bold)
**Total number of pore volumes injected at which recovery values are quoted
***a.m.: active matter concentration
****Interfacial tension (system description is given in Table 2.2)

Alcohols:
EtOH: ethanol
i-BuOH: iso-butanol
n-PrOH: n-propanol

Anionic surfactant:
SAS: Hostapur SAS 60 (Secondary alkanesulfonate)

Non-ionic surfactant:
W2722: Witconol 2722 (Polysorbate 80)

Table 2.2 – Experimental results

Washing Solution	Active Matter	TCE in Sample[a]	Kinematic Viscosity	Initial Density	Density at Equilibrium		Interfacial Tension	Contact Angle	N_T[b]
					Aqueous	Organic			
	% mass	% mass	$x10^{-3}$ Pa*s	kg/m^3	kg/m^3	kg/m^3	$x10^{-3}$ N/m	deg	(dimentionless)
Solubilizing systems: negative slope tie-lines, a.m.[c] concentration below critical tie-line									
W2722/SAS=2/1	20	35	11.3	1025.0	1409.0	-[d]	3.30	-	$6.56x10^{-6}$
EtOH/SAS=2/1	20	51	4.0	989.0	1113.0	1403.0	0.06	-	$4.05x10^{-4}$
EtOH	50	33	4.7	894.0	935.9	1359.6	1.31	28	-
EtOH	20	50	3.6	958.0	971.9	1454.9	13.58	-	$2.28x10^{-6}$
i-BuOH/SAS=2/1	5	49	1.8	997.0	100.2	1443.8	0.70	-	$3.76x10^{-5}$
Mostly mobilizing systems: negative slope tie-lines, a.m. concentration above critical tie-line									
EtOH/SAS=2/1	50	52	11.3	960.0	1116.6	1399.6	0.05	-	$7.29x10^{-4}$
EtOH	80	70	2.7	831.0	979.2	1250.6	0.11	-	$2.64x10^{-4}$
i-BuOH/SAS=2/1	20	55	4.8	988.0	1072.3	1381.7	0.09	-	$3.10x10^{-4}$
Mobilizing systems: positive slope tie-lines (3 samples/system)									
i-BuOH	85	10	5.0	835.0	981.6	987.8	2.93	-	$1.12x10^{-5}$
i-BuOH	85	30	5.0	835.0	989.3	1061.6	5.90	-	$5.50x10^{-6}$
i-BuOH	85	45	5.0	835.0	991.7	1316.0	8.60	38	$3.76x10^{-6}$
n-PrOH	50	14	4.9	903.0	951.7	966.3	0.29	-	$1.18x10^{-4}$
n-PrOH	50	33	4.9	903.0	974.3	1070.4	1.47	24	$2.24x10^{-5}$
n-PrOH	50	60	4.9	903.0	978.5	1240.7	3.05	20	$1.07x10^{-5}$
n-PrOH	20	21	3.8	960.0	978.0	1323.1	3.98	24	$7.79x10^{-6}$
n-PrOH	20	44	3.8	960.0	981.6	1380.6	5.35	20	$5.76x10^{-6}$
n-PrOH	20	71	3.8	960.0	983.4	1425.0	7.67	-	$4.01x10^{-6}$

[a] TCE concentration in overall sample composition

[b] From equation 1, 2 and 3 (section 2.1.3), where: q_w (velocity) = $1.68x10^{-6}$ m/s; k (absolute permeability) = $1.73x10^{-11}$ m^2; k_{rw} (relative permeability of water, approx. value) = 0.3

[c] Active matter concentration (% mass)

[d] Organic phase not available (turned into a macroemulsion), interfacial tension measured with pure TCE

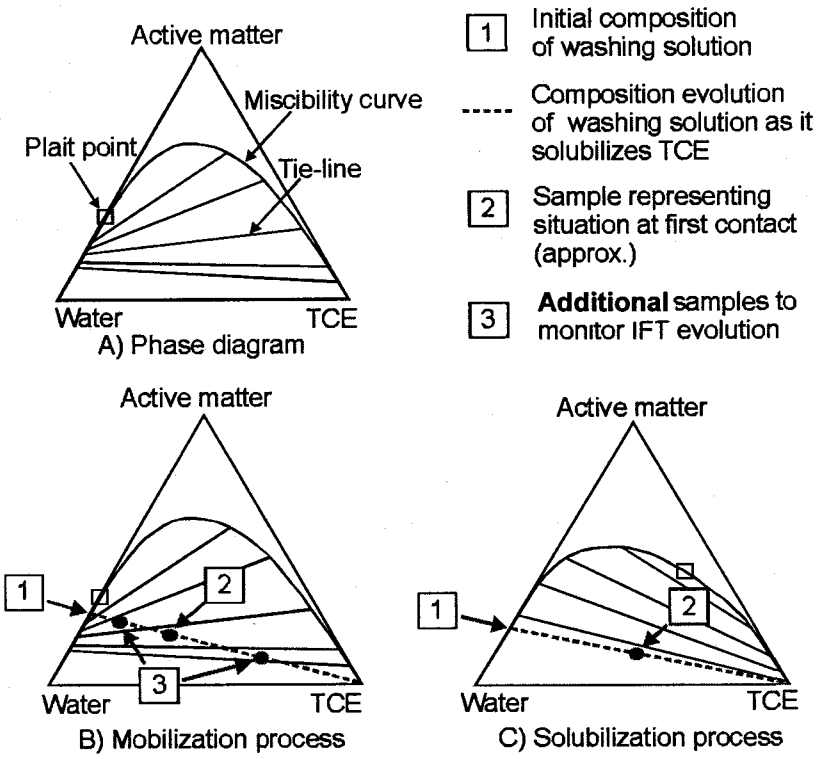

FIGURE 2.1 - Phase diagrams used for sample selection. The component proportions are determined on a mass basis.

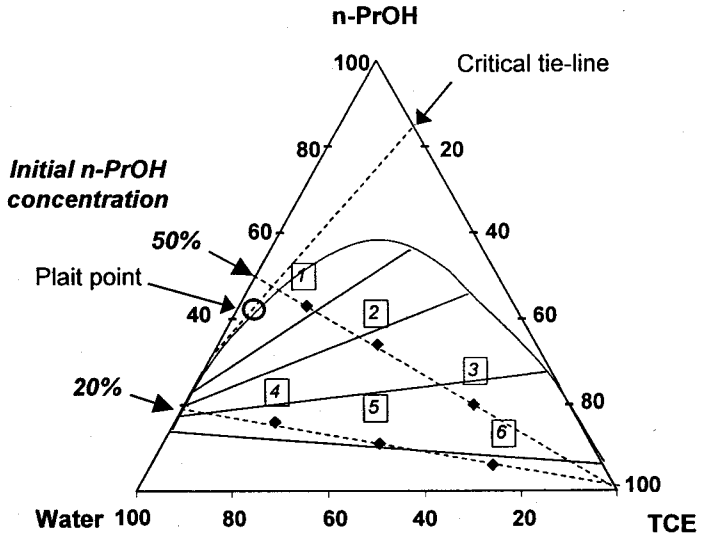

(a)

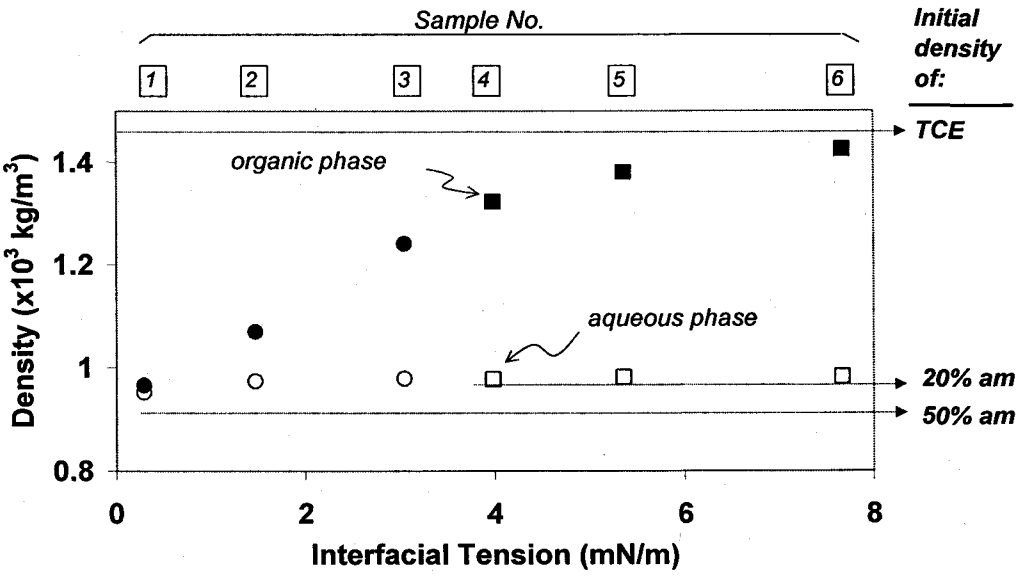

(b)

FIGURE 2.2 – (a) Swelling and solubilization with n-PrOH mobilizing system. Location of overall samples #1 to 6 on the water/n-propanol/TCE phase diagram. (b) Density of the equilibrated aqueous (white symbol) and organic (black symbol) phases as a function of the interfacial tension measured between the two phases (squares: 20% n-PrOH; circles: 50% n-PrOH). Also showing initial densities of TCE, and washing solutions.

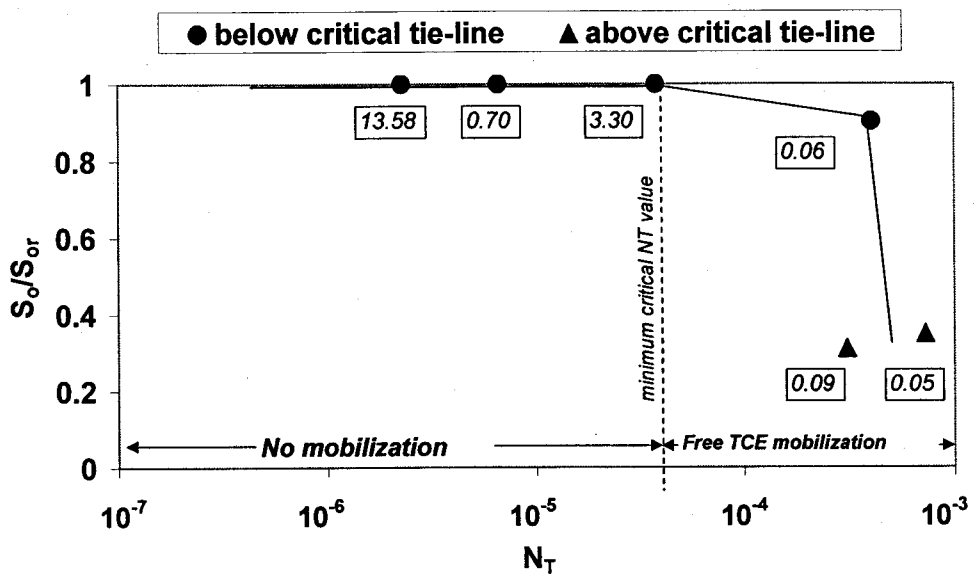

FIGURE 2.3 - Desaturation curve showing effects of mobilization on the reduction of TCE (organic phase) saturation S_o. IFT values are given (boxes, in mN/m). The minimum critical N_T value is picked where S_o/S_{or} starts to decrease.

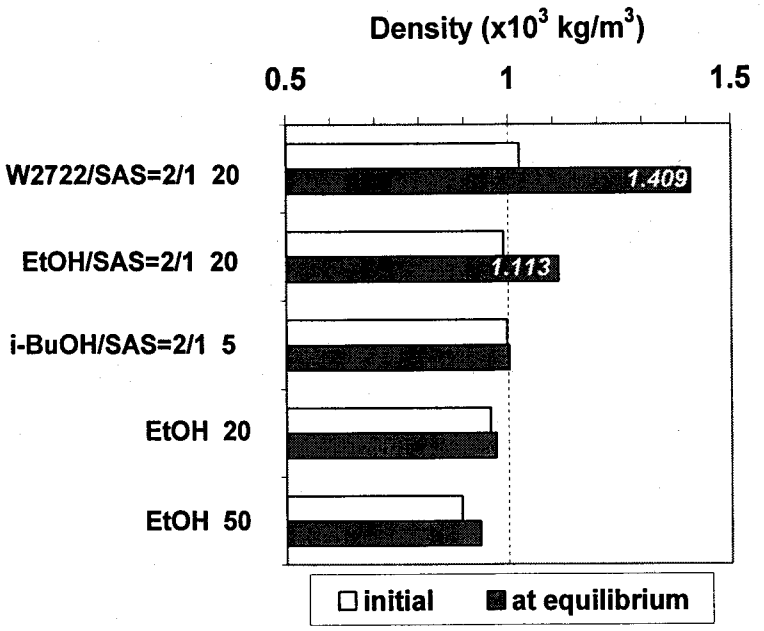

FIGURE 2.4 - Density of washing solution before and after TCE solubilization. Density of surrounding water is around 1 g/cm^3.

CHAPITRE 3

VISUALIZATION OF TCE RECOVERY MECHANISMS USING SURFACTANT-POLYMER SOLUTIONS IN A TWO-DIMENSIONAL HETEROGENEOUS SAND MODEL

RÉSUMÉ

L'injection de solutions micellaires est une technologie en émergence pour la réhabilitation *in situ* des zones sources d'aquifères contaminés par du TCE. Cette recherche vise à optimiser la récupération du TCE dans un modèle physique 2D représentant les caractéristiques d'un aquifère granulaire hétérogène. Une solution de lavage performante, composée de deux tensioactifs, a été identifiée antérieurement pour solubiliser efficacement le TCE piégé à saturation résiduelle en milieu poreux. Une stratégie d'injection utilisant un gradient de concentration ascendant en tensioactifs dans la solution de lavage a été employée pendant l'expérience pour minimiser les conditions favorisant la mobilisation du TCE. Un polymère rhéofluidifiant a été ajouté à la solution de lavage pour augmenter son efficacité de balayage dans le milieu hétérogène et pour atténuer les effets d'hétérogénéité sur le patron d'écoulement. Avant l'injection de la solution micellaire-polymère, le TCE fut introduit dans le bac par infiltration à partir de la surface pour former dans le milieu poreux saturé en eau des zones à saturation résiduelle et des accumulations (cuvettes) de TCE. L'analyse de photographies et d'images digitales a permis d'illustrer les interactions entre le TCE et les fluides injectés. Les tensioactifs ont interagi avec le polymère et la viscosité globale du mélange a été réduite. Suite au premier contact avec la solution de lavage, les accumulations de TCE se sont drainées. Le

TCE remobilisé n'a pas pénétré de couches précédemment non contaminées, et la surface de contact TCE/solution de lavage a été augmentée. L'augmentation de la concentration en tensioactifs dans les volumes de solution de lavage injectés plus tardivement n'a pas causé davantage de remobilisation. Le TCE a été principalement dissous pendant la séquence de lavage avec la plus grande concentration en matière active. L'obstruction de l'entrée de la chambre par des microgels ou des croissances bactériologiques a compromis la fin de l'expérience. Cependant, plus de 90% du TCE initialement en place a été récupéré avec la circulation de moins de 6 volumes de pores de solution micellaire-polymère. Ce type d'expérience permet l'observation directe de processus de récupération qui pourraient être difficilement caractérisés uniquement à partir de l'analyse des effluents.

ABSTRACT

Surfactant solution flooding is a promising technique for the remediation of source zones in DNAPL-contaminated aquifers. This research aimed to optimize TCE recovery in a 2D physical model providing a realistic representation of a heterogeneous granular aquifer. Earlier studies identified a promising surfactant formulation containing a combination of two surfactants which showed the potential to effectively dissolve TCE trapped at residual saturation with minimal displacement. The injection strategy used a surfactant concentration increase during the experiment to minimize the conditions favoring TCE remobilization. A shear-thinning polymer was added to optimize the sweep efficiency of the surfactant solution in the heterogeneous media. Before the injection of the surfactant-polymer solution, TCE was introduced in the sand pack where it infiltrated to form both mobile TCE pools and residual saturation zones. Photographs and digital image analysis illustrated interactions between TCE and the injected fluids. The effects of varying layer permeability inside the sand pack were greatly reduced by the shear-thinning polymer. The polymer also improved the contact between the TCE blobs and the solution, thus promoting dissolution. There was an interaction between the surfactants and the polymer, and the overall viscosity of the solution was lower than expected. At first contact with the initial 0.5% surfactant solution, the TCE pools drained and remobilization occurred. However, TCE did not penetrate any previously uncontaminated areas. As a result, TCE

surface area was increased. Subsequently injected higher surfactant concentration solution did not trigger more remobilization. TCE was mainly dissolved during the highest surfactant concentration solution flood. Plugging from bacterial growth or microgel formation at the inflow screen prevented the full completion of the experiment. However, more than 90% of TCE was recovered with the circulation of less than 6 pore volumes of surfactant polymer solution. Visualization experiments allow the direct observation of processes which may be difficult to properly identify based solely on effluent concentrations as in conventional experiments, especially for a heterogeneous medium.

3.1 INTRODUCTION

3.1.1 Overview

Aquifer contamination by dense non aqueous-phase liquid (DNAPL), especially chlorinated solvents, is highly problematic because of these organic compound's chemical, physical and biological properties (Pankow and Cherry, 1996). For example, TCE (trichloroethene, a common chlorinated solvent) is highly mobile inside granular aquifer material (gravel, sand, silt) because of its high density (1,460 vs. 998 kg/m^3 for groundwater), low viscosity and low partitioning on solid grains. Coming from surface or underground leaks, spills or intentional disposal, a DNAPL can potentially sink in the sub-surface, migrate through aquifers, and can accumulate in pools over less permeable stratigraphic layers. Along the migration path, droplets remain trapped in the porous media by capillary forces. In aquifers, TCE is very persistent because of its low water-solubility (1100 mg/l) and low degradability. Therefore, the DNAPL-contaminated zones become long-term sources of dissolved organic compounds. The US EPA standard for dissolved TCE in groundwater is very severe ($\leq$ 5 μg/l) (the Canadian standard is 50 μg/l), therefore source-zones do not have to be widespread to produce and feed large contaminated groundwater plumes for decades. For these reasons, it becomes relevant for any remediation effort to target the most complete removal of source-zones as possible.

Surfactant flooding is a promising *in situ* technique for the remediation of source zones in DNAPL-contaminated aquifers. It consists of sweeping source-zones with washing solutions containing surfactants and/or alcohols (Falta, 1998; Pope and Wade, 1995; Baran *et al.*, 1994; Martel *et al.*, 1993). Depending on the type and concentration of the selected active matter (surfactant, alcohol), there are three potential DNAPL recovery mechanisms: (1) Active matter partitions into the organic phase, which causes swelling and important interfacial tension reductions, causing mobilization (also called displacement) of a free organic phase ahead of the washing solution (St-Pierre, 2001; Pennell *et al.*, 1996; Brandes and Farley, 1993; Fountain *et al.*, 1991). (2) Surfactants molecules aggregate and form micelles which increase the aqueous solubility of the DNAPL and accelerate its dissolution (Ramsburg and Pennell, 2001; Taylor *et al.*, 2001; St-Pierre, 2001; Sabatini *et al.*, 2000; Boving and Brusseau, 2000). (3) Under specific conditions (optimum salinity window, ultra-low interfacial tensions) microemulsions can form and promote DNAPL solubilization (Dwarakanath *et al.*, 1999; Kostarelos *et al.*, 1998; Shiau *et al.*, 1996). Following the injection of surfactant solutions into the targeted sub-surface area, the contaminants can be recovered at pumping wells either as an organic phase or as dissolved in the washing solutions.

The focus of our research is TCE solubilization by surfactant solutions (Conrad *et al.*, 2001; St-Pierre, 2001; Robert *et al.*, 2001). In the literature, although micellar solubilization generally provided good results during laboratory and field experiments carried out under controlled conditions, it becomes apparent that several factors can mitigate the success of a realistic field application. These obstacles can be grouped into six limiting factors. TCE remobilization, dense plume sinking, heterogeneities and layer topography in the sub-surface, pools of TCE, rate-limited solubilization and costs can make TCE solubilization either endangering, incomplete, or economically impractical (Table 3.1). Several researchers proposed interesting solutions to overcome these limitations (Table 3.1). This paper presents the steps that our research group undertook during the design and application of a solubilization flood in a two-dimensional heterogeneous aquifer model, while considering some of the proposed options to overcome the limiting factors. Sand box experiments are interesting since they can

reproduce field-like environments, while insuring a good control over the experiment (Conrad *et al.*, 2001). When such experiments are taking place inside a glass-wall box, they allow the direct observation of processes which may be difficult to properly identify based solely on effluent concentrations as in conventional experiments, especially for heterogeneous medium.

3.1.2 Previous studies

A great number of washing solutions containing surfactants and alcohols were initially evaluated with phase diagrams (Water/Active Matter/TCE) based on the lowest miscibility curve criteria (St-Pierre, 2001; Martel *et al.*, 1993). The most promising solutions for TCE recovery were tried in sand column experiments, where efficiency and recovery mechanisms (solubilization vs. mobilization) were evaluated (St-Pierre, 2001). Interfacial tensions and liquid phase densities were measured in order to better understand the recovery processes (Robert *et al.*, 2001). For solubilizing systems, a minimum critical capillary number was found around 2×10^{-5} over which TCE mobilization occurred in Ottawa sand (d_{50}=0.33 mm). The density increase of washing solution due to TCE solubilization was found to be a potential problem for two well-performing solubilizing system. A combination of two surfactants, W2722 (Witconol 2722, polysorbate 80, nonionic) and SAS (Hostapur SAS 60, secondary alkanesulfonate, anionic), at a mass ratio of W2722/SAS=2/1, was selected for its high solubilizing power of TCE at residual saturation and high enough interfacial tension with TCE (measured in batch) in order to prevent TCE remobilization.

Concurrently, Conrad *et al.* (2001) performed two TCE recovery visualization experiments using a reproducible 2D chamber providing a good representative heterogeneous environment. Experiments demonstrated that extreme reductions in DNAPL/water interfacial tension (27 mN/m to 0.6 mN/m) occurred when using a 1.6% Aerosol MA (sulfosuccinate, anionic), 4% isopropanol, and 0.3% NaCl aqueous solution, resulting in massive pool drainage into low permeability layers and overall poor TCE recovery results. More modest reductions in interfacial tension occurred (27 mN/m to 9

mN/m) when using a 5% Tween 80 (polysorbate 80, nonionic) aqueous solution, resulting in modest TCE remobilization, restricted to the pathway of original DNAPL migration. In this experiment, capillary forces remained sufficiently high to exclude DNAPL migration into low hydraulic conductivity regions. Almost 90% of the DNAPL was recovered within 8.6 pore volumes of washing solution. It was found that, as a rule of thumb, pooled TCE drainage can be expected once the IFT between the TCE and the washing solution becomes less than half the IFT between the TCE and the water (therefore around 13-14 mN/m).

3.1.3 Objectives

The present study combined the findings of the previous experiments while considering the application of some of the options presented in Table 3.1. The main goal was to find a field-applicable remediation strategy that optimizes the solubilization process in an economically viable and environmentally safe manner. Four steps were undertaken in order to reach this goal:

- Visualize the ability of a polymer solution (without surfactants), and the enhanced viscous forces it induces inside the sand pack, to increase TCE surface-to-volume ratio (spreading), without reducing the interfacial tensions and causing important TCE remobilization or penetration into low conductivity layers. In addition, TCE pools are low conductivity regions (water saturation is low and consequently its relative permeability is low), and the polymer should allow greater contact with TCE, promoting its dissolution. The combination of these actions should diminish the propensity of TCE pools to drain during the subsequent surfactant flood, even if interfacial tension is reduced;

- Optimize solubilization efficiency with a washing solution formulation benefiting from extensive laboratory optimization (phase diagrams, sand column experiments, IFT and density measurements). This experiment should also verify if predictions regarding recovery processes, solubilization efficiency, and the identification of

conditions favoring TCE remobilization, formulated upon the analysis of phase diagrams, sand column experiments and IFT measurements, apply to this field-like heterogeneous situation;

- Add a shear-thinning polymer to the washing solution. Shear thinning polymers have the ability to reduce the washing solution viscosity in low hydraulic conductivity layers, and increase the washing solution viscosity in high hydraulic conductivity layers (Martel, K.E. *et al.*, 1998), thus uniformizing the flow and promoting the sweep of fine-grained layers. Also, with a uniform front, less washing solution should be needed in order to entirely sweep the chamber. Again, the polymer should allow greater contact between surfactant and TCE, promoting its dissolution;

- Apply a surfactant gradient approach. Observe TCE behavior under the influence of increasing surfactant concentration and reducing interfacial tensions (formation and migration of a free TCE phase in the initially residual saturation zones, drainage of pools, penetration of previously uncontaminated finer sand layers and aquitards). The goal of this gradient approach is to avoid massive drainage and have dissolution diminish the propensity for the pools to drain by minimizing the reduction of the capillary forces when the gravity forces are at their highest values. Afterwards, active matter concentrations can be increased to effectively solubilize TCE without the risk of massive mobilization.

3.2 EXPERIMENTAL SETUP

3.2.1 Chamber setup

The full description of the chamber is given in Conrad *et al.* (2001). The chamber setup is designed to simulate field-scale applications of surfactant-enhanced aquifer remediation (SEAR). It is thin but extensive (internal dimensions: 0.01m thick, 0.61 m wide and 0.60

m tall), with an internal volume of 3.9 liters. It is mounted in a dark room, in front of a controlled output diffuse light source. Its glass walls allow visual observation of the interaction between red-dyed TCE and washing solutions in saturated heterogeneous aquifer material. Figure 3.1 presents a schematic view of the experimental setup. Entry pressures were maintained under a 10 cm of water limit to prevent bowing in the glass walls of the chamber. Such bowing allows sand grains to redistribute and adversely affects the image analyses.

3.2.2 Sand pack

The sand pack is an analog model presenting heterogeneities reminiscent of fluvial lithologies (Figure 3.1). It consists of four translucent hydrophilic silica sands with non-overlapping grain size distributions, where textures vary sharply across facies boundaries (Table 3.2). Permeabilities range over a factor of 20, and capillary contrasts for non-wetting fluid entry pressures range over a factor of 4. Glass *et al.* (2000) reported pressure saturation curves for three of these sands within the chamber geometry. Sand distribution was designed to allow TCE to be initially present in both residual saturation state and pooled state, while preventing it from reaching one of the chamber boundaries. It was also designed to include a bottom pool overlaying an aquitard. Glass *et al.* (2000) give details on the filling and settling procedure. One pore volume of the chamber is 1.45 liters and a bulk value for hydraulic conductivity was measured to be 3.13×10^{-3} m/s. The average porosity of the sand is 0.37.

3.2.3 Sampling and data analysis

Samples were collected during the experiment for TCE concentration and fluid density measurements. Taken at the outflow manifold, these measurements represent bulk values for the whole chamber effluent at a given time. No discrete sampling of a specific sand lens was taken. The sampling port for GC samples is located downstream of the outflow manifold (Figure 3.1). Approximately 250 µl were drawn with a syringe through the septum located on the port. The sample was then injected in a 4 ml vial previously filled

with water. It was then split in two 2ml vials for GC analysis. The GC used is SRI Instruments model 8610C, equipped with a FID detector and an auto sampler. The column used was Carbo-Wax from Supalco. Standards were run prior to sample analysis to build a calibration curve, and were also run every ten samples for constant calibration check. For density measurements, 15-ml vials were filled at the end of the outflow tubing (Figure 3.1). The density of the fluids was measured with a hand-held Anton Paar densimeter model DMA 35N. The tool has a ±1 kg/m^3 uncertainty. Densities were measured until three consecutive values fell within a range of ±5 kg/m^3, the highest value being considered.

Since dyes affect the transmission of light through the chamber, standard and digital imaging can well illustrate spatial and temporal differences occurring inside the chamber during the experiment. However, several factors such as the presence of remedial fluids, the presence of undissolved dye or the range of sand textures affect the ability of using light transmission techniques to quantitatively track the removal of TCE. Images were taken by standard 35 mm color cameras and video cameras. Digital images were obtained using a 1024x1024 pixel, 4096 gray levels, shuttered, monochromatic Charge Coupled Device camera, providing a resolution of 0.6 mm per pixel. Imaging software was used for digital image processing.

Two types of image processing techniques were used (Conrad *et al.*, 2001). The analysis of the differences in light intensity between two digital images taken at times corresponding to the beginning and the end of a flood can identify: (1) regions where TCE saturation has decreased (from drainage or dissolution), and regions where TCE saturation has increased, and (2) solubilization patterns, illustrated by color sequences showing earliest to latest dissolution. These techniques provided valuable qualitative evaluation of the TCE mobilization and solubilization processes.

3.3 WASHING SOLUTION FORMULATION

A combination of two surfactants, W2722 (Witconol 2722, polysorbate 80, nonionic) and SAS (Hostapur SAS 60, secondary alkanesulfonate, anionic), at a mass ratio of W2722/SAS=2/1, was selected for its high solubilizing power and high enough interfacial tension with TCE, as observed during previous sand column (TCE at residual saturation) and batch experiments (Robert *et al.*, 2001; Gabriel *et al.*, 2001; St-Pierre, 2001).

Xanthan gum, which is a food grade, shear-thinning polymer, was added to the solution. At a concentration of 500 mg/l, it provides good shear thinning behavior and the viscosity is not significantly affected by salt or bactericide (Martel K. E. *et al.*, 1998). Viscosities inside the sand pack vary between 10 and 20 mPa·s (observed viscosity during experiments is usually higher than when measured with a viscometer). A polymer flood can also prevent subsequent surfactant adsorption in the media by occupying available sites prior to the injection of surfactants (Martel K. E. *et al.*, 1998), although this was not expected to be a significant process in the clean silica sands.

Physical and chemical properties of the selected system for different active matter concentrations are illustrated in Figure 3.2. With this system, TCE solubilization should be maximized while the conditions favoring TCE redistribution and dense plume sinking should be minimized (Table 3.1).

3.4 TCE INJECTION AND REDISTRIBUTION

The chamber was saturated with water prior to the TCE injection. For best visualization, a red dye (Oil-Red-O, 0.9 g/l) was added to the TCE. The density of the dyed TCE was measured at 1,4585 kg/m^3. The interfacial tension of dyed TCE with water was measured at 27 mN/m. The TCE injection procedure is described in detail by Conrad *et al.* (2001). Sixty (60) ml of TCE was injected in the chamber. TCE migrated in the chamber in the manner observed and described in detail elsewhere (Conrad *et al.*, 2001; Glass *et al.*,

2001; Glass *et al.*, 2000). At the end of the injection sequence (Figure 3.3), TCE was present in the chamber in both a residual saturation state (original migration paths and drained regions of pools and fingers) and a almost fully saturated state (pools). TCE did not penetrate the bottom aquitard of the chamber, but it did hit the outflow manifold. This TCE was considered as the extension of the lower pool. Unfortunately, this substantial leak prevented mass balance calculations. After redistribution was complete, water was injected in the chamber from side to side at a 5 ml/min rate. TCE did not significantly remobilize during this period. A new value of hydraulic conductivity was measured at 2.74×10^{-3} m/s. The presence of TCE thus reduced the effective hydraulic conductivity in the chamber by 12 %.

3.5 OVERVIEW OF THE REMEDIATION EXPERIMENT SEQUENCE

The injection sequence was divided into three general steps: a water flood, a polymer flood, and a surfactant-polymer flood. The use of dyes at the beginning of the water and polymer floods allowed visualization of the flow behavior. No dye was used during the surfactant-polymer solution flood to allow qualitative TCE saturation estimations with the processing of digital images without interference.

The purpose the of polymer flood was to test the ability of enhanced viscous forces in increasing the TCE surface-to-volume ratio by spreading at least some pooled TCE, without reducing the interfacial tensions. 1.52 PV of polymer solution were injected in the chamber. A flow interruption of 10.3 hours followed.

The surfactant-polymer flood was divided into three distinctive floods (polymer concentration was constant in all three floods at 500 mg/l): a 0.5% surfactant flood (1.52 PV, followed by a 14.4 hours interruption), a 2% surfactant flood (1.20 PV followed by a 9.4 hour interruption), and a 5% surfactant flood (3.75 PV, with a 65 hours flow interruption taking place after the first PV). The goal of this gradient approach was to minimize the reduction of the capillary forces when the gravity forces were at their

highest (undissolved TCE pools). After the reduction of gravity forces from dissolution and modest mobilization, progressively lower IFTs could safely be accomodated, increasing the washing solution solubilization power.

3.6 RESULTS AND DISCUSSION

Appendix C-3, presented at the end of this document, presents the results of the entire flooding experiment. The flow rate, the TCE concentration in the effluent and the effluent density are plotted against injected pore volume and time. Both figures presented in the appendix C-3 illustrate the difficulty of using such data to perform a vigorous interpretation of the mechanisms that took place inside the chamber throughout the experiment. The visual observation of the processes occurring inside the chamber provided a better mean for any description or interpretation, which mostly remained qualitative.

TCE concentration measurements in the effluent did not provide a good means to quantify the TCE solubilization, for three reasons : (1) scattered data following the breakthrough of the polymer solution indicated that either xanthan gum had a perturbing effect on the flow of the samples inside the GC column or that the sampling technique was deficient; (2) Important dilution inside the chamber (not all washing solution encountered TCE as it progressed inside the chamber) prevented us from identifying effects of rate-limitations or flow interruptions, and from comparing data with solubility values; (3) Poor mass balance obtained at the end of the experiment, mainly due to TCE leaking through the outflow manifold under the aquitard following its injection, made an accurate quantification of the solubilization process impossible. We could observe, however, that TCE concentration trends during the experiment were in good agreement with density measurements. Also, the cumulative TCE recovery curve provided valuable information on relative solubilization efficiency through the analysis of the slope variation of the curve.

Flow rate and head difference data were recorded throughout the experiment. Based on the assumption that effective hydraulic conductivity (K_e) is somewhat uniform vertically throughout the chamber (because of the shear-thinning behavior of the solutions), any variation in K_e becomes a good indication of viscosity effects and relative permeability to water variations. The propensity for density-related aqueous plume sinking was also analyzed following the measurement of the effluent density.

3.6.1 Polymer flood

The most significant data we gathered during the polymer flood came from direct observation of processes. In order to visualize the behavior of the shear-thinning polymer solution inside the chamber, a blue dye was added to the first polymer solution slug, and compared with a previously circulated water-only blue pulse of similar volume. These pulses showed that (1) shear-thinning behavior did occur inside the chamber during the polymer flood, (2) sweep efficiency was increased with the polymer, (3) TCE saturation from one pool to another is variable and (4) enhanced viscous forces did have a noticeable effect on TCE distribution, causing both enhanced dissolution and remobilization. All these processes are well illustrated by photographs taken during the polymer flood (Figure 3.4). Also, GC data showed that TCE solubilization increased by a factor of 4 after the breakthrough of the polymer solution. Finally, flow data showed that bulk viscosity increased inside the sand pack as more polymer solution progressed towards the outflow side of the chamber.

Figure 3.4 (a) shows the water flow behavior inside the chamber. The large irregularity of the dyed-water front was clearly controlled by the differences in hydraulic conductivity between sand layers, with water flowing at higher velocity inside the higher permeability zones. Figure 3.4 (b) shows the contrasting polymer solution flow behavior. Contrary to the water flow pattern, the front of the dyed-water-polymer solution showed much more stability. The effects of varying permeabilities were thus greatly reduced by the shear-thinning behavior of the polymer. Breakthrough of the dyed water occurred after the injection of only 0.30 pore volume (PV), and breakthrough of the polymer solution

occurred after 0.77 PV. Moreover, a complete sweep of the chamber, i.e. the moment when the dye reached the full length of the downstream edge of the chamber, was achieved after the injection of 1.41 PV for the water flood, but only 1.07 PV for the polymer flood. Concretely, this means 24% less fluid was needed to sweep the whole chamber with the polymer included in the flowing water. In a larger-scale field situation, this could translate into significant cost reductions. These observations provided good indications of the flow homogeneity induced in the sand pack by the polymer.

Dye pulses also showed that sweep efficiency was increased with the polymer solution. In the enhanced oil recovery literature, sweep efficiency is defined as the ratio of the volume of oil contacted by the displacing agent over the volumes of oil originally in place (Lake, 1989). Figure 3.5 shows sweeping of the bottom pools and aquitard by the dyed water and the dyed polymer solution. During the water flood (Figure 3.5 (a)), blue water slowly progressed horizontally through the aquitard, and broke through upwards into the upper coarser layer after sweeping less than 14 cm of aquitard material. This front did not progress further into the aquitard until the end of the pulse experiment. The water swept only the very top part of pool 7a and entirely by-passed pool 7b. In contrast (Figure 3.5 (b)), the polymer solution progressed further into the aquitard and into pool 7a, and kept on moving until the end of this pulse experiment (it swept more than 20 cm of aquitard material). As a result, deeper penetration occurred into pool 7a, and pool 7b was not entirely by-passed. In the case of the water flood, the heterogeneity of the sand pack and the topography of the layers were responsible for the by-pass : the low permeability of the bottom aquitard prevented water from easily flowing through it, and the aquitard topography diverted the fluid flowing into the upper coarser sand over the two bottom pools, sitting in depressions. The homogeneity induced in the sand pack by the polymer, with more fluid able to flow inside the finer aquitard sand, resulted in more TCE contacted by the polymer solution, and an increase in sweep efficiency.

The sweeping of TCE pools 1 to 6 allowed a good qualitative evaluation of TCE saturation. Indeed, it was observed that both solutions did not get to the hearts of pools 4 and 5, meaning that TCE saturation was high inside these pools. There, TCE occupied not

only the center of the larger pores, but most of the pore space, preventing even a shear-thinning solution from flowing through the center of these pools (Figure 3.6). On the contrary, pools 1, 2, 3 and 6 seem to have been completely swept by the blue dye in both pulse experiments, indicating lower TCE saturations in these pools. These qualitative levels of saturation will become relevant in the evaluation of the solubilization process.

Figure 3.7 shows the differences in light intensity between two digital images taken at times corresponding to the beginning and the end of the polymer flood. Dark regions show a decrease in TCE saturation whereas white regions show an increase in TCE saturation (Conrad *et al.*, 2001). As a result of enhanced viscous forces acting on TCE blobs and pools, dissolution in lower saturation zones and modest TCE remobilization in higher saturation zones was observed. More than likely, a combination of the two processes was observed at the edge of pools 2, 3 and 7a (pool 7a is not shown), and some TCE moved beneath pools 4 and towards pool 5. Enhanced dissolution occurred because the shear-thinning polymer allowed greater penetration of the water-polymer solution into the low relative water-permeability zones (fine-grained sand layers and TCE contaminated regions), and forced more contact with TCE. Moreover, pools 2, 3 and 7a are low-saturation pools (as indicated by the dye pulse), thus more susceptible to enhanced dissolution (greater TCE surface-to-volume ratio). Since the interfacial tension (IFT) between the water-polymer solution and TCE (dyed with 0.9 g/l Oil-Red-O) is the same as the water-only and TCE IFT, 27 mN/m as measured in our lab, we believe the polymer does not improve TCE dissolution in any manner other than improved physical contact. This hypothesis is confirmed by the very similar phase diagrams obtained with both systems (surfactants/water/TCE vs. surfactants/water-polymer/TCE). Remobilization occurred when the viscous forces were increased and, in combination with existing buoyancy forces, slightly overcame capillary forces responsible for initial TCE trapping and pooling. The resulting (and very modest) TCE remobilization was restrained under a high saturation pool, where buoyancy forces exert the most pressure (in this case, pool 4).

Following the polymer flood breakthrough at 0.77 PV (from the pulse test), the TCE solubilization rate, which corresponds to the slope of the cumulative recovery curve

presented in Figure 3.8, is increased by a factor of 4 (from 0.16 grams to 0.61 grams of solubilized TCE per circulated pore volume of polymer solution – changing average TCE concentrations from 110 mg/l prior to breakthrough to 420 mg/l after the breakthrough). This confirms the effects of increased sweep efficiency and enhanced dissolution observed visually during the progression of the polymer solution inside the chamber. These two effects are consequences of the shear-thinning behavior of the polymer-water solution, inducing more homogeneous flow in the sand pack and allowing greater contact with TCE blobs and pools.

During this experiment, the reduction in effective hydraulic conductivity (K_e) from the gradual bulk viscosity increase caused an important reduction in the flow rate (Figure 3.9). The 10 cm inflow head pressure limit prevented us from keeping the flow rate constant throughout the experiment, complicating the analysis of the results and making the injection sequences a lot more time consuming. Shear-thinning behavior can also be alleviated by low flow rates. During the design of future experimental (or field) setups using a polymer, it will be important to consider these effects to warranty that enough pressure is available at the injection well to accommodate the K_e reduction.

3.6.2 First surfactant flood (0.5% surfactant-polymer solution)

Again, the most significant data we gathered during this first surfactant flood came from direct observation of processes. Two main observations stood out from this flood : (1) viscous fingering by the surfactant-polymer solution occurred through the previously circulated polymer solution and (2) significant TCE remobilization occurred at first contact between the washing solution and the TCE pools. These processes are well illustrated by photographs taken during the flood. The cumulative TCE recovery curve (Figure 3.8) shows that TCE dissolution doubled after breakthrough of the first surfactant-polymer solution flood. The flow data (Figure 3.9) clearly shows the reduction in bulk viscosity inside the sand pack as less viscous fluid progresses towards the outflow side of the chamber, causing the observed viscous fingering.

Blue dye trapped in the inflow manometer was released in a very low concentration when the flood began. The evolution inside the chamber of this very faint pulse indicated some early fingering of the surfactant-polymer solution inside the previously circulated polymer solution. Also, TCE remobilization from pool 5 caused by the reduction of interfacial tensions by surfactants began earlier than it would have been expected with a stable front. In this case, the surfactant-polymer solution flowed faster in the high permeability medium-coarse sand towards pool 5. Viscous fingering occurs in the porous media when the displacing fluid is less viscous than the displaced fluid (Lake, 1989). This phenomenon can be expressed quantitatively by this simplified expression of the Mobility ratio (M), introduced in the enhanced oil recovery literature (Mungan, 1982) and more recently adapted for fluids with similar densities by (Martel K. E. *et al.*, 1998):

$$M = \frac{\mu_d}{\mu_D} \qquad (4)$$

where μ_d : viscosity of the displaced fluid

μ_D : viscosity of the displacing fluid

In the case where $M < 1$, the mobility ratio is said to be favorable, displacement fronts are stable and no viscous fingering occurs. This is similar to what we observed during the polymer flood, along with the shear-thinning behavior. On the other hand, when M > 1, the mobility ratio is said to be unfavorable, displacement fronts are unstable and viscous fingering occurs. In the case of this flood, no viscosity measurements were carried out prior to the experiment, since we did not expect that such a small quantity of surfactants (0.5% by weight) would have impacted the overall viscosity of the solution containing 500 mg/l of xanthan gum.

In order to investigate the causes of the observed viscous fingering, viscosity measurements were carried out after the experiment on identical solutions as well as on a higher polymer concentration solution (Figure 3.10). The results indicate that an amount

of active matter as small as 0.5% by weight in the solution significantly reduces its viscosity, and further increases in surfactant concentration do not decrease its viscosity further. Moreover, with higher surfactant concentration, overall viscosity increases in a similar manner as observed with surfactant-only solutions when the concentration of surfactant is increased (the viscosity of a 5% W2722/SAS=2/1 solution is 1.5 times higher than a 0.5% solution). Also, the shear-thinning behavior of the solution is maintained (viscosity still reduces with an increasing shear-rate), but the slopes of the curves presented in Figure 3.10 slightly decrease with the viscosity.

Polysaccharides (xanthan gum belongs to this class of bio-polymers) increase a solution viscosity by adding a more rigid structure into it, through the snagging of its long polymer chains (Lake, 1989). The shear-thinning behavior is therefore caused by the uncoiling and unsnagging of the polymer chains occuring when the solutions are exposed to high shear rates (usually greater than 1.0 s^{-1}). Chen and Sheppard (1979; 1980) recognized the lack of stability of the polysaccharide *Xantomonas Campestris* (xanthan gum) and investigated its modes of degradation. Several factors were found to cause breakup of the polymer chains and reduction of the solution viscosity. Amoung other things, they found that only a small amount of NaCl (0.5%) decreased the viscosity drastically and further increases in NaCl concentration did not decrease the viscosity further. This behavior is not unlike what was observed with the addition of surfactants into polymer solutions, and we can therefore suspect that our surfactant degrades the polymer to a certain extent, breaking up the chains and causing a drop in solution viscosity. The presence of a bactericide agent can also adversely affect polymer solution viscosity, while maintaining their shear-thinning behavior (Martel K. E. *et al.*, 1998).

Following previous studies and these measurements, the observed viscous fingering can therefore be explained by the unfavorable mobility ratio created by the less viscous washing solution pushing against the more viscous polymer solution. A bulk-scale approximate mobility ratio may be obtained by looking at the ratio of the viscosities at any given shear rate, since shear-thinning character is maintained. Using equation (4), the different mobility ratios between all the floods of this experiment are presented in Table

3.3 for comparison. It is possible to see that all surfactant-polymer floods were carried out under stable conditions, except for the first 0.5% flood.

Interfacial tensions around 6.2 mN/m were anticipated between TCE and the washing solution (originally at 27 mN/m). In a manner already observed by Conrad *et al.* (2001) during a previous experiment (using a surfactant formulation that reduced the interfacial tensions down to 9.0 mN/m), the pools drained when first contacted by the surfactant-polymer solution (Figure 3.11). The reduction of the interfacial tension and of the capillary forces responsible for TCE trapping and pooling caused this remobilization. TCE roughly followed pre-existing paths from the original migration, an indication that capillary forces continued to influence the migration. TCE did not penetrate any previously uncontaminated sand layers, with the exception of one finger in the medium-coarse sand. More importantly, no TCE entered the bottom aquitard. The two bottom pools 7a and 7b did not fill up as a result of the TCE remobilization. Rather, following the drainage of the upper pools, TCE invaded larger regions than the original path in mainly three different locations inside the sand pack (white regions in Figure 3.11 (b)): under pool 4, under pool 5, where almost a new pool was formed in the medium-coarse layer over the medium sand, and under pool 6. Also, the solubilization pattern observed during the rest of the experiment, and described in the following sections, will show that TCE in those three areas took longer to solubilize than elsewhere in the chamber, indicating high levels of saturation. Overall, with this TCE spread over a larger area, more surface became exposed to the incoming washing solution. Under these conditions, this remobilization was considered a benefit, since it had no negative impacts (no penetration in the aquitard) on the future recovery by the surfactant solutions. No mobile TCE phase formation was observed at the front of the washing solution in the regions where the sand pack was contaminated initially at a residual saturation level. This is in agreement with the onset of mobilization predictions based on the previous batch and column experiments carried out with residual TCE saturations (Robert *et al.*, 2001). IFT is still too high to reduce the residual saturation level and promote mobilization.

Again, the cumulative curve presented in Figure 3.8 shows an increase in TCE recovery following the breakthrough of the first surfactant-polymer solution. The solubilization rate (slope of the cumulative curve) doubles from 0.997 to 2.14 grams of solubilized TCE per circulated pore volume of polymer solution (which translates into average TCE concentration in the effluent increasing from 690 mg/l to 1480 mg/l).

Since viscous fingering should not alter the shear thinning behavior of the surfactant solution, the hypothesis formulated during the analysis of the polymer flood flow data still applies to this flood: the hydraulic conductivity (K) is uniform (vertically) inside the chamber. Therefore, the rise in K_e observed at the beginning of the surfactant-polymer flood, starting at 1.5 PV on figure 3.9, is from the gradual bulk viscosity decrease inside the sand pack as the less viscous washing solution progresses towards the outflow side of the chamber. The small kick observed on the K_e curve after the injection of 0.5 PV of surfactant-polymer solution could be from a sudden rise in relative permeability to water happening as a result of almost instantaneous TCE pool drainage in the middle of the chamber. The fact that K_e reaches a constant value after only 0.5 PV of solution injected is an indication of early breakthrough, an obvious consequence of the viscous fingering.

3.6.3 Second and third surfactant floods (2% and 5% surfactant-polymer solutions)

During these higher concentration surfactant-polymer floods, plugging gradually occurred at or near the inflow screen. It disturbed the experiment flow data and prevented completion of the experiment and full recovery of TCE. Direct observation of the processes, image analysis and GC data showed that no remobilization occurred with additional interfacial tension reductions and the factors controlling TCE solubilization are (in order of importance) : (1) surfactant concentration in the solution, (2) TCE saturation in the media, (3) heterogeneous stratigraphy of the sand pack and (4) disposition of the pools in relation with the flow pattern of the washing solution. The comparison between the observations and the GC data shows that a plateau reached on the cumulative TCE recovery curve does not imply that the experiment is near completion, but rather that only

TCE located within the zone swept by the washing solutions is fully recovered, and that an increase in solubilization power is needed or the flow pattern has to be changed in order to complete TCE recovery in an optimum amount of time. Only an effluent concentration of zero should be considered as a reliable proof of complete TCE removal.

Interfacial tensions around 4.8 mN/m and 3.8 mN/m were anticipated between the TCE and the 2% and 5% surfactant-polymer solutions respectively. No TCE remobilization occurred when both washing solutions encountered either pooled or residual TCE. Throughout those floods, capillary forces remained higher than buoyancy and viscous forces, and only solubilization occurred.

As predicted by the batch study results presented in Figure 3.2, surfactant concentration was the main factor controlling TCE solubilization. Indeed, the slope of the cumulative TCE recovery curve (Figure 3.8) shows that the rate of solubilization was increased 1.8 times after the breakthrough of the 2% solution, and increased another 1.7 times after the breakthrough of the 5% solution, and the last rate was maintained throughout most of the flood, although progressively less TCE was available (because of the ongoing dissolution).

Figure 3.12 illustrates the solubilization pattern during the 2% and the 5% floods. The bottom pools 7a and 7b were cut off on these images since the persistence of blue dye flowing out of the aquitard throughout the experiment perturbed the image processing. For each flood, solubilization is illustrated in a time sequence. Each color represents TCE solubilization happening during the same time interval. The solubilization pattern is given by the following color sequence: orange (earliest dissolution), yellow, green and blue (latest dissolution). The bright red color inside the pools are areas were TCE remained undissolved at the end of the illustrated flood.

Figure 3.12 (c) shows the last TCE remaining not long before the end of the experiment. These persistent zones correspond to regions where remobilized TCE accumulated following the first interfacial tension reduction. Note that original pool locations were

more readily dissolved than those more recent accumulations. Those zones are well swept in either flow patterns presented in Figure 3.4 (a : worst uniformity case, K_e variable vertically and b: best uniformity case, vertically uniform K_e). Therefore, even if the shear-thinning behavior of this flood was compromised by the low shear rates induced by low flow rates resulting from the plugging issue, poor sweep efficiency or low permeability cannot be held responsible for the persistence of TCE inside those zones (those factors are responsible for the incomplete TCE recovery from the two bottom pools, and that is discussed later). In this case, high levels of TCE saturation are believed to be responsible for the persistence of those zones (high saturation means lower surface-to-volume ratios). It is also possible to conclude that TCE saturation in original pools is not as high as TCE saturation in new accumulation zones.

The stratigraphy controlled solubilization of bottom pools 7a and 7b (not shown here). TCE present over the aquitard was not completely dissolved at the end of this experiment. The topography allowed the fine sand of the aquitard to divert the flow of the washing solutions over the pools, according to the flow behavior analyzed during the dye pulse tests, presented in Figure 3.5 .

Also, the images presented in Figure 3.12 may give the wrong impression that TCE was dissolved mainly from the top of the pools and in areas facing the incoming flow rather than from all sides in contact with washing solutions, including beneath the pools. Conrad *et al.* (2001) explained in their previous experiment that as mass is removed by washing solutions from all sides of pools, pressure equilibrium within the pools was maintained by preferentially vacating the pores along the top of the pools, where the gravity potential is lower. This can very well be the case for this experiment, since we were working at even lower interfacial tension, easing TCE downward displacement. The white arrow placed in Figure 3.12 (b) points at the outflow-facing edge of a pool or what seems to be evidence of such a downward TCE migration.

The cumulative recovery curve presented in Figure 3.8 shows a drastic drop in TCE solubilization rate after the injection of 6.3 PV (1.5 PV of polymer solution + 4.8 PV of

surfactant-polymer solution). After this time, more than 90% of the TCE was recovered (this result is based solely on visual evaluation and is given here as a qualitative information). Only TCE present over the aquitard remained in the chamber, outside of the washing solution swept zone (depicted in Figures 3.4 and 3.5). Indeed, pool 7b was still fully saturated after the injection of 8 PV of solution. At that time, the pool was 9.6 cm wide and 1.25 cm high, representing 5 grams of TCE (a conservative approximation). With the rate of solubilization at that time being 0.5 grams of solubilized TCE per circulated pore volume of polymer solution (Figure 3.8), another 10 PV of washing solution would have been necessary to remove all the TCE left in pool 7b. This is more than the total amount of washing solution injected so far for the whole experiment. It clearly illustrates that when it comes to the end of experiments, after most of the TCE is removed, there are still some crucial polishing steps to consider. Polishing steps can include flow reversals or the circulation of a higher density, better solubilizing solution, with the ability to scrub the bottom of pools (for example, a 10% active matter W2722/SAS=2/1 solution with an initial density of 1,040 kg/m^3). TCE molecular diffusion in the aquitard must also be considered. Indeed, as TCE remains for some time over an aquitard, molecular diffusion into this aquitard has to occur. Therefore, there has to be sufficient clear water circulated after a SEAR experiment to allow the reversal of diffusion effects. Basically, the monitoring of the effluent concentration should be considered as a reliable proof of complete TCE removal. Since this experiment was not completed after experiencing plugging problems, these options were not tried and the latter assumption was not verified.

During these floods, a white macroemulsion began to appear around TCE blobs and pools. This phenomena was observed and reported by other researchers using nonionic surfactants such as Witconol 2722 or Tween 80 (Fountain *et al.*, 1991; Pennell *et al.*, 1994; Okuda *et al.*, 1996, Oostrom *et al.*, 1999; Taylor *et al.*, 2001). It was also observed during the previous batch test experiments (Robert *et al.* 2001).

3.6.4 Plugging issues

Polymers were included in the experiment for a little more than 48 hours prior to the apparition of the first plugging clues. A manometer installed on the top of the chamber during the last surfactant-polymer flood showed that almost all of the pressure drop was happening at the screen and confirmed the hypothesis of plugging. A bactericide solution (500 mg/l Thymol) was flushed in the inflow manifold from top to bottom and a water back flush was performed. As a result, physical evidence of bacterial growth or polymer microgel accumulations was recovered. These actions did not entirely resolve the plugging problem.

Xanthan gum is a polysaccharide bio-polymer, which is similar to a sugar. Formation of microgels and biodegradation are two phenomena related to the use of such polymers, and are reported both in the enhanced oil recovery (EOR) and surfactant enhanced aquifer remediation (SEAR) literature. In EOR, residence time in reservoirs for polymers is often several years, temperatures are high and permeabilities are usually very low (10^{-15} to 10^{-12} m^2). Under these conditions, the use of a bactericide becomes necessary, as well as ultrafiltration to remove microgels prior to the injection of the solutions inside reservoirs (Martel K.E. *et al.,* 1998; Lake, 1989; Mungan, 1981). On the other hand, the use of a bactericide is not recommended for site remediation experiments since residence time in aquifers is short (days), temperatures are relatively low, and polymer biodegradation is considered as an important last step of the remediation sequence (Martel K. E. *et al.*, 1998). As for surfactants, a number of researchers, both in the fields of EOR and SEAR, performed several column, sand box or field experiments without ever experiencing bacterial growth or setup plugging. This confirms the hypothesis that the problem is linked to the polymer itself.

This experiment was conducted at 21 °C. At warm temperatures and using a setup designed for fine sands, it is safe to recommend preventive ultrafiltration as well as the use of a bactericide with xanthan gum to avoid such problems. Future work will include batch tests to identify possible bactericide candidates that are not too aggressive for the

environment. Walker *et al.* (1998) successfully used trace amounts of Thymol and Mercuric Chloride to prevent bacterial growth from occurring during SEAR experiments involving nonionic surfactants.

3.6.5 Density-related plume sinking

Density-related plume sinking occurs when the washing solution dissolves enough TCE that its density becomes higher than the density of the ambient groundwater (Kostarelos *et al.*, 1998; Pennell *et al.*, 1996; Oostrom *et al.*, 1992). Density-related plume sinking depends mainly on (1) the magnitude of the velocity and (2) the relative density difference between dense plume and ambient groundwater. The chamber used for this experiment did not include an ambient groundwater zone underlying the surfactant-polymer swept zone, except for a relatively thin aquitard layer within which plume sinking became hard to identify. However, effluent density measurements show a marked increase in the bulk density of the aqueous solution as more TCE dissolution occurs (Appendix C-3). Densities at the peak of the solubilization process (after 6 PV injected) approach the values identified by Oostrom *et al.* (1999) for which sinking occurred (1,003.9 for this experiment vs. 1,004.5 kg/m^3 for Oostrom *et al.*). In this experiment, the injection rates were much lower and flow interruptions were included, thus further promoting sinking. Therefore, there is evidence pointing to the possibility of aqueous phase plume sinking in larger-scale experiments. In the field, this problem could be remediated by the design of extraction well deeper than injection wells, or special injection/pumping strategies.

3.7 CONCLUSIONS AND RECOMMENDATIONS

A TCE-solubilization experiment was carried out under field-like conditions (inter-well fluid circulation, heterogeneous media with bottom aquitard, TCE present both at residual saturation and in pools) using a surfactant-polymer washing solution. The process was optimized with the use of a washing solution formulation benefiting from extensive

characterization and optimization, and with the addition of a shear-thinning polymer. Significant discoveries with implications for field-applicability (or larger-scale laboratory experiments) of such remediation experiments were made.

The original intent of the polymer flush was to push TCE out of pools using the viscous forces provided by the shear-thinning polymer. The following observations were made:

- The effects of varying layer permeability inside the sand pack were greatly reduced by the shear-thinning polymer;
- Enhanced viscous forces did produce some TCE mobilization, but not enough to have a significant impact on TCE distribution;
- Adding a polymer increases the contact between TCE and the aqueous phase leading to a significant increase in solubilization;
- Better flow uniformity translates into better sweep efficiency and significant cost reductions;
- Polymers could be used alone to provide a very low risk method of improving pump and treat, or they could be used together with surfactants to improve the performance of surfactant flooding.

A first low-active matter surfactant-polymer flood was used for limiting TCE remobilization following interfacial tension reduction:

- Interactions between surfactant and polymer molecules were not anticipated, and the viscosity of surfactant-polymer solutions was lower than expected, leading to viscous fingering inside the chamber;
- However, surfactant-polymer solutions have a similar shear-thinning behavior as polymer solutions, but the viscosity variation is attenuated;
- Pooled TCE was remobilized following the reduction of the interfacial tensions and capillary forces. The remobilization was not damaging, and more TCE became exposed to incoming washing solutions. No free TCE phase formation was observed at the front of the washing solution in the regions where the sand pack was

contaminated initially at a residual saturation level. This is in agreement with the onset of mobilization predictions based on the previous batch and column experiments carried out with residual TCE saturations;

- The TCE solubilization rate doubled after the breakthrough of the surfactant-polymer solution;
- The mechanisms responsible for the viscosity reduction of the surfactant-polymer solutions were quantified to facilitate better planning of future experiments.

Higher concentration surfactant-polymer floods were then circulated inside the chamber to accelerate TCE solubilization :

- Plugging gradually occurred at or near the inflow screen. It disturbed the experiment flow data and prevented completion of the experiment and full recovery of TCE;
- No remobilization occurred with additional interfacial tension reductions, thus confirming the effectiveness of a gradient approach;
- The factors controlling TCE solubilization are (in order of importance) : (1) active matter concentration in the surfactant-polymer solution, (2) TCE saturation in the media, (3) heterogeneous stratigraphy of the sand pack and (4) disposition of the pools in relation to the flow pattern of the washing solution;
- A plateau reached on the cumulative TCE recovery curve does not imply that the experiment is near completion, but rather that crucial polishing steps are to be undertaken (increase in solubilization power and solution density, change in the flow pattern). The monitoring of the effluent concentration should be considered as a reliable proof of complete TCE removal.

Densities at the peak of the solubilization process provided evidence pointing to the possibility of aqueous phase plume sinking in larger-scale experiments. This problem could be mitigated by the design of extraction wells deeper than injection wells or by using appropriate injection/pumping sequences.

3.8 ACKNOWLEDGEMENTS

The author wishes to thank Uta Gabriel and William J. Peplinski for much appreciated guidance and technical support. Laboratory characterization experiments were done at the Hydrogeology Laboratory at the Quebec Geoscience Center, and at the Geology and Geological Engineering Department at Laval University, with the support of NSERC and FCAR research grants. The 2D chamber experiment was done at Sandia National Laboratories, Albuquerque, New Mexico, with support from the Environmental Management Science Program, US Department of Energy.

Table 3.1 – Limiting factors in the recovery of TCE through solubilization with micellar solutions

Limiting factor	Description of the problem	*References*	Options to overcome the limits	*References*
1. TCE remobilization	- Best solubilization is achieved with high active matter concentrations, which reduces interfacial tensions (IFT) and capillary forces, responsible for TCE trapping; - Capillary forces are overcome by buoyancy and viscous forces; - A dense, free organic phase forms and migrates downward, with the risk of penetrating uncontaminated layers or bottom aquitards.	-St-Pierre, 2001; -Conrad *et al.*, 2001; -Ramsburg and Pennel, 2001; -Taylor *et al.*, 2001; -Sabatini *et al.*, 2000; -Boving and Brusseau, 2000; -Pennell *et al.*, 1996,1994.	- Select best solubilizing system generating the least IFT reduction (from phase diagrams, batch tests, column and sand box experiments) - Limit the amount of active matter - Use the Capillary and Bond number approach (for cases where TCE is at residual saturation) to take into account buoyancy and viscous forces, and aim to work at the corresponding optimal interfacial tension. - Use an active-matter gradient approach	-This research; -St-Pierre, 2001; -Martel *et al.*, 1993; -Pennell *et al.*, 1996; -Sabatini *et al.*, 2000.
2. Dense plume sinking	- The washing solution solubilizes dense TCE; - The aqueous phase becomes denser than the surrounding water; - It sinks beyond the influence zone of extracting wells and into uncontaminated layers or bottom aquitard.	-Taylor *et al.*, 2001; -Oostrom *et al.*, 1999; -Kostarelos *et al.*, 1998; -Istok and Humphrey, 1995.	- Limit the amount of active matter - Include a light alcohol in the solution which does not partition into the organic phase and swells it (causing mobilization) - Use high flow rates - Tighten well spacing	-This research; -Taylor *et al.*, 2001.
3. Heterogeneities and layer topography in the sub-surface	- Finer sand lens or impermeable layers (clay, compact till) causes pooling of the TCE (point #4); - Washing solutions flow preferencially through high permeability zones, and by-passes low permeability zones; - Topography of an aquitard diverts the flow of the washing solutions over pools located in dips.	-Conrad *et al.*, 2001; -Fountain *et al.*, 1991, 1996.	- Include a shear-thinning polymer in the washing solution to reduce the effects of heterogeneities.	-Zhong *et al.*, 2001; -Dwarakanath *et al.*, 1999; -Martel K.E. *et al.*, 1998.
4. Pools of TCE	- Low exposition to incoming washing solutions (low surface-to-volume ratio, and usually small vertical cross-section: pools lay mostly horizontally - Conditions favoring remobilization are hard to predict (variable height across one pool, variable IFT reduction when encountering washing solutions, variable pore sizes between sand layers)	-Conrad *et al.*, 2001; -Pankow and Cherry 1996.	- Use an active-matter gradient approach; - Use enhanced viscous forces to promote TCE remobilization (and spreading) without reduction of IFT, by adding a polymer to the washing solution.	-Sabatini *et al.*, 2000; -This research.
5. Rate-limited solubilization	- TCE dissolution depends on time in stagnant conditions, and depends on flow velocity during flooding.	-Taylor *et al.*, 2001; -Pennell *et al.*, 1994.	- Include flow interruption periods during flooding.	-Taylor *et al.*, 2001.
6. Costs	- Micellar solutions are expensive and TCE solubilization is not the most efficient means time-wise and volume-wise to recover TCE (compared with mobilization).		- All of the above points aim to optimise the efficiency of the recovery, therefore should significantly lower the cost of a project. - Recycle active ingredients during floods.	 -Lee *et al.*, 2001.

Table 3.2 - Sand properties

Sand Type	n^a	k^b	$d_{50}{}^c$
	%	m^2	mm
Coarse	34.8	6.32×10^{-10}	1.10
Medium-coarse	34.8	2.55×10^{-10}	0.71
Medium	35.4	1.20×10^{-10}	0.53
Fine	36.2	2.97×10^{-11}	0.26
Ottawa (C-109)	33.0	1.73×10^{-11}	0.33

[a] Porosity; [b] Intrinsic permeability; [c] Mean diameter of grains

Table 3.3 - Mobility ratios throughout the experiment

Flood	μ_d [a] mPa*s	μ_D [b] mPa*s	M [c]	Remarks[e]
Preflush	1	43.53	0.02	Very favorable
0.5% a.m.[d]	43.53	16.42	2.65	Very unfavorable
2% a.m.	16.42	18.46	0.89	Favorable
5% a.m.	18.46	19.64	0.94	Favorable

[a] Viscosity of the displaced fluid; [b] Viscosity of the displacing fluid; [c] Mobility ratio obtained from equation (4); [d] Percentage by mass of active matter (W2722/SAS = 2/1) in water; [e] M values were compared with similar ratios obtained by K. E. Martel *et al.* (1998).

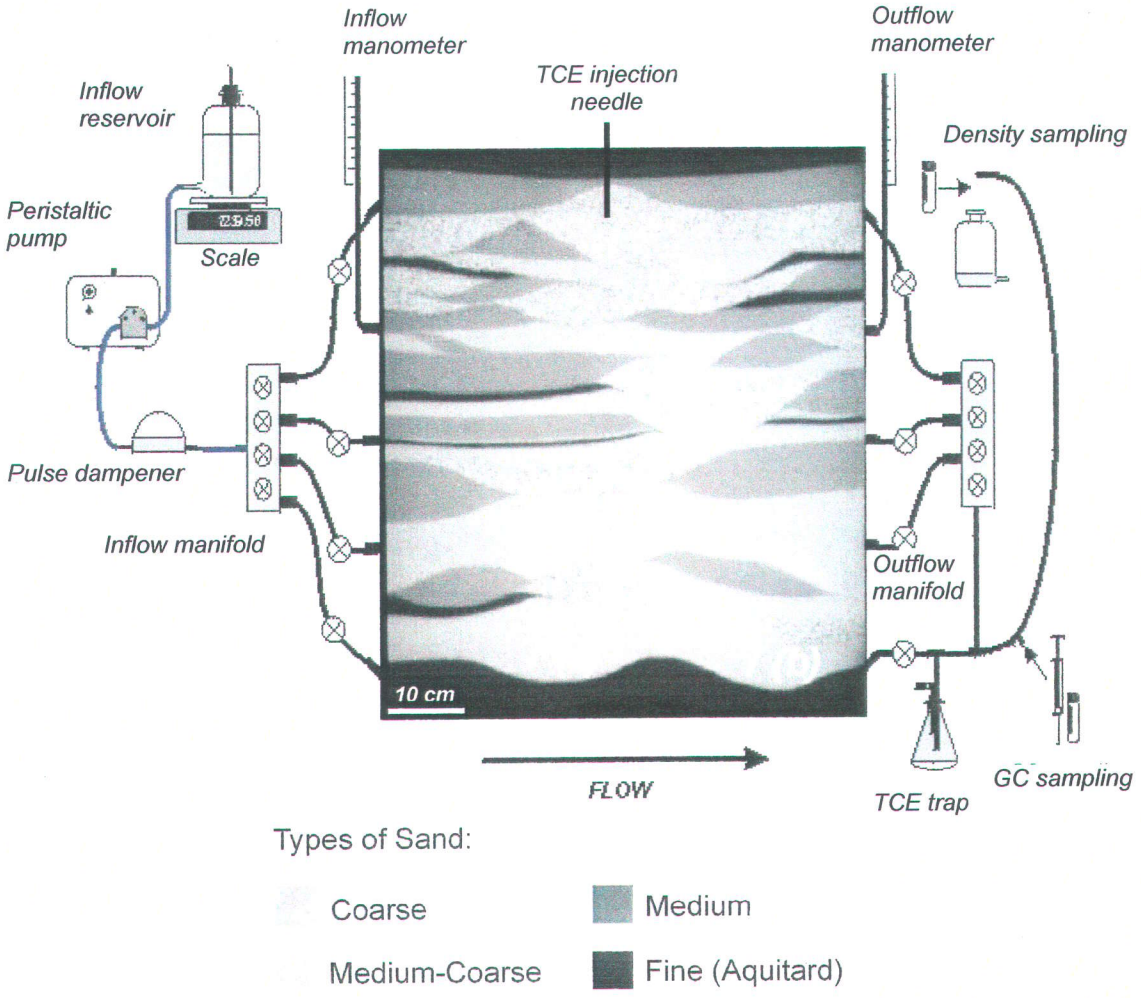

FIGURE 3.1 - Chamber Setup. Numbers indicate locations of pools.

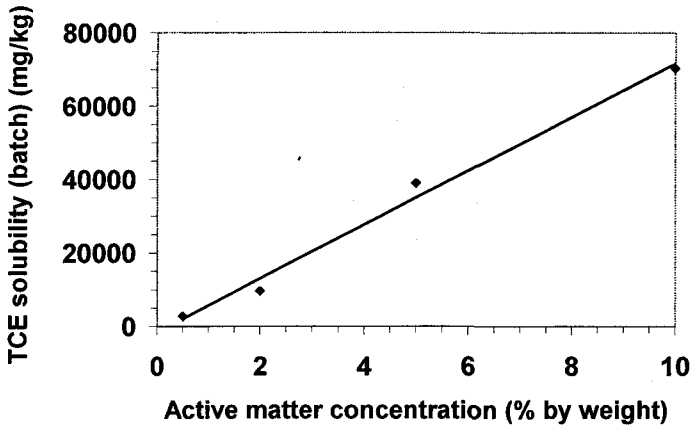

(a)

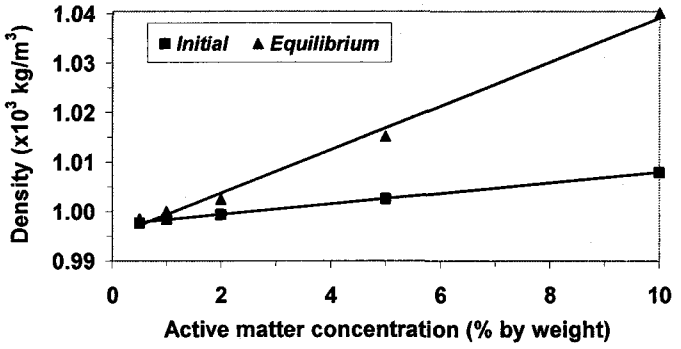

(b)

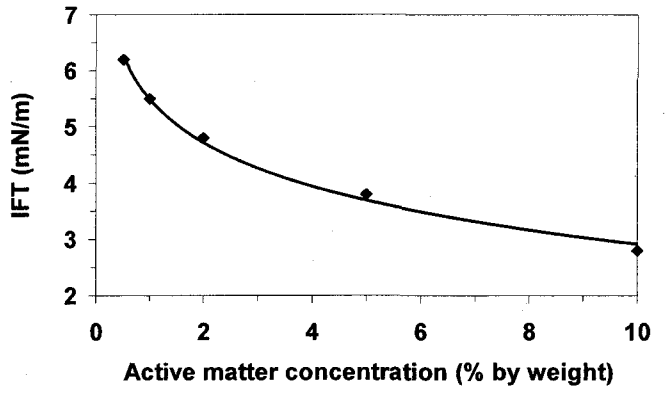

(c)

FIGURE 3.2 - Micellar-polymer solution properties (W2722/SAS = 2/1; Xanthan Gum 500 mg/l).

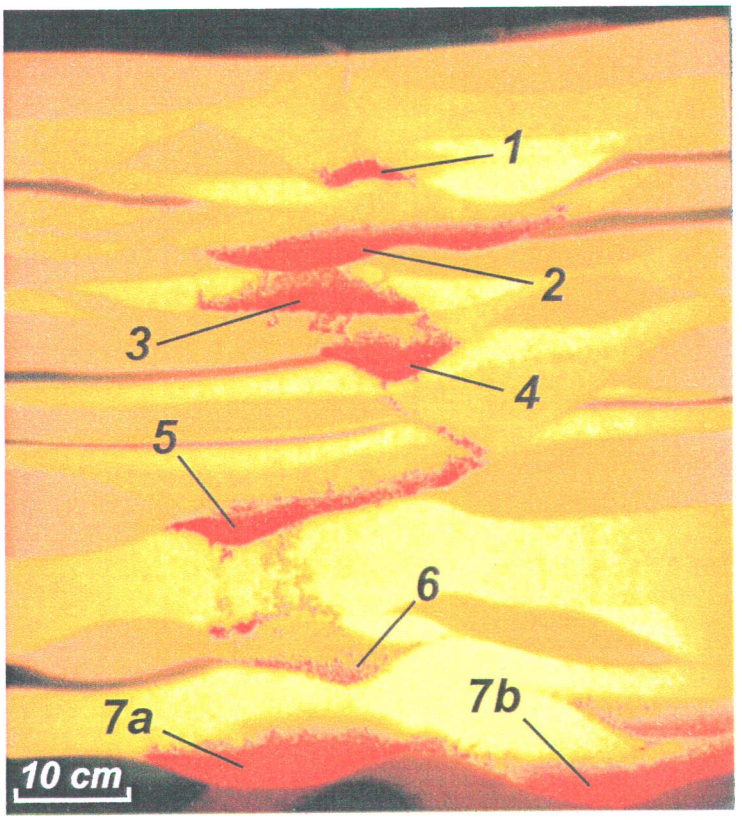

FIGURE 3.3 - Initial TCE distribution prior to flooding. Pool numbers are indicated.

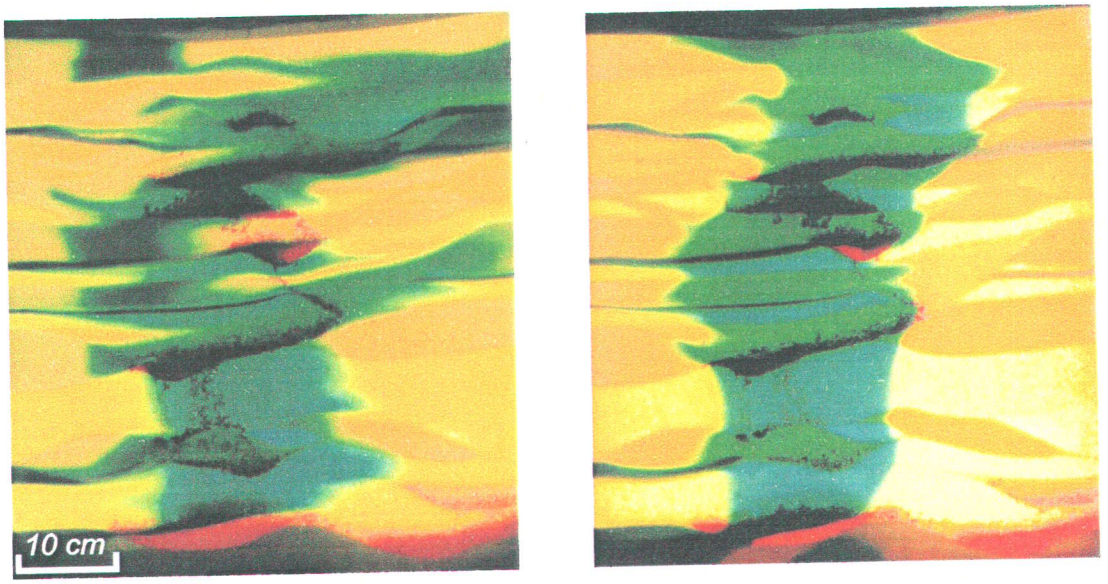

FIGURE 3.4 – Blue dye pulses. (a) Behavior of dyed water pulse. (b) Behavior of dyed polymer solution pulse. Flow is from left to right. Pictures taken after approximately 0.3 pore volumes of dye solution is injected and followed by another 0.3 PV of water for (a) or polymer solution for (b).

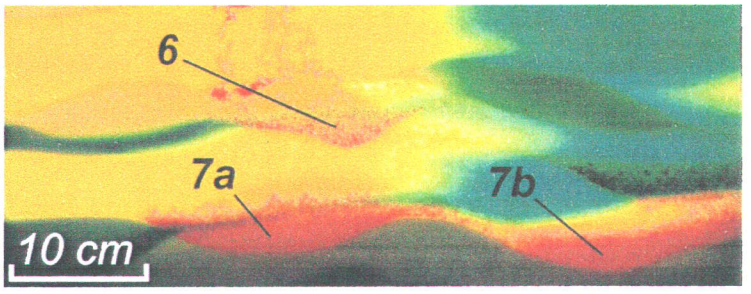

(a)

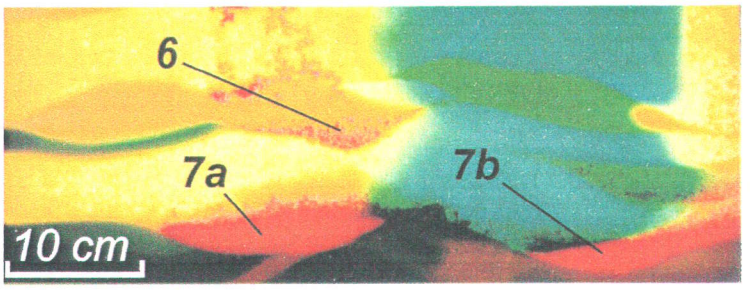

(b)

FIGURE 3.5 - Sweeping of the aquitard by (a) water solution and (b) Polymer-water solution.

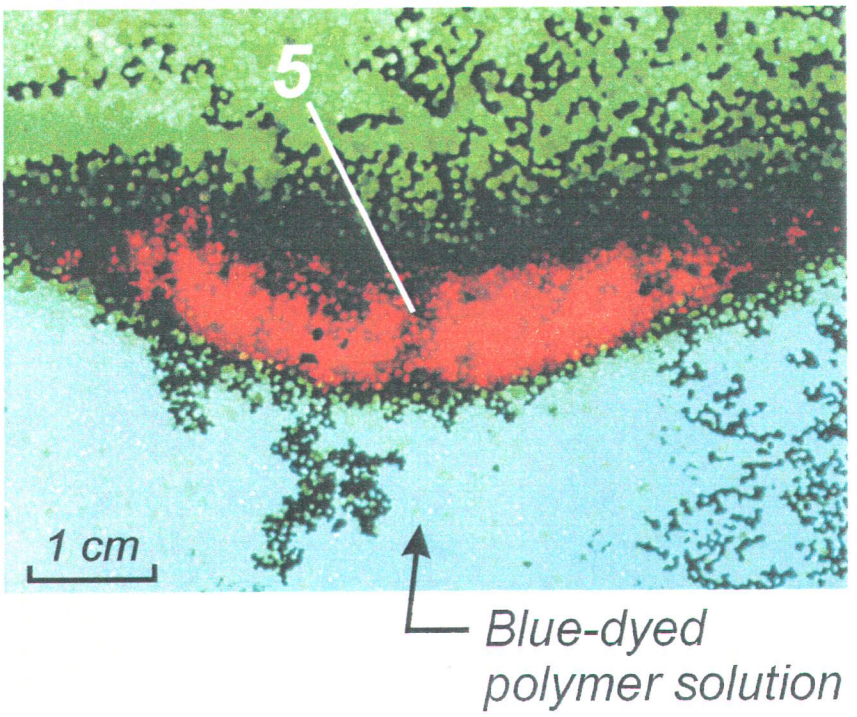

FIGURE 3.6 – Incomplete sweeping of high saturation pool 5 with the blue-dyed polymer solution.

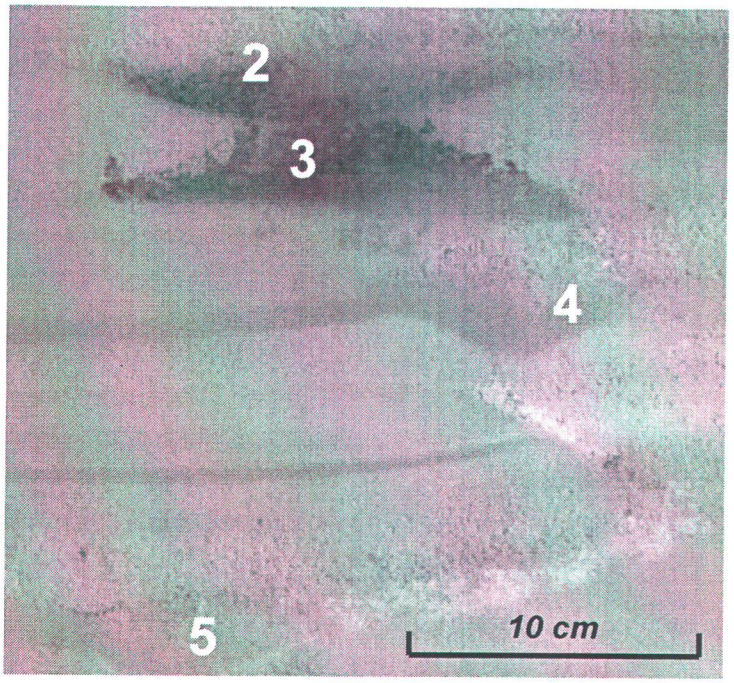

FIGURE 3.7 - Coupled effects of enhanced dissolution and TCE remobilization under increased viscous forces. Dark regions show where the light intensity has increased, indicating locations from where the TCE has migrated (pools 2 and 3). White regions show where the light intensity has decreased, indicating regions to where the TCE has migrated (between pools 4 and 5).

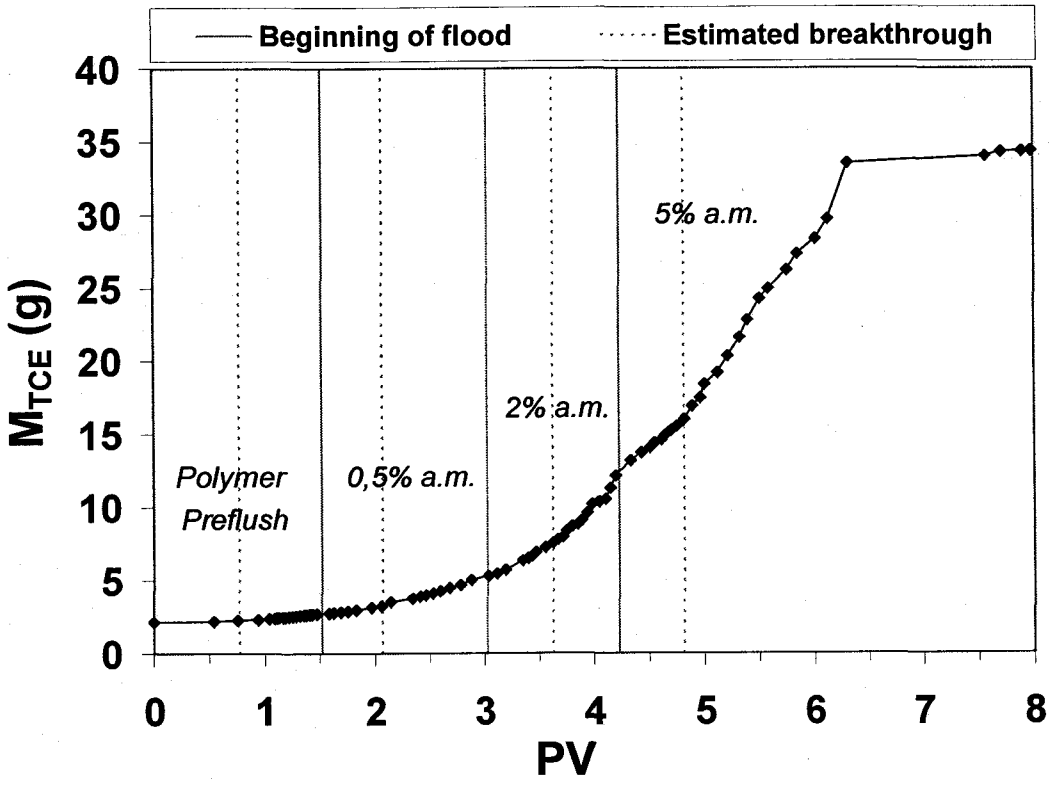

FIGURE 3.8 - Cumulative mass of TCE recovered.

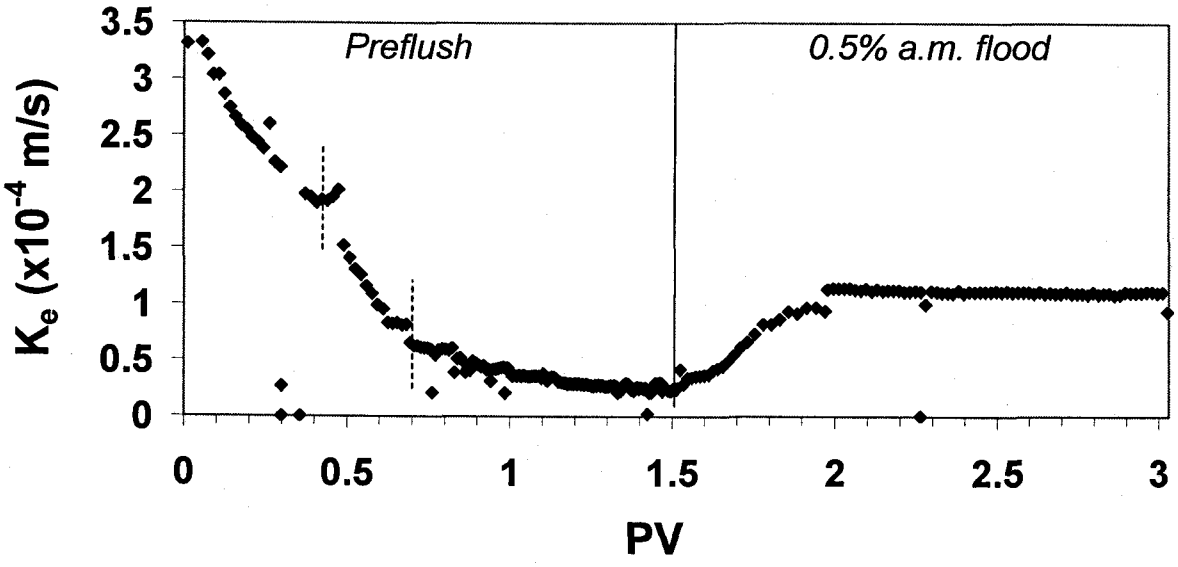

FIGURE 3.9 - Effective hydraulic conductivity (K_e) variation during the first two floods. The dashed lines show the interval when the washing solution first contacted TCE.

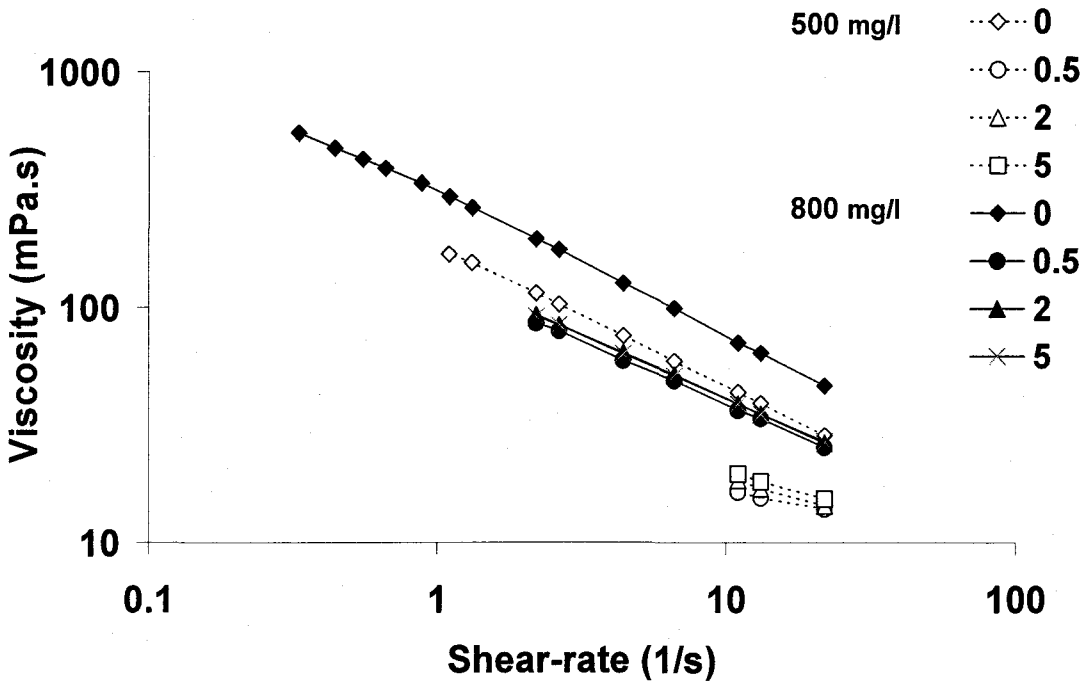

FIGURE 3.10 - Viscosity as a function of shear-rates of 800 mg/l and 500 mg/l of xanthan gum solutions containing either 0, 0.5, 2 or 5 % (by weight) of active matter (W2722/SAS=2/1).

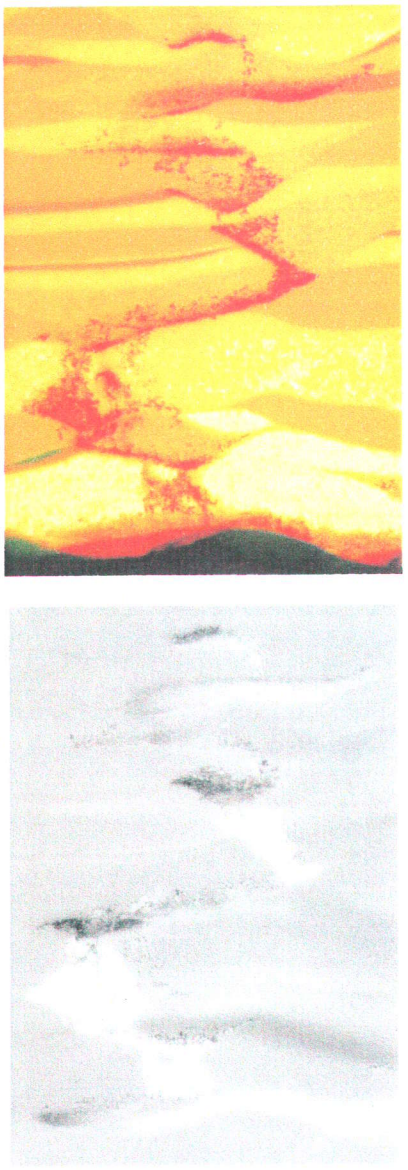

FIGURE 3.11 - TCE remobilization – final state (after the injection of 1.51PV of 0.5% surfactant solution). The picture is presented along with a difference image (movement of dye is perturbing the image).

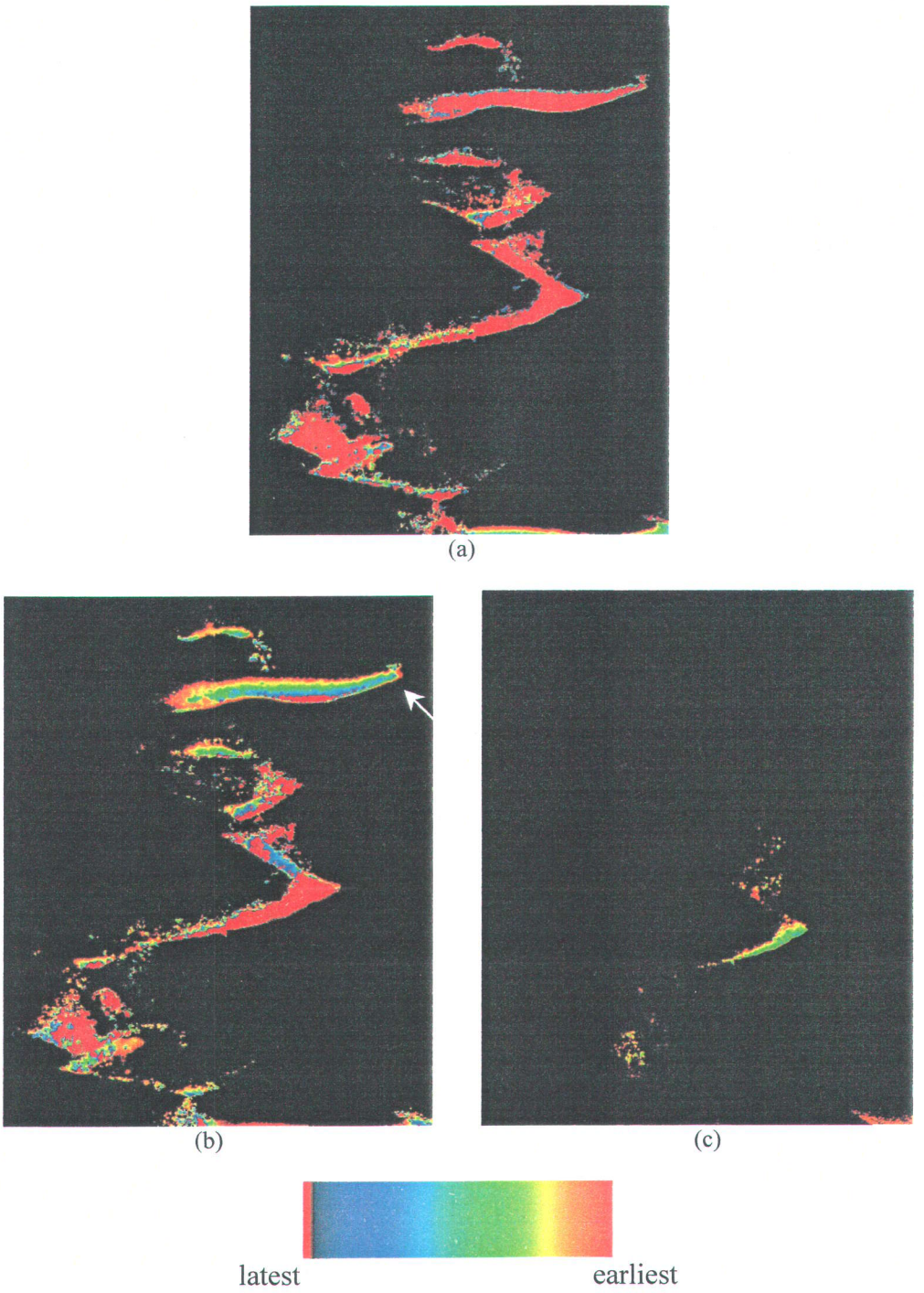

FIGURE 3.12 - Solubilization pattern. (a) 2% active matter flood (1.2 PV injected). (b) 5% active matter flood, prior to unplugging attempts and prolonged flow interruption (0.4 PV injected). (c) Final 5% active matter flood (3 PV).

CHAPITRE 4

CONCLUSION GÉNÉRALE ET RECOMMENDATIONS

Des travaux déjà entrepris sur la récupération de TCE par lavage de sol avec des solutions tensioactives ont été poursuivis dans le but d'élaborer un procédé de lavage de sol aux solutions tensioactives qui soit applicable à d'éventuels cas de terrain. Dans un premier temps, la compréhension des mécanismes de récupération du TCE, observés lors de la réalisation de diagrammes de phase et d'essais en colonne de sable, a été approfondie par la réalisation de mesures complémentaires. La mesure des tensions interfaciales, des angles de contact, des densités et des viscosités sur des mélanges préparés en vrac, dont la composition se rapprochait de celle des fluides retrouvés à l'intérieur des colonnes de sable lors des expériences antérieures, a permis de mieux caractériser les mécanismes de solubilisation et de mobilisation du TCE. Pour les systèmes mobilisants, il a été démontré entre autres choses que c'est le gonflement de la phase organique qui est le facteur responsable de la récupération du TCE, et que ce gonflement dépend de la nature et de la concentration des tensioactifs employés. De plus, pour les systèmes solubilisants, il a été démontré que la remobilisation du TCE en phase libre, qui doit être évitée, n'est pas seulement liée à la réduction des tensions interfaciales, mais aussi à d'autres facteurs tels que la viscosité des solutions de lavage et les débits d'écoulement. Aussi, l'approche des nombres capillaire et de Bond a permis d'identifier des combinaisons de conditions causant la remobilisation du TCE. Des problèmes liés à l'augmentation de la densité des solutions lors de la solubilisation du TCE ont été anticipés pour de futures applications avec un écoulement horizontal des solutions de lavage.

Un procédé de récupération du TCE par solubilisation dans un milieu hétérogène, à l'intérieur duquel le TCE se retrouvait autant à saturation résiduelle que dans des accumulations locales, a ensuite été développé puis testé en laboratoire. L'expérience a été réalisée dans un bac de sable 2D hétérogène en collaboration avec le laboratoire de visualisation d'hydrogéologie des Laboratoires Sandia (Nouveau-Mexique). La visualisation des procédés s'est avérée être la source d'information la plus révélatrice liée à l'utilisation combinée des polymères et des tensioactifs. L'utilisation d'un polymère rhéofluidifiant a favorisé le balayage des couches de plus faible perméabilité, uniformisant le front d'écoulement des solutions. C'est le premier contact entre la solution tensioactive et les accumulations locales de TCE, et la réduction des tensions interfaciales résultante, qui a causé la totalité de la remobilisation du TCE. Cependant, comme il avait été prévu que les tensions interfaciales ne seraient pas ultra basses à cet instant, la remobilisation n'a pas eu d'effets néfastes.. Les facteurs contrôlant la solubilisation du TCE ont également été observés, le plus important étant la concentration en matière active dans la solution de lavage. L'importance d'appliquer un gradient de concentration en matière active a été ainsi démontré. L'expérience a mis en évidence la pertinence de bien planifier les dernières étapes de la séquence de lavage des sols, afin d'assurer le nettoyage complet des zones contaminées.

Le procédé de récupération du TCE présenté dans le chapitre 3 doit être optimisé. Comme le pré-lavage n'a pas permis de remobiliser les accumulations locales de TCE, cette étape pourrait être mise de coté, si les problèmes d'adsorption des tensioactifs dans le milieu poreux ne sont pas envisagés. Ensuite, le gradient de concentration pourrait se faire en trois étapes : (1) un premier lavage avec une très faible concentration en tensioactif pour drainer les accumulations tout en maintenant des forces capillaires capables d'influencer de façon significative la remobilisation du TCE, (2) un deuxième lavage avec une concentration importante en tensioactif qui assurerait le plus gros de la solubilisation du TCE, et (3) un lavage final avec une solution lourde très riche en tensioactif, qui permettrait de laver en profondeurs le peu de TCE présent dans le fond des anciennes accumulations locales. Une stratégie d'injection et de pompage doit être développée pour

permettre la récupération de cette solution. Les problèmes de colmatage des installations et de croissance bactériologique à l'intérieur du milieu poreux doivent également être corrigés par l'utilisation d'un bactéricide.

Lors d'un second essais en bac de sable, il serait également très important de prendre toutes les mesures nécessaires à l'établissement d'un bilan de masse, ce qui permettrait la quantification du processus de solubilisation.

LISTE DES RÉFÉRENCES

Baran, J.R., Pope, G.A., Wade, W.H. and Weerasooriya, V., 1994. Phase behavior of water/perchloroethylene/anionic surfactant systems. *Langmuir*, 10, p. 1146-1150.

Boving, T.B. and Brusseau, M.L., 2000. Solubilization and removal of residual trichloroethene from porous media: comparison of several solubilization agents. *Journal of Contaminant Hydrology*, 42 (1), p. 51-67.

Brandes, D. and Farley, K.J., 1993. Importance of phase behavior on the removal of residual DNAPLs from porous media by alcohol flooding. *Water Environment Research*, 65 (7), p. 869-878.

Chen, C.S.H. and Sheppard, E.W., 1979. Conformation and hydrolytic stability of polysaccharide from Xanthomonas campestris. *Journal of Micromolecular science and chemistry*, A13 (2), p. 239-259.

Chen, C.S.H. and Sheppard, E.W., 1980. Conformation and shear stability of xanthan gum in solution. *Polymer Engineering and science*, Mid-May, 20 (7), p. 512-516.

Cohen, R.M. and Mercer, J.W., 1993. DNAPL Site Evaluation. C.K. Smoley, CRC Press, Boca Raton, Florida, 225 pages.

Conrad, S.H., Glass, H.C. and Peplinski, W.J., 2001. Bench-scale visualization of DNAPL remediation processes in analog heterogeneous aquifers: Surfactant floods, and in situ oxidation using permanganate. *Journal of Contaminant Hydrology*, submitted.

Dwarakanath, V., Kostarelos, K., Pope, G.A., Shotts, D. and Wade, W.H., 1999. Anionic surfactant remediation of soil columns contaminated by nonaqueous phase liquids. *Journal of Contaminant Hydrology*, 38, p. 465-488.

Falta, R.W., 1998. Using phase diagrams to predict the performance of cosolvent floods for NAPL remediation. *Ground Water Monitoring and Remediation*, 19 (3), p. 1-9.

Farley, K.J., Falta, R.W., Brandes, D., Milazzo, J.T. and Brame, S.E., 1993. Remediation of hydrocarbon-contaminated groundwater by alcohol flooding. Final report, Submitted to Hazardous Waste Management Research Fund, 148 pages.

Fountain, J.C., Klimek, A., Beikirch, M.G. and Middleton, M., 1991. The use of surfactants for in-situ extraction of organic polluants from a contaminated aquifer. *Journal of Hazardous Materials*, 28, p. 295-311.

Fountain, J.C., Starr, R.C., Middleton, T., Beikirch, M.G., Taylor, C. and Hodge, D., 1996. A controlled field test of surfactant-enhenced aquifer remediation. *Ground Water*, 34 (35), p. 910-916.

Gabriel, U., Robert, T., Lefebvre R., and Martel R., 2001. TCE recovery mechanisms with alcohol and surfactants solutions in sand columns. *Proceedings, 54rd Canadian Geotechnical Conference*, Geotechnical Group of Montreal, Canadian Geotechnical Society.

Glass, R.J., Conrad, S.H. and Peplinski, W.J., 2000. Gravity-destabilized nonwetting phase invasion in macroheterogeneous porous media: Experimental observations of invasion dynamics and scale analysis. *Water Resources Research*, 36 (11), p.121-3137.

Istok, J.D., and Humphrey, M.D., 1995. Laboratory investigation of buoyancy-induced flow (plume sinking) during two-well tracer tests. *Ground Water*, 33 (4), p. 597-604.

Knox, R.C., Sabatini, D.A., Harwell, J.H., Brown, R.E., West, C.C., Blaha, F. and Griffith, C., 1997. Surfactant remediation field demonstration using a vertical circulation well. *Ground Water*, 35 (6), p. 948-953.

Kostarelos, K., G.A. Pope, B.A. Rouse, and G.M. Shook, 1998. A new concept: the use of neutrally-buoyant micro-emulsions for DNAPL remediation. *Journal of Contaminant Hydrology*, 34, p. 383-397.

Lake, L. W., 1989. Enhanced Oil Recovery. Prentice Hall, Englewood Cliffs, N.J., 550 pages.

Lee, D.-H., Cody, R.D. and Hoyle, B.L., 2001. Laboratory evaluation of the use of surfactants for ground water remediation and the potential for recycling them. *Ground Water Monitoring and Remediation,* Winter 2001, p. 49-57.

Lunn, S.R.D. and Kueper, B.H., 1999a. Risk reduction during chemical flooding: Preconditioning DNAPL density in situ prior to recovery by miscible displacement. *Environmental Science and Technology*, 33 (10), p. 1703-1708.

Lunn, S.R.D. and Kueper, B.H., 1999b, Manipulation of density and viscosity for the optimization of DNAPL recovery by alcohol flooding. *Journal of Contaminant Hydrology*, 38 (4), p. 427-445.

Mackay, D.M., Roberts, P.V. and Cherry, J.A., 1989. Transport of organic contaminants in groundwater – distribution and fate of chemicals in sand and gravel aquifers. *Environmental Science and Technology*, 19 (5), p. 384-392.

Martel, R., Gélinas, P.J., Desnoyers, J.E., and Masson, A., 1993. Phase diagrams to optimize surfactant solutions for oil and DNAPL recovery in aquifers. *Ground Water*, 31, p. 789-800.

Martel, R., Gélinas, P.J. and Desnoyers, J.E., 1998a. Aquifer washing by micellar solutions: 1-Optimization of alcohol–surfactant–solvent solutions. *Journal Of Contaminant Hydrology*, 29, p. 319-346.

Martel, R., Lefebvre, R., Gélinas, P.J., 1998b. Aquifer washing by micellar solutions : 2-DNAPL recovery mechanisms for an optimized alcohol/surfactant/solvent solution. *Journal of Contaminant Hydrology*, 30, p. 1-31.

Martel, R., Gélinas, P.J. and Saumure, L., 1998c. Aquifer washing by micellar solutions: 3-Field test at the Thouin sand pit (L'Assomption, Québec, Canada). *Journal of Contaminant Hydrology* 30, p. 33-48.

Martel, K. E., Martel, R., Lefebvre, R. and Gélinas, P. J., 1998. Laboratory study of solutions used for mobility control during in situ NAPL recovery. *Ground Water Monitoring and Remediation,* Summer 1998, p. 103-113.

Mercer, J.W., and Cohen, R.M., 1990. A review of immiscible fluids in the subsurface: properties, models, characterization and remediation. *Journal of Contaminant Hydrology*, 6, p. 107-163.

Mungan, N., 1982. Enhenced oil recovery using water as a driving fluid, part 8 – Application of polymer solutions to improve waterflooding. *World Oil*, February 1, p. 95-106.

Okuda, I., McBride, J.F., Gleyzer, S.N. and Miller, C.T., 1996. Physicochemical transport processes affecting the removal of residual DNAPL by nonionic surfactant solutions. *Environmental Science and Technology*, 30, p. 1852-1860.

Oostrom, M., Dane, J. H., Gueven, O., and Hayworth, J.S., 1992. Experimental investigation of dense solute plumes in an unconfined aquifer model. *Water Resources Research*, 28 (9), p. 2315-2326.

Oostrom, M., Hofstee, C., Walker, R.C. and Dane, J.H., 1999. Movement and remediation of trichloroethylene in a saturated, heterogeneous porous medium - 2. Pump and treat surfactant flushing. *Journal Of Contaminant Hydrology*, 37, p. 179-197.

Pankow, J.F. and Cherry, J.A., 1996. Dense chlorinated solvents and other DNAPLs in ground water. Waterloo Press, Portland, Or., 522 pages.

Pennell, K.D., Jin, M., Abriola, L.M. and Pope G.A., 1994. Surfactant enhanced remediation of soil columns contaminated by residuel tetrachloroethylene. *Journal of Contaminant Hydrology*, 16, p. 35-53.

Pennell, K.D., Pope, G.A., and Abriola, L.W., 1996. Influence of Viscous and Buoyancy Forces on the mobilization of residual tetrachlorethylene during surfactant flooding. *Environmental Science and Technology,* 30 (4), p. 1328-1335.

Pope, G. A., and Wade, W. H., 1995. Lessons from enhenced oil recovery research for surfactant-enhanced aquifer remediation, *Surfactant-Enhanced Subsurface Remediation - Emerging Technologies*: Washington, DC, American Chemical Society, p. 142-160.

Quirion, F., and Desnoyer, J.E., 1984, Effects of alcohols and surfactants on the lowering of the interfacial tension between water and benzene: a correlation with phase diagrams. *AOSTRA Journal of Research*, 1 (2), p. 121-126.

Ramsburg, A.C. and Pennell, K.D., Experimental and economic assessment of two surfactant formulations for source-zone remediation at a former dry cleaning facility. *Ground Water Monitoring and Remediation*, Fall 2001, p. 68-82.

Robert, T., U. Gabriel, R. Lefebvre, and Martel, R., 2001. TCE Recovery during in situ flushing: Experimental study of the controlling Parameters. *Proceedings, 54rd Canadian Geotechnical Conference*. Geotechnical Group of Montreal, Canadian Geotechnical Society.

Roeder, E., Falta, R.W., Lee, C.M., and Coates, J.T., 2001. DNAPL to LNAPL transitions during horizontal co-solvent flooding. *Ground Water Monitoring and Remediation*, Winter, p. 77-88.

Sabatini, D. A., Knox, R. C., Harwell, J. H., Soerens, T., Chen, L., Brown, R.E. and West, C.C., 1997. Design of a surfactant remediation field demonstration based on laboratory and modeling studies: *Ground Water*, 35 (6), p. 954-963.

Sabatini, D.A., Knox, R.C., Harwell, J.H., and Wu, B., 2000. Integrated design of surfactant enhanced DNAPL remediation: efficient supersolubilization and gradiant systems. *Journal of Contaminant Hydrology*, 45, p. 99-121.

Shiau, B.-J., Sabatini, D. A., Harwell, J. H. and Vu, D.Q., 1996. Microemulsion of mixed chlorinated solvents using food grade (edible) surfactants. *Environmental Science and Technology*, 30 (1), p. 97-103

Shiau, B.-J., Sabatini, D. A., and Harwell, J. H., 1994. Solubilization and Microemulsification of chlorinated solvents using direct food additive (edible) surfactants. *Ground Water*, 32 (4), p. 561-569.

St-Pierre, C., 2001. Étude en laboratoire des mécanismes de récupération du trichloroéthène (TCE) en phase résiduelle lors de l'injection de solutions micellaires dans des sables, *Mémoire de maîtrise*: Université du Québec - INRS Géoressources, 80 pages.

Taylor, T.P., Pennell, K.D., Abriola, L.M. and Dane, J.H., 2001. Surfactant enhanced recovery of tetrachloroethylene from a porous medium containing low permeability lenses - 1. Experimental studies. *Journal of Contaminant Hydrology*, 48, p. 325-350.

Walker, R.C., Hofstee, C. Dane, J.H. and Hill, W.E., 1998. Surfactant enhanced removal of PCE in a nominally two-dimensional, saturated, stratified porous medium. *Journal of Contaminant Hydrology*, 34, p. 17-30.

Zhong, L. and Mayer, A., 2001. Visualization of surfactant-enhanced nonaqueous phase liquid mobilization and solubilization in a two-dimensional micromodel. *Water Resource Research*, 37 (3), p. 523-537.

APPENDICE A

Mesures complémentaires : Résultats expérimentaux

EtOH; initial 20% active matter

Ratio	
W	0,4451
TCE	0,4461
A.M.	0,10881

Density	g/cm3
Aqueous phase:	0,9719
Organic phase:	1,4549

Mea. Tem.: 10 deg. Celcius
Comments:

IFT (av.):	**13,58**	dynes/cm
DV max:	2,123	ul
IFT (DV max):	13,7	dynes/cm

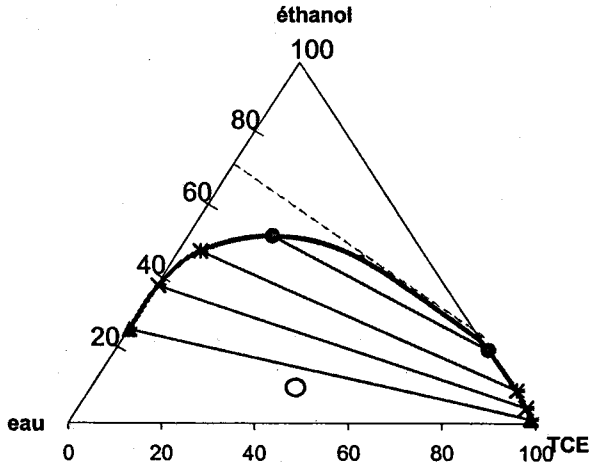

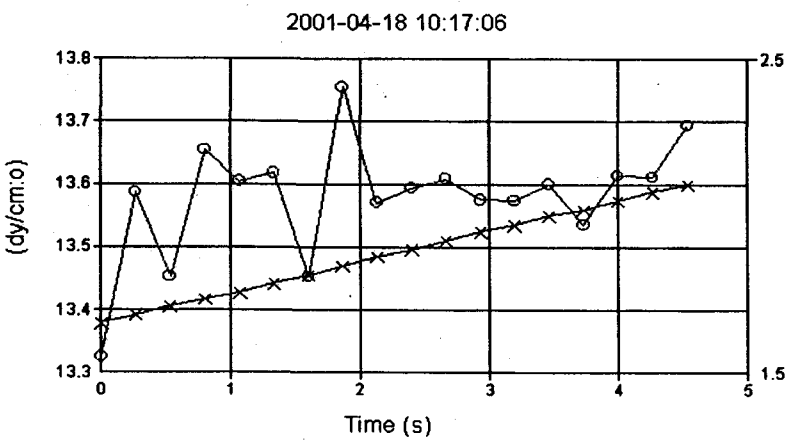

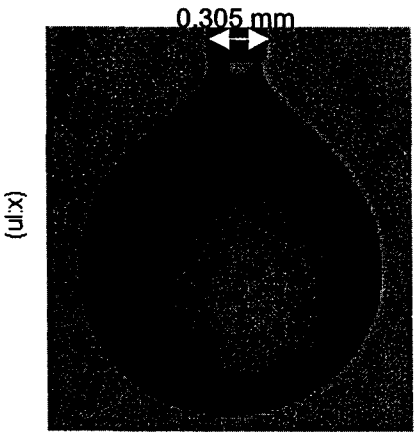

EtOH; initial 50% active matter

Ratio	
W	0,33
TCE	0,3301
A.M.	0,3399

Density	g/cm3
Aqueous phase:	0,9359
Organic phase:	1,3596

Mea. Tem.: 8 deg. Celcius
Comments:

IFT (av.):	**1,31**	dynes/cm
DV max:	0,2123	ul
IFT (DV max):	1,327	dynes/cm

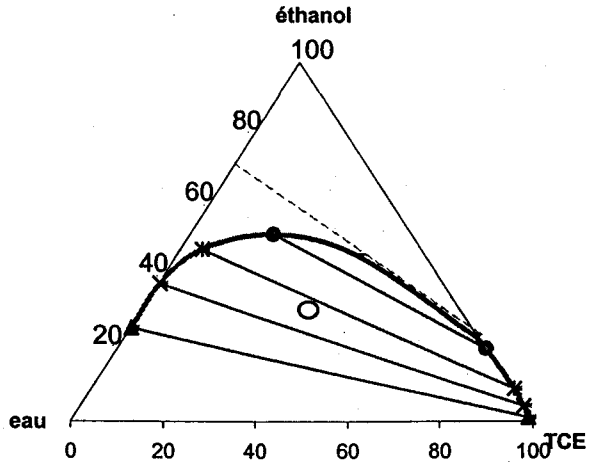

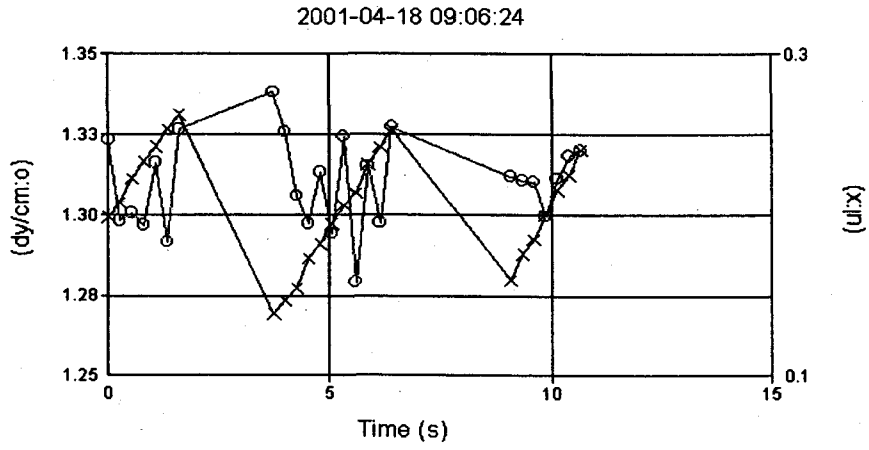

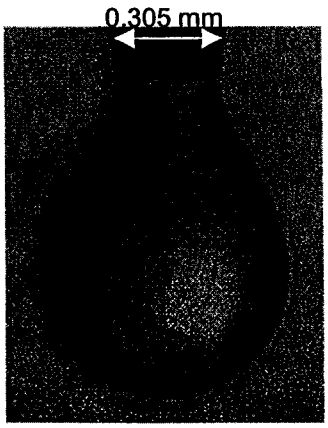

n-PrOH; initial 50% active matter

Ratio	
W	0,2002
TCE	0,5997
A.M.	0,2002

Density	g/cm3
Aqueous phase:	0,9785
Organic phase:	1,2407

Mea. Tem.: 12 deg. Celcius
Comments:

IFT (av.):	3,05	dynes/cm
DV max:	0,895	ul
IFT (DV max):	3,102	dynes/cm

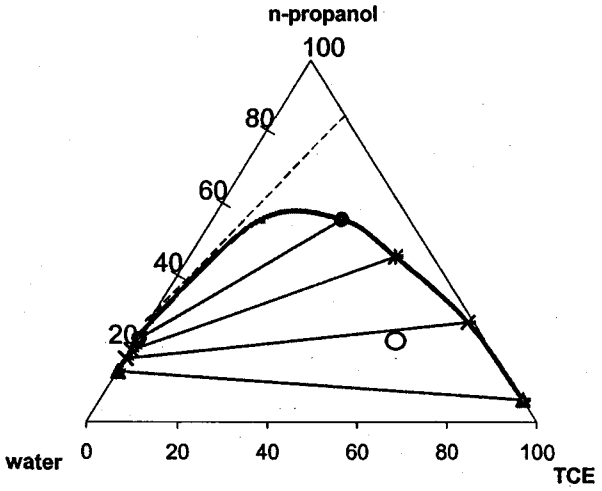

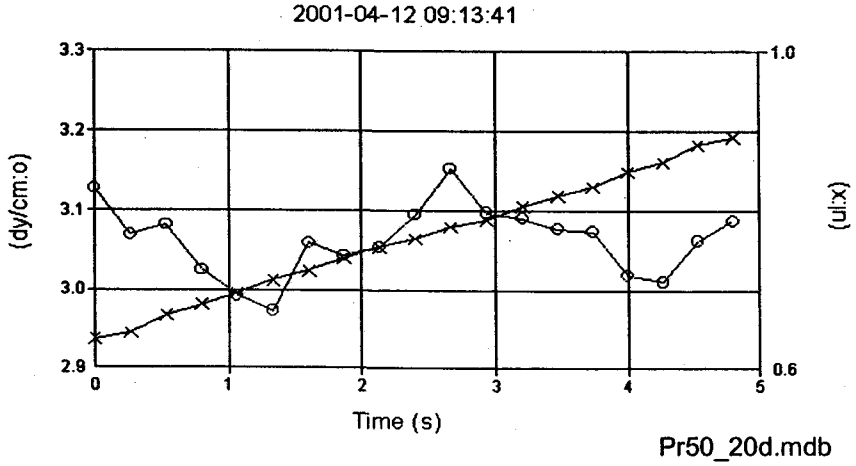

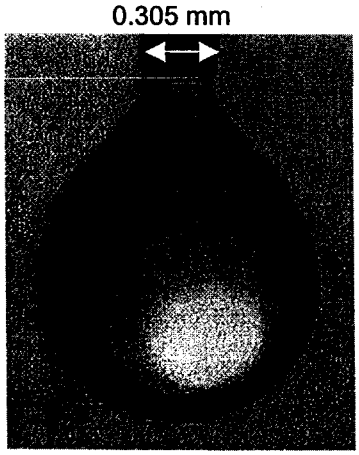

Pr50_20d.mdb

n-PrOH; initial 50% active matter

Ratio	
W	0,3289
TCE	0,3323
A.M.	0,3388

Density	g/cm3
Aqueous phase:	0,9743
Organic phase:	1,0704

Mea. Tem.: 12,5 deg. Celcius
Comments:

IFT (av.):	1,47	dynes/cm
DV max:	1,065	ul
IFT (DV max):	1,502	dynes/cm

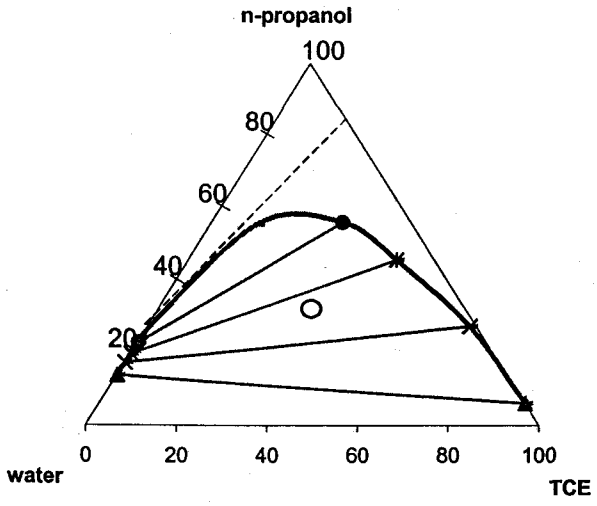

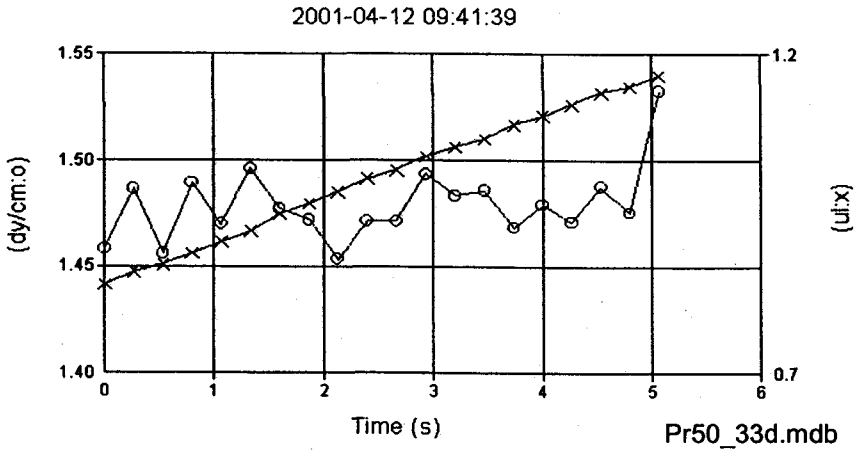

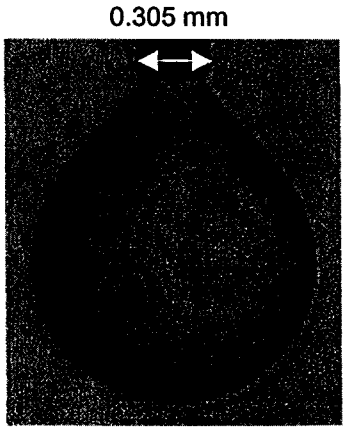

n-PrOH; initial 50% active matter

Ratio	
W	0,4291
TCE	0,1423
A.M.	0,4287

Density	g/cm3
Aqueous phase:	0,9517
Organic phase:	0,9663

Mea. Tem.: 12,5 deg. Celcius
Comments:

IFT (av.):	0,29	dynes/cm
DV max:	0,6003	ul
IFT (DV max):	0,2949	dynes/cm

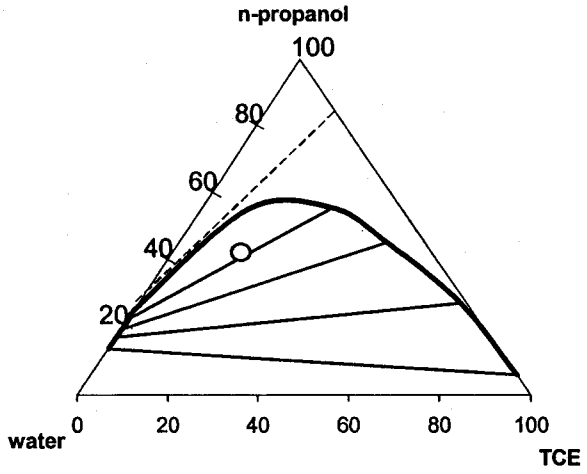

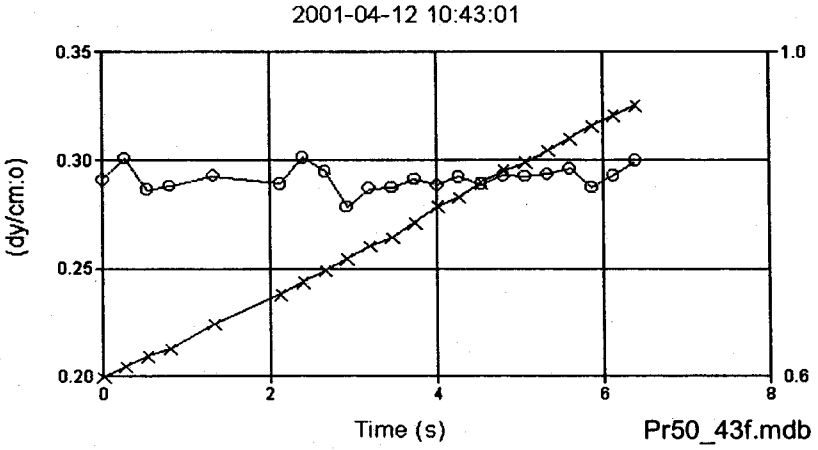

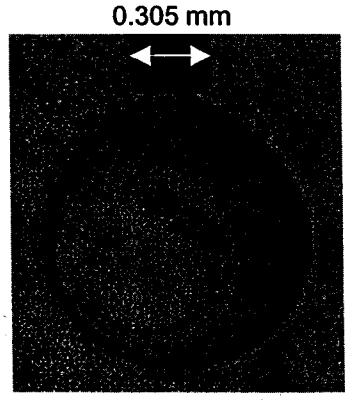

n-PrOH; initial 20% active matter

Ratio	
W	0,24
TCE	0,71
A.M.	0,06

Density	g/cm3
Aqueous phase:	0,9834
Organic phase:	1,425

Mea. Tem.: 12 deg. Celcius
Comments:

IFT (av.):	7.67	dynes/cm
DV max:	1.301	ul
IFT (DV max):	7.699	dynes/cm

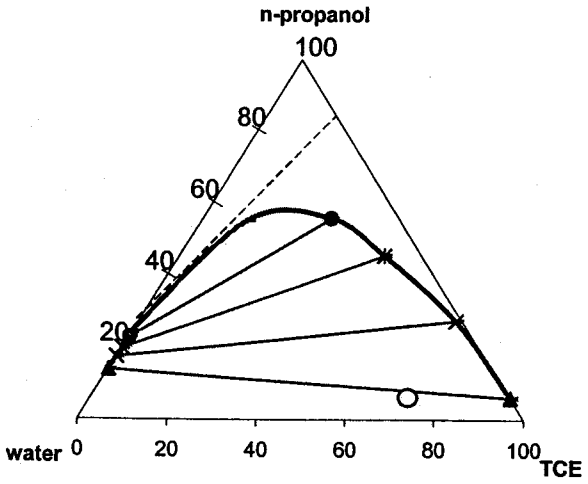

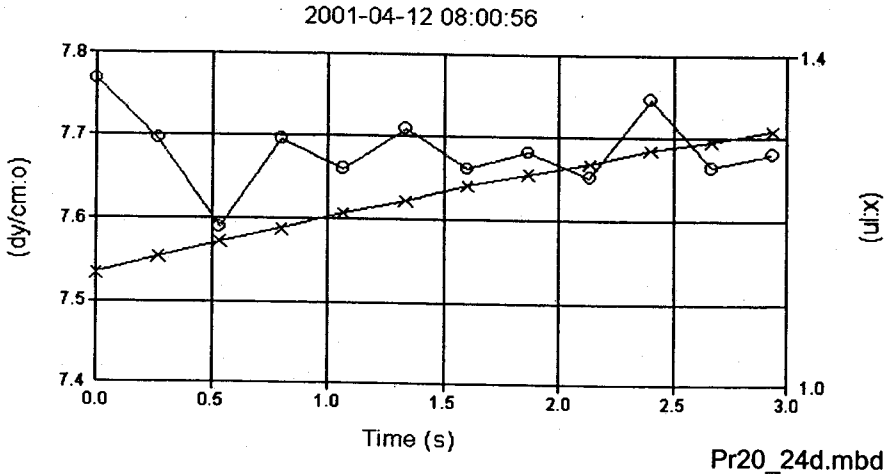

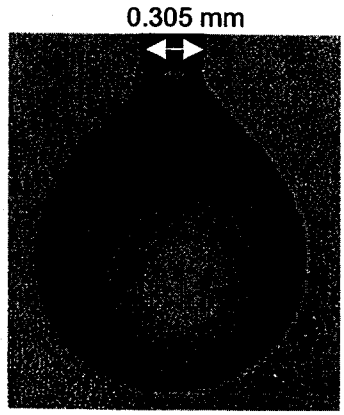

Pr20_24d.mbd

n-PrOH; initial 20% active matter

Ratio	
W	0,4461
TCE	0,4447
A.M.	0,1092

Density	g/cm3
Aqueous phase:	0,9816
Organic phase:	1,3806

Mea. Tem.: 12 deg. Celcius
Comments:

IFT (av.):	5,35	dynes/cm
DV max:	0,9674	ul
IFT (DV max):	5,337	dynes/cm

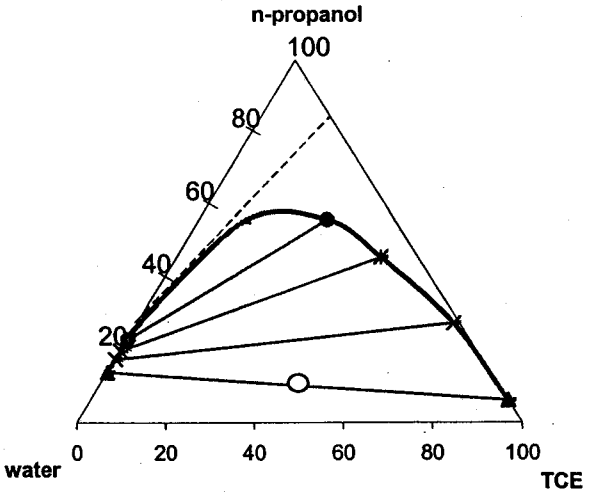

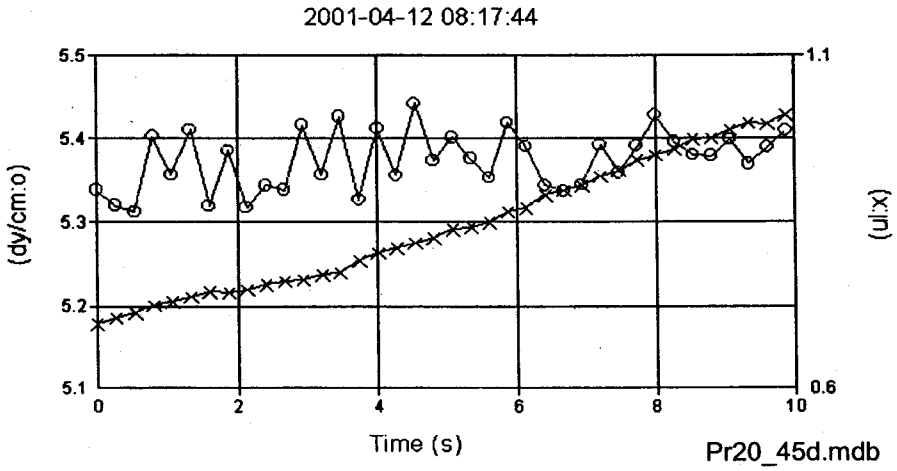

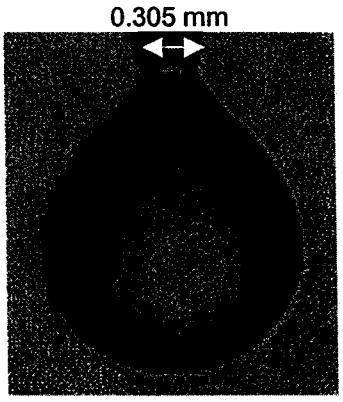

n-PrOH; initial 20% active matter

Ratio	
W	0,6305
TCE	0,2096
A.M.	0,1599

Density	g/cm3
Aqueous phase:	0,978
Organic phase:	1,3231

Mea. Tem.: 12 deg. Celcius
Comments:

IFT (av.):	3,98	dynes/cm
DV max:	0,8346	ul
IFT (DV max):	3,911	dynes/cm

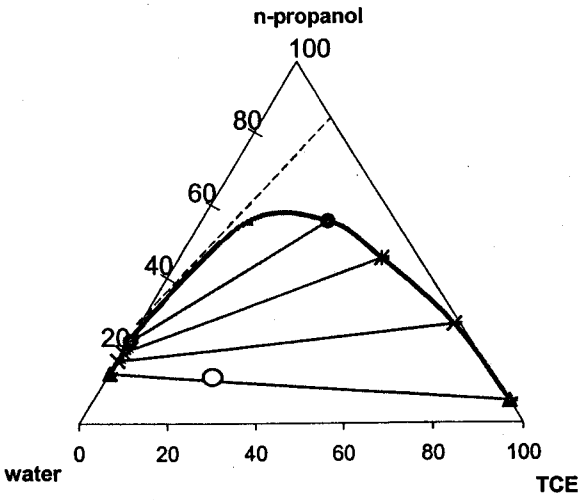

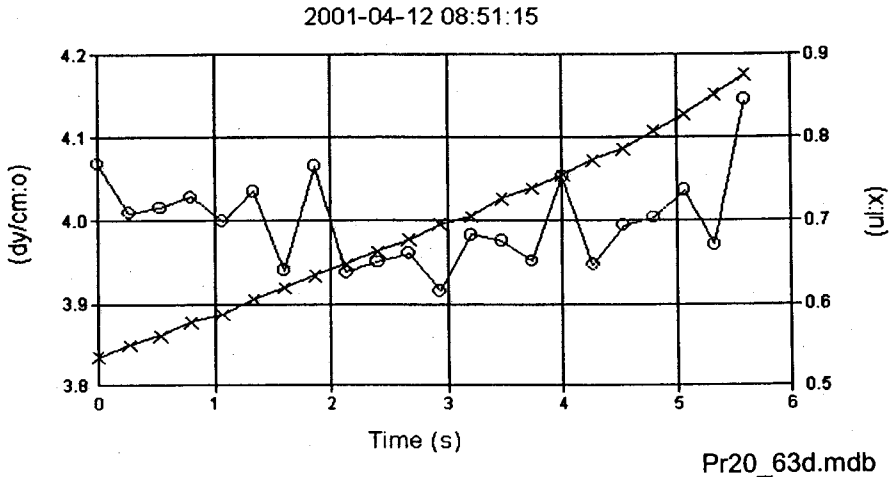

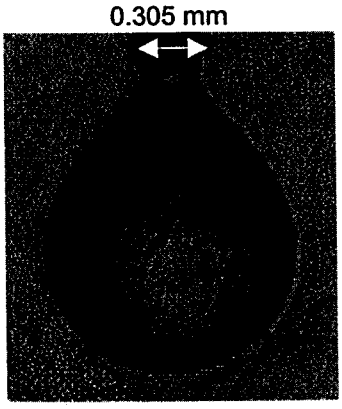

Pr20_63d.mdb

i-BuOH/SAS = 2 ; initial 5% active matter

Ratio	
W	0,4873
TCE	0,4877
A.M.	0,025

Density	g/cm3
Aqueous phase:	1,002
Organic phase:	1,4438

Mea. Tem.: 8 deg. Celcius
Comments:

IFT (av.):	**0,695**	dynes/cm
DV max:	0,1066	ul
IFT (DV max):	0,7008	dynes/cm

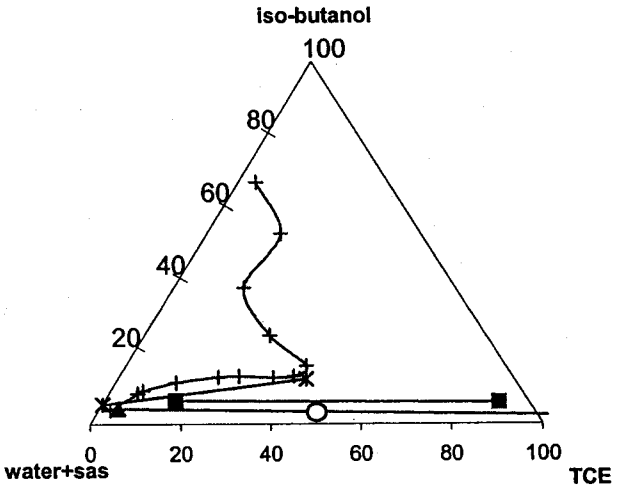

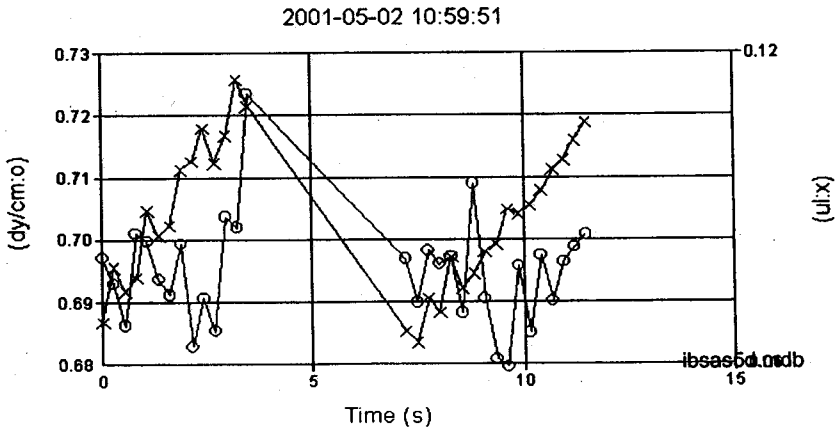

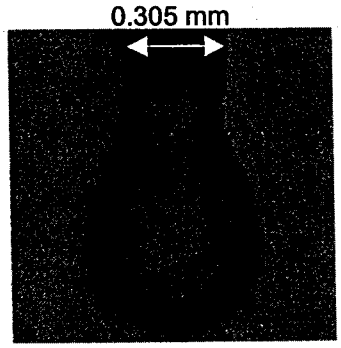

i-BuOH/SAS = 2 ; initial 20% active matter

Ratio	
W	0,3597
TCE	0,5504
A.M.	0,0899

Density	g/cm3
Aqueous phase:	1,0723
Organic phase:	1,3817

Mea. Tem.: 8 deg. Celcius
Comments:

IFT (av.):	**0,088**	dynes/cm
DV max:	-	ul
IFT (DV max):	-	dynes/cm

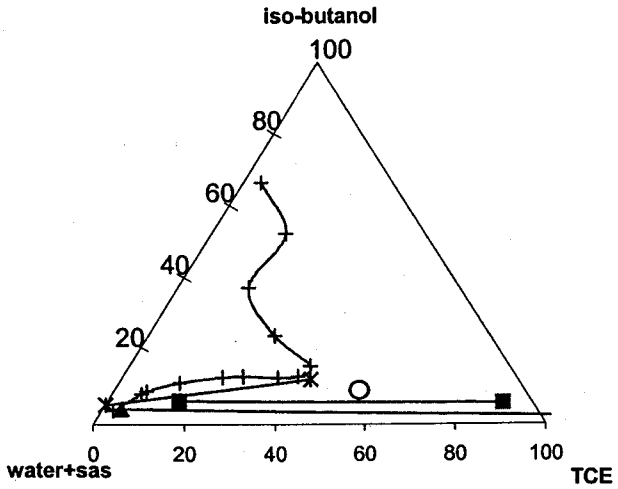

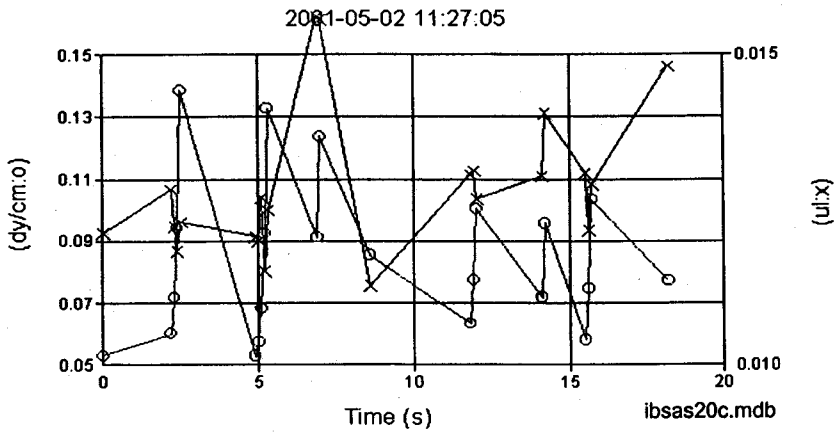

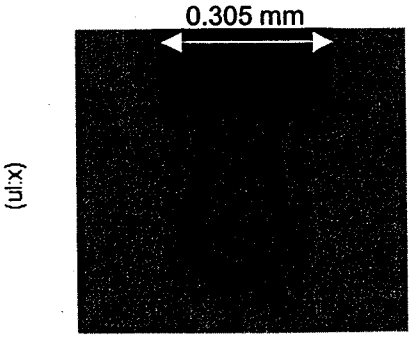

EtOH/SAS = 2 ; initial 20% active matter

Ratio		
W	0,24	
TCE	0,5065	
A.M.	0,254	(0,085 SAS)
		(0,325 water+SAS)
Mea. Tem.:	10	deg. Celcius
Comments:		

Density	g/cm3
Aqueous phase:	1,113
Organic phase:	1,403

IFT (av.):	**0,055**	dynes/cm
DV max:	-	ul
IFT (DV max):	-	dynes/cm

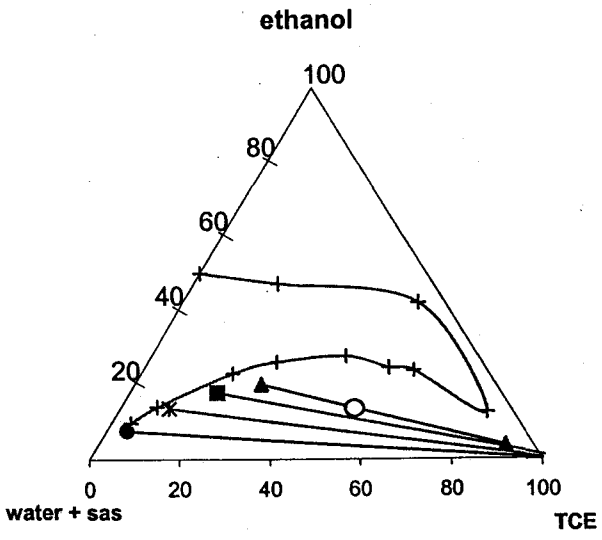

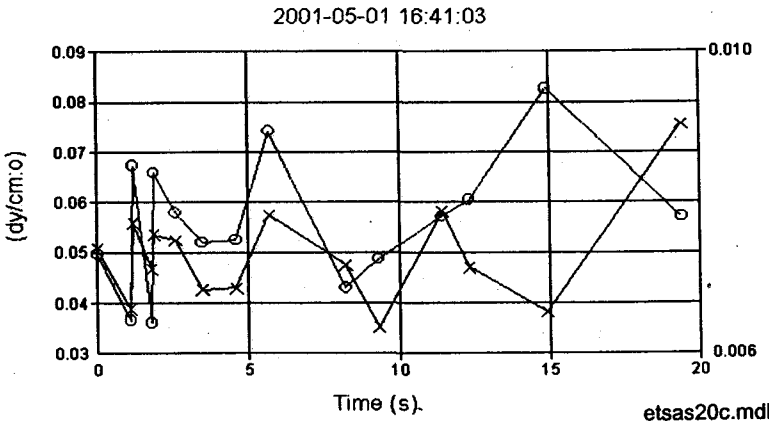

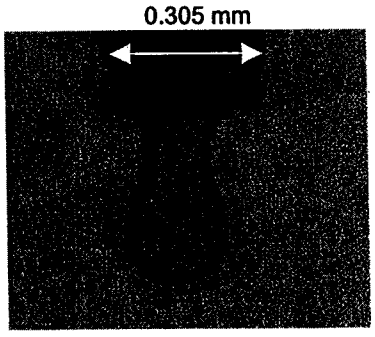

EtOH/SAS = 2 ; initial 50% active matter

Ratio		
W	0,2413	
TCE	0,518	
A.M.	0,241	(0,08 SAS)
		(0,3213 water + SAS)

Density	g/cm3
Aqueous phase:	1,1166
Organic phase:	1,3996

Mea. Tem.: 10 deg. Celcius

Comments:

Two IFT domains: Larger values represent drops falling and are ignored

IFT (av.):	**0,048**	dynes/cm
DV max:	-	ul
TIF (DV max):	-	dynes/cm

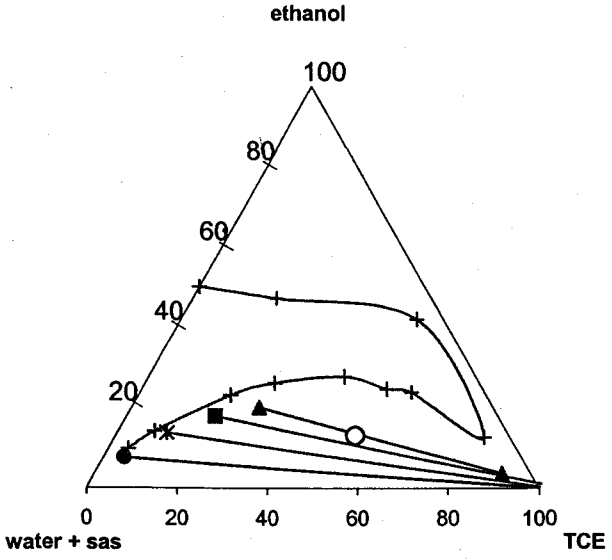

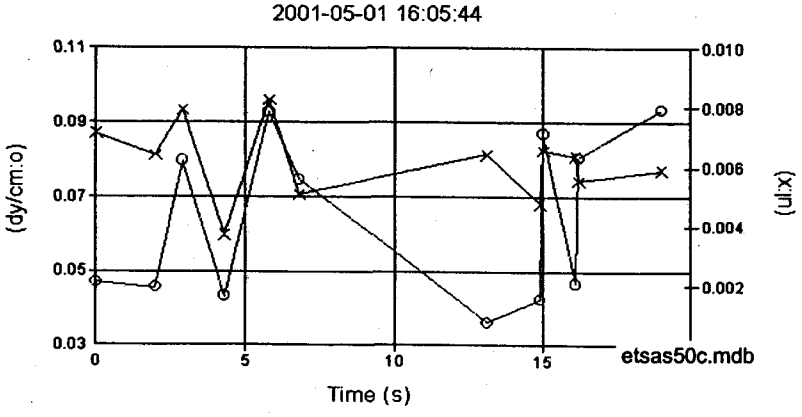

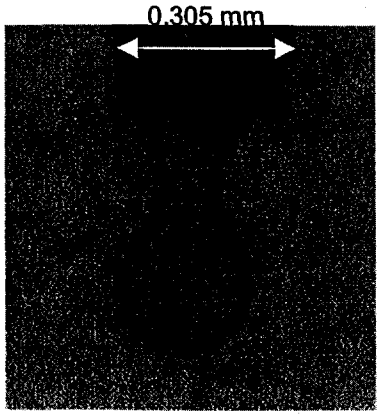

i-BuOH; initial 85% active matter

Ratio	
W	0,3996
TCE	0,0997
A.M.	0,5007

Density	g/cm3
Aqueous phase:	0,8916
Organic phase:	0,9878

Mea. Tem.: 13 deg. Celcius
Comments:

IFT (av.):	2,925	dynes/cm
DV max:	1,346	ul
IFT (DV max):	2,938	dynes/cm

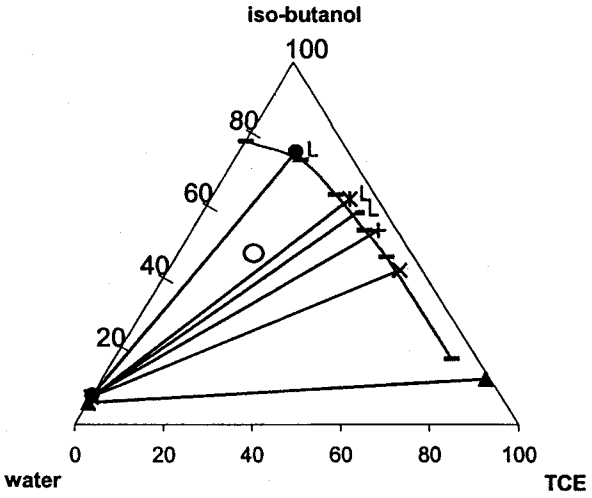

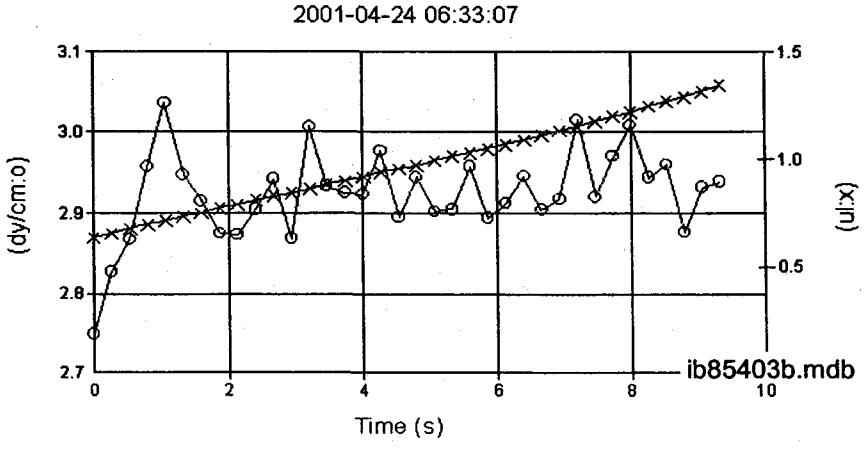

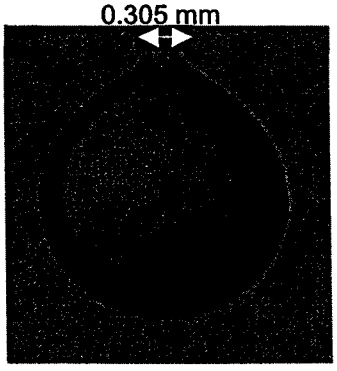

i-BuOH; initial 85% active matter

Ratio	
W	0,3997
TCE	0,301
A.M.	0,2993

Density	g/cm3
Aqueous phase:	0,9893
Organic phase:	1,0616

Mea. Tem.: 14 deg. Celcius
Comments:

IFT (av.):	5,9	dynes/cm
DV max:	6,629	ul
IFT (DV max):	6,101	dynes/cm

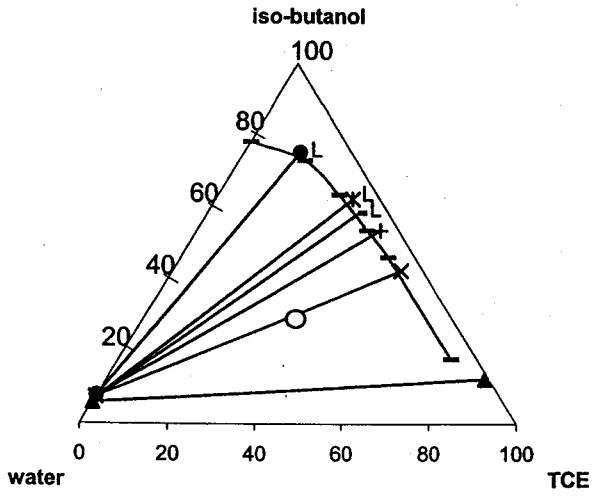

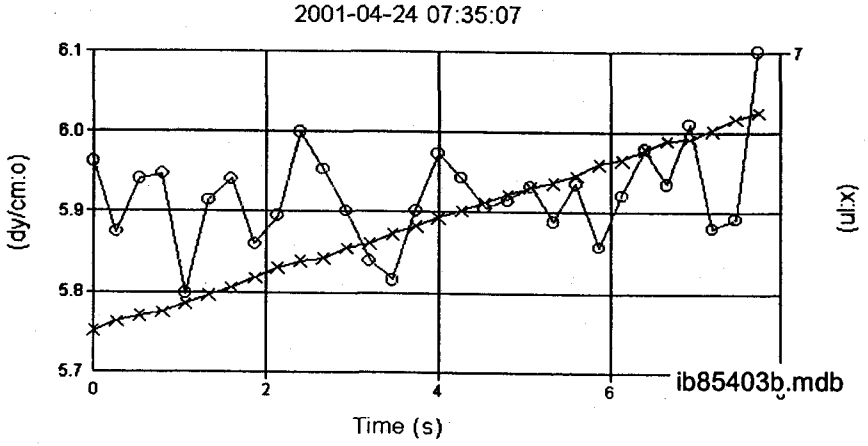

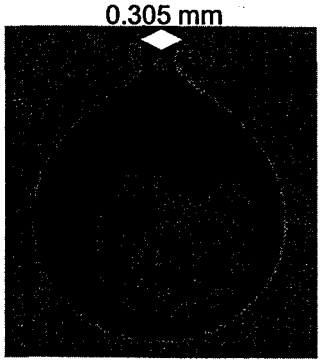

i-BuOH; initial 85% active matter

Ratio	
W	0,4496
TCE	0,4505
A.M.	0,0999

Density	g/cm3
Aqueous phase:	0,9917
Organic phase:	1,316

Mea. Tem.: 12,5 deg. Celcius
Comments:

IFT (av.):	8,6	dynes/cm
DV max:	1,984	ul
IFT (DV max):	8,631	dynes/cm

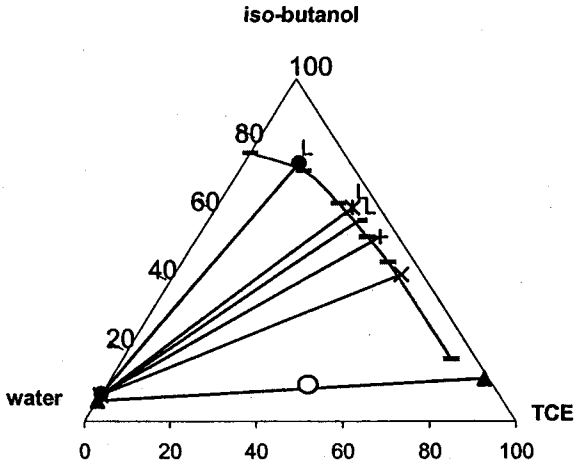

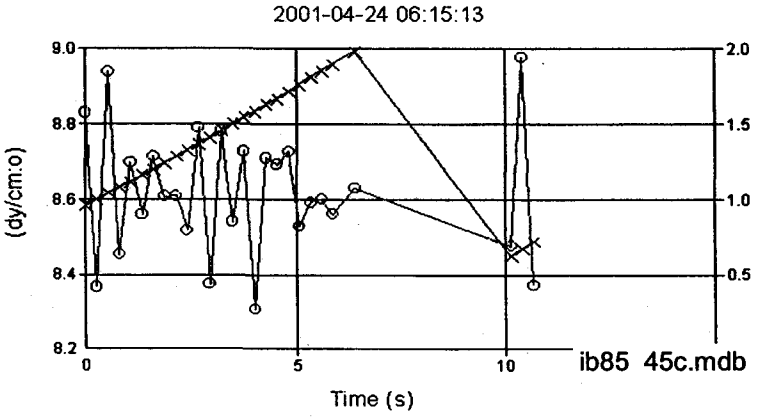

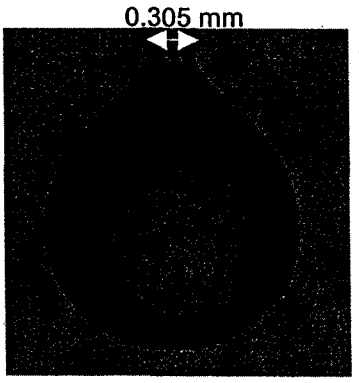

APPENDICE B

Diagrammes de phase des systèmes isopropanol/tensioactifs, diethylamine/tensioactifs et dimethylamine/tensioactifs

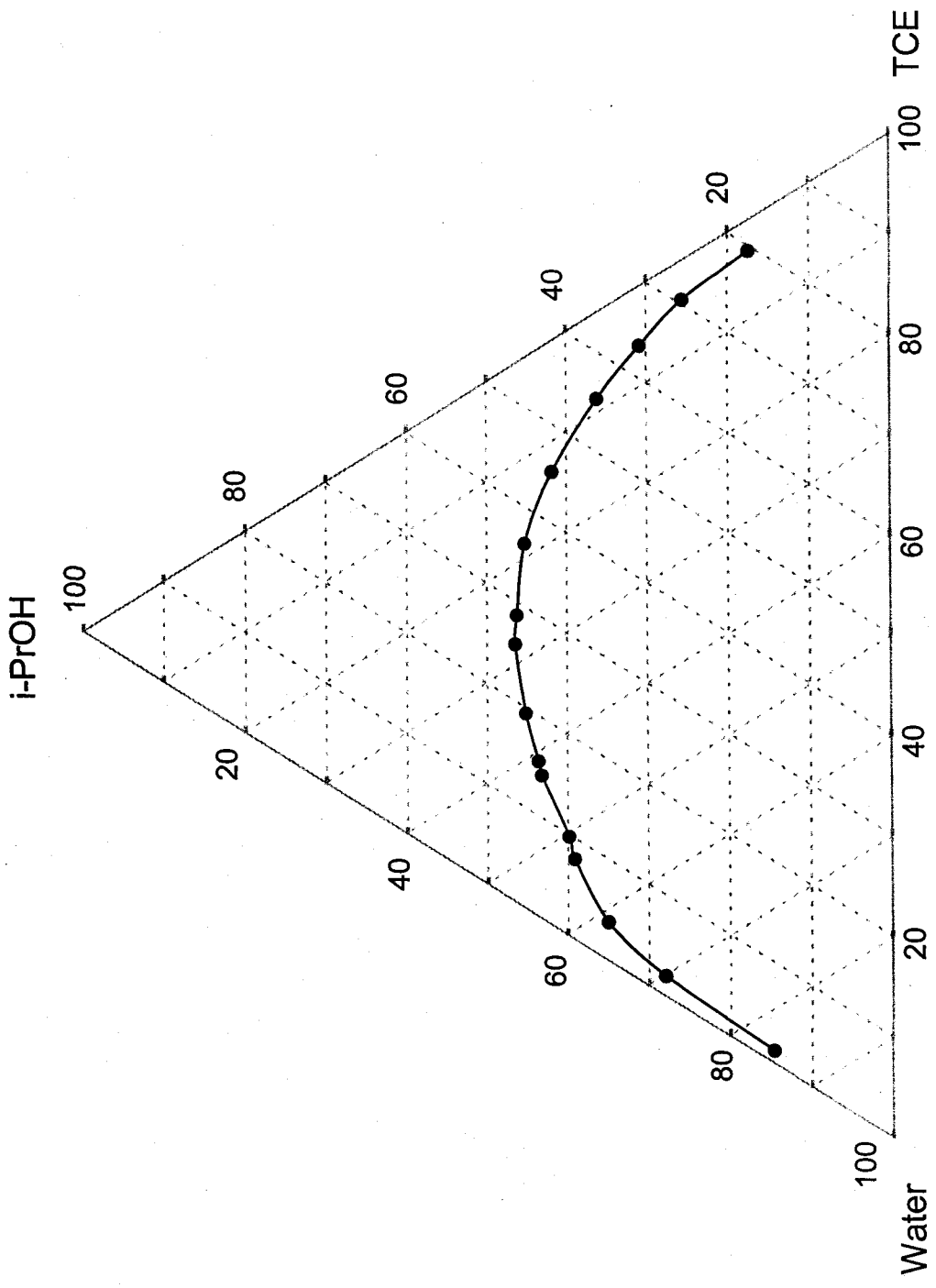
i-PrOH
100
80
60
40
20
TCE
100
80
60
40
20
Water
100
80
60
40
20

i-PrOH

% tce	% a.m.	% water
79,4017737	17,4859073	3,11231891
70,4547306	25,5551754	3,99009401
63,230929	30,8251327	5,94393835
55,2513224	36,1753507	8,57332686
45,2072552	41,7793111	13,0134337
36,2758586	45,2368169	18,4873245
28,6159547	46,2535155	25,1305297
25,6322066	46,4848125	27,8829808
19,4430547	45,1525918	35,4043535
15,5079593	43,5949769	40,8970638
14,271997	43,2117848	42,5162182
9,84074779	39,8390168	50,3202354
7,93883536	39,1355956	52,9255691
3,83409206	34,9485753	61,2173327
2,01242018	27,9600445	70,0275353
1,27191065	14,6269725	84,1011169

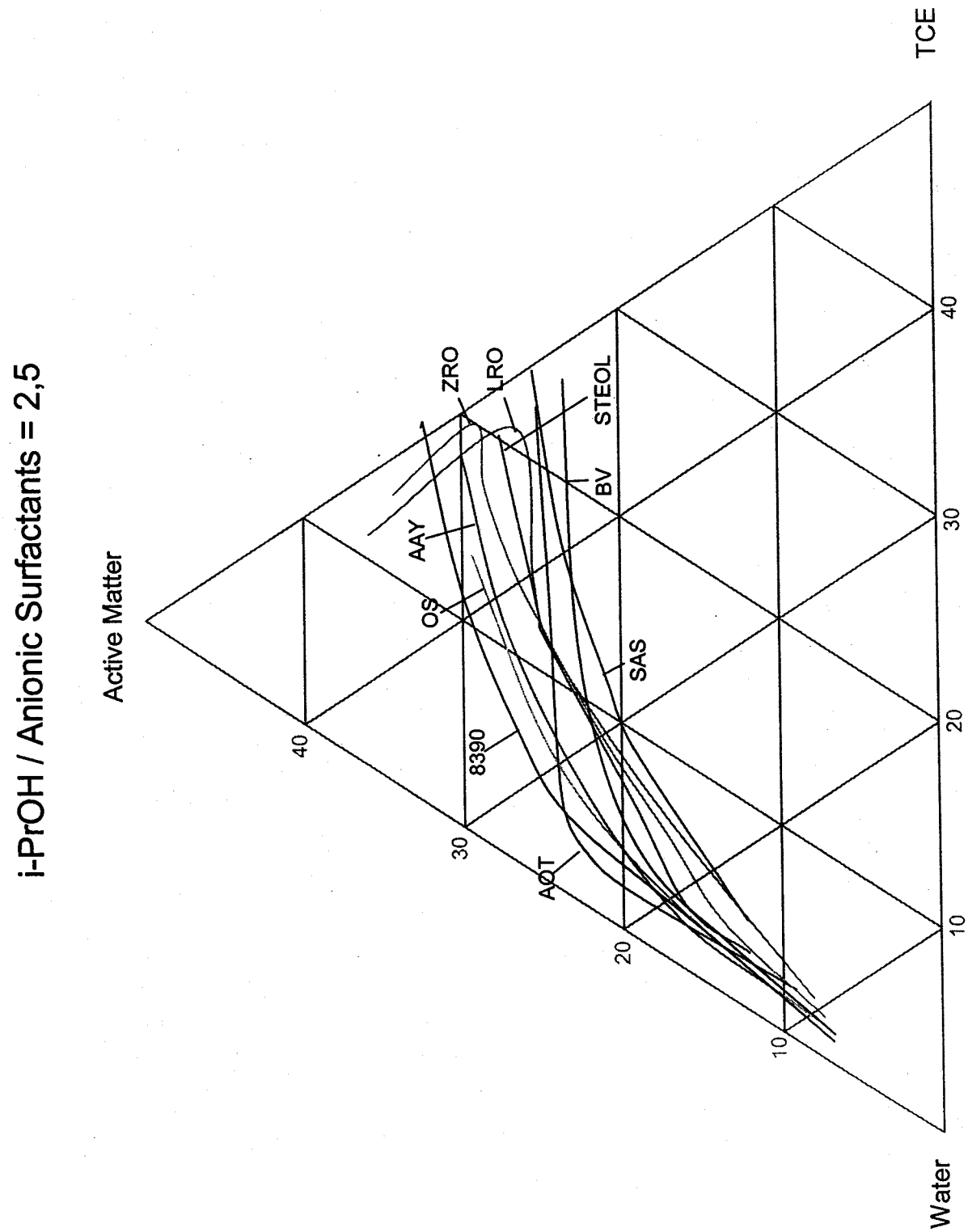
i-PrOH / Anionic Surfactants = 2,5
Active Matter
Water
TCE
40
30
20
10
40
30
20
10
AOT
8390
OS
AAY
ZRO
LRO
STEOL
BV
SAS

Anionic Surfactants

i-PrOH/AOT=2,5

% tce	% a.m.	% water
33,7913968	26,4201239	39,7884793
22,7009055	25,2013466	52,0977479
14,386377	24,5191423	61,0944808
4,34584154	23,7905797	71,8635787
2,44376926	22,0556038	75,5006269
2,04721324	19,5437197	78,4090671
2,45620789	9,205273	88,3385191

i-PrOH/AAY=2,5

% tce	% a.m.	% water
23,374877	30,4194832	46,2056398
18,0457791	29,9678237	51,9863972
10,9913328	27,2209621	61,7877051
5,19468214	21,9265485	72,8787694
2,23346467	16,3079784	81,4585569
1,72351507	10,2495551	88,0269299

i-PrOH/ZRO=2,5

% tce	% a.m.	% water
13,9118457	34,3473667	51,7407876
19,9155444	29,1766493	50,9078063
17,2458015	28,5620242	54,1921743
14,6364372	27,164171	58,1993918
12,8166122	25,6446766	61,5387112
8,66797386	21,1500599	70,1819662
6,00101712	17,2131138	76,7858691
3,45587166	13,6455946	82,8985338
1,99713938	7,39750246	90,6053582

i-PrOH/LRO=2,5

% tce	% a.m.	% water
11,1700774	35,9303058	52,8996168
21,0131457	26,614941	52,3719134
14,2787608	25,4716454	60,2495938
11,6935538	24,5600072	63,746439
8,48952282	20,144948	71,3655292
5,72987096	15,0572607	79,2128684
2,58738649	8,09446521	89,3181483

i-PrOH/OS=2,5

% tce	% a.m.	% water
20,9758924	31,5740508	47,4500568
13,4804733	29,3628957	57,1566311
6,65509318	24,6963884	68,6485184
3,58193125	19,2619005	77,1561682
1,97109862	12,0524395	85,9764619
1,61245969	7,47488675	90,9126536

i-PrOH/STEOL=2,5

% tce	% a.m.	% water
29,2671182	28,2875941	42,4452877
20,1774965	27,5530135	52,2694901
12,4338552	25,0869911	62,4791537
12,0444579	25,1107469	62,8447952
6,46990363	19,272651	74,2574454
3,05864184	15,9275467	81,0138115
2,79913197	12,1013639	85,0995042

i-PrOH/SAS=2,5

% tce	% a.m.	% water
40,1414728	24,6605498	35,1979773
35,4494667	25,6363223	38,9142109
24,357783	25,4170558	50,2251612
16,7046973	23,6102255	59,6850772
11,3766503	20,7706219	67,8527278
9,15224076	19,28936	71,5583992
4,30415208	12,1999359	83,495912

i-PrOH/8390=2,5

% tce	% a.m.	% water
18,0828111	32,5132961	49,4038929
18,3804794	32,3951502	49,2243704
11,3804399	30,0425804	58,5769797
6,42697466	26,576838	66,9961874
3,75117107	23,3278968	72,9209322
2,50998901	15,3073923	82,1826187
1,11486863	6,83804299	92,0470884

i-PrOH/BV=2,5

% tce	% a.m.	% water
59,4052811	17,9018309	22,692888
39,4327943	23,0220369	37,5451687
24,8968116	23,4805557	51,6226327
13,5635999	22,8705091	63,5658909
7,29451895	21,1682082	71,5372729
3,81226398	18,2311468	77,9565892
2,62313644	13,3974249	83,9794387
1,47610122	6,76628162	91,7576172

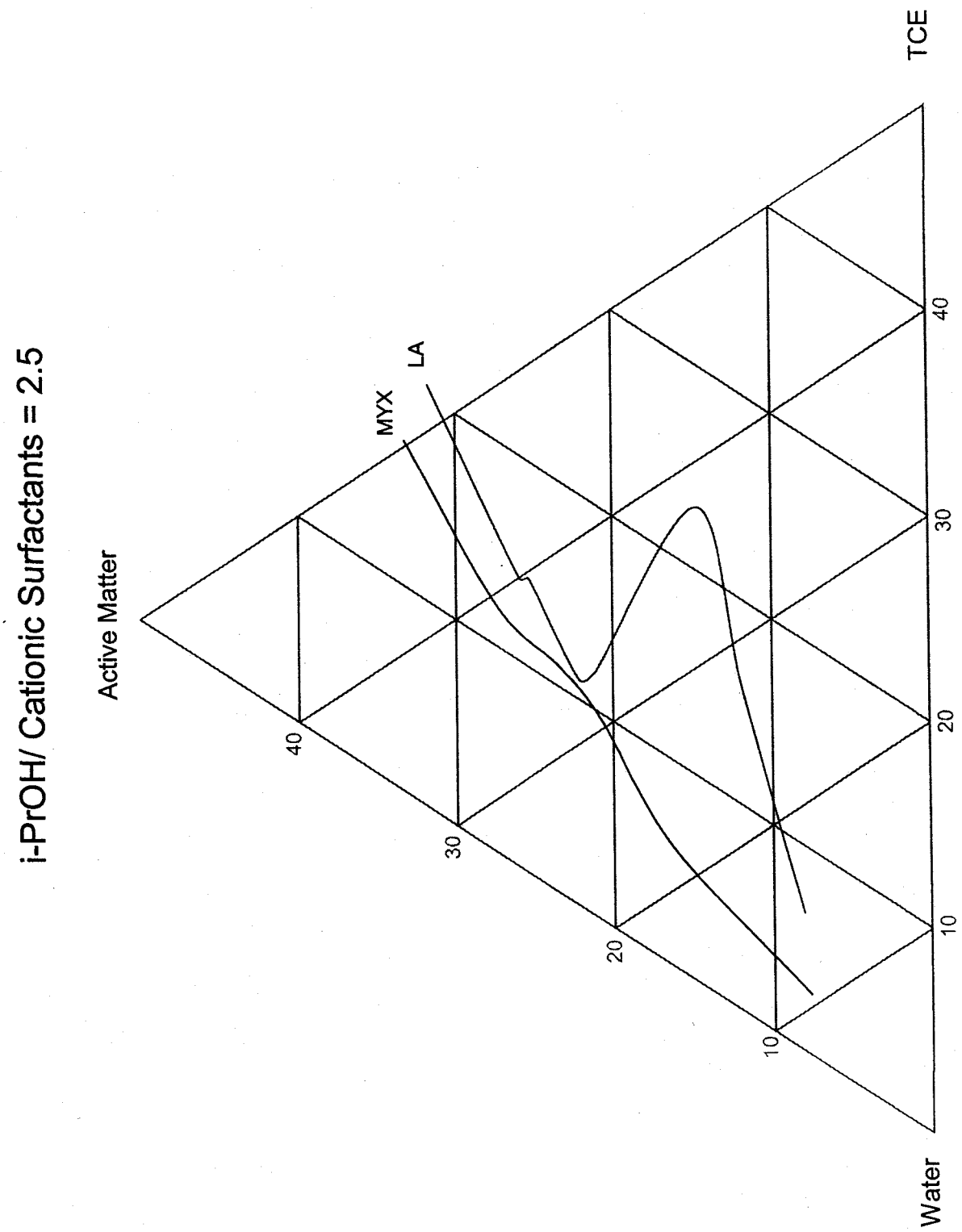
i-PrOH/ Cationic Surfactants = 2.5
Active Matter
MYX
LA
40
30
20
10
Water
TCE
40
30
20
10

Cationic Surfactants

i-PrOH/MYX = 2,5

% tce	% a.m.	% water
17,0607772	33,2501982	49,6890247
11,9066517	27,3041683	60,7891801
11,0049213	23,4699636	65,5251151
9,7208582	20,8149444	69,4641974
5,79976337	16,2911685	77,9090682
2,92312414	7,68332128	89,3935546

i-PrOH/LA = 2,5

% tce	% a.m.	% water
20,511583	31,7447415	47,7436755
14,0172255	25,9494879	60,0332866
14,3129245	25,3400733	60,3470021
10,9491295	22,1522332	66,8986373
11,9226946	21,1083315	66,9689739
23,072783	14,7012383	62,2259787
15,6235029	11,8869189	72,4895782
6,70361573	8,07971367	85,2166706

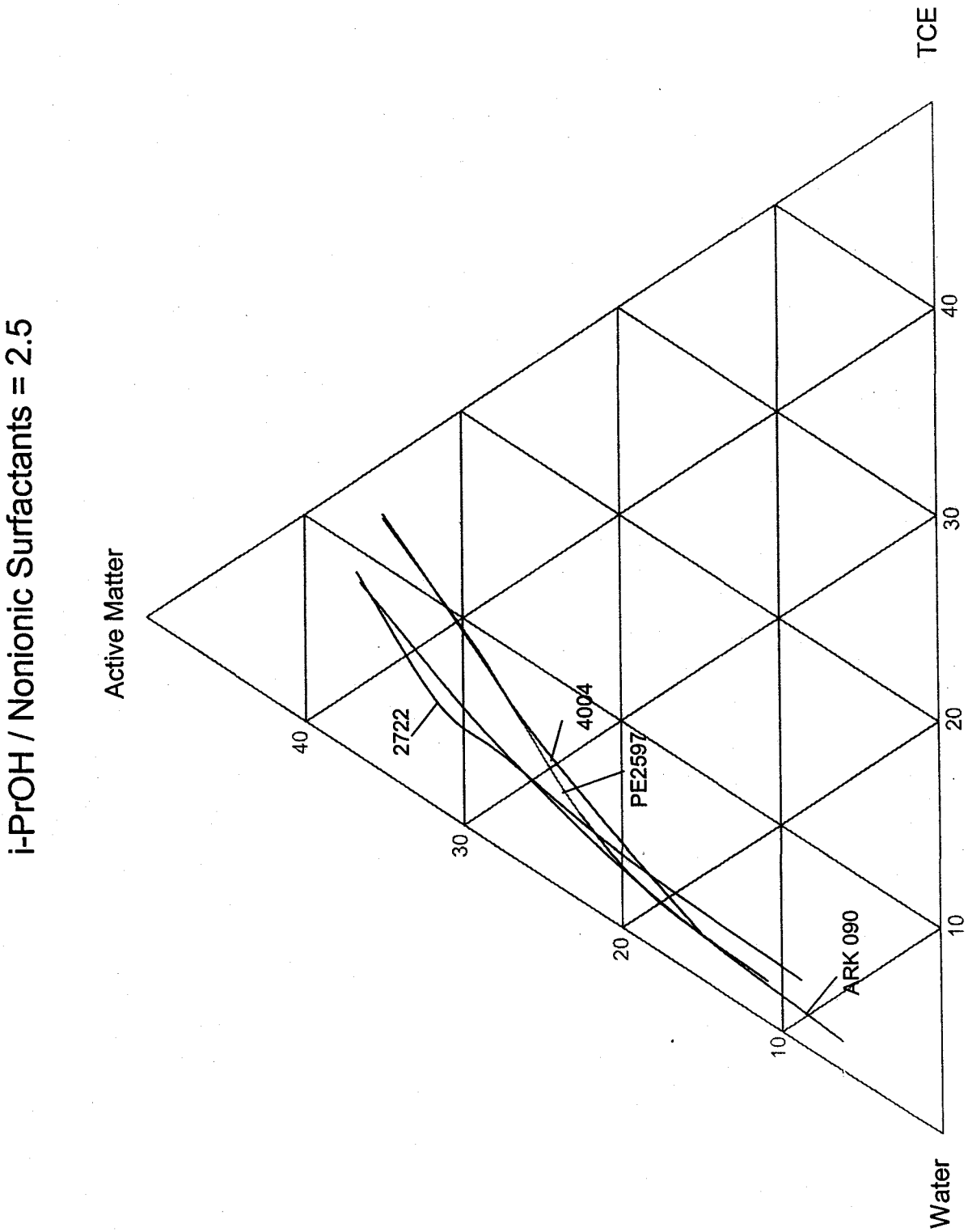
i-PrOH / Nonionic Surfactants = 2.5
Active Matter
Water
TCE
40
30
20
10
2722
4004
PE2597
ARK 090

Nonionic Surfactants

i-PrOH/4004 = 2,5

% tce	% a.m.	% water
12,3028587	35,0477925	52,6493488
8,99475834	29,2150913	61,7901503
7,01094583	26,3975965	66,5914577
4,60116536	21,184212	74,2146226
2,16816225	15,043464	82,7883737

i-PrOH/2722 = 2,5

% tce	% a.m.	% water
8,85843988	36,7433039	54,3982562
5,07492042	31,615946	63,3091336
4,58197798	27,391935	68,026087
3,50933751	19,5348271	76,9558353
3,09764795	8,77501661	88,1273354

i-PrOH/ARK = 2,5

% tce	% a.m.	% water
8,4563011	36,502855	55,0408439
5,02319485	28,2001684	66,7766367
2,52721617	18,0508215	79,4219623
1,4313193	6,21267049	92,3560102

i-PrOH/PE2597 = 2,5

% tce	% a.m.	% water
12,4986911	35,0548864	52,4464225
8,54348747	28,7101892	62,7463234
6,76703902	26,2375123	66,9954487
4,21276353	22,6588179	73,1284186
2,44045794	17,9210761	79,6384659
1,99609683	10,9074551	87,096448

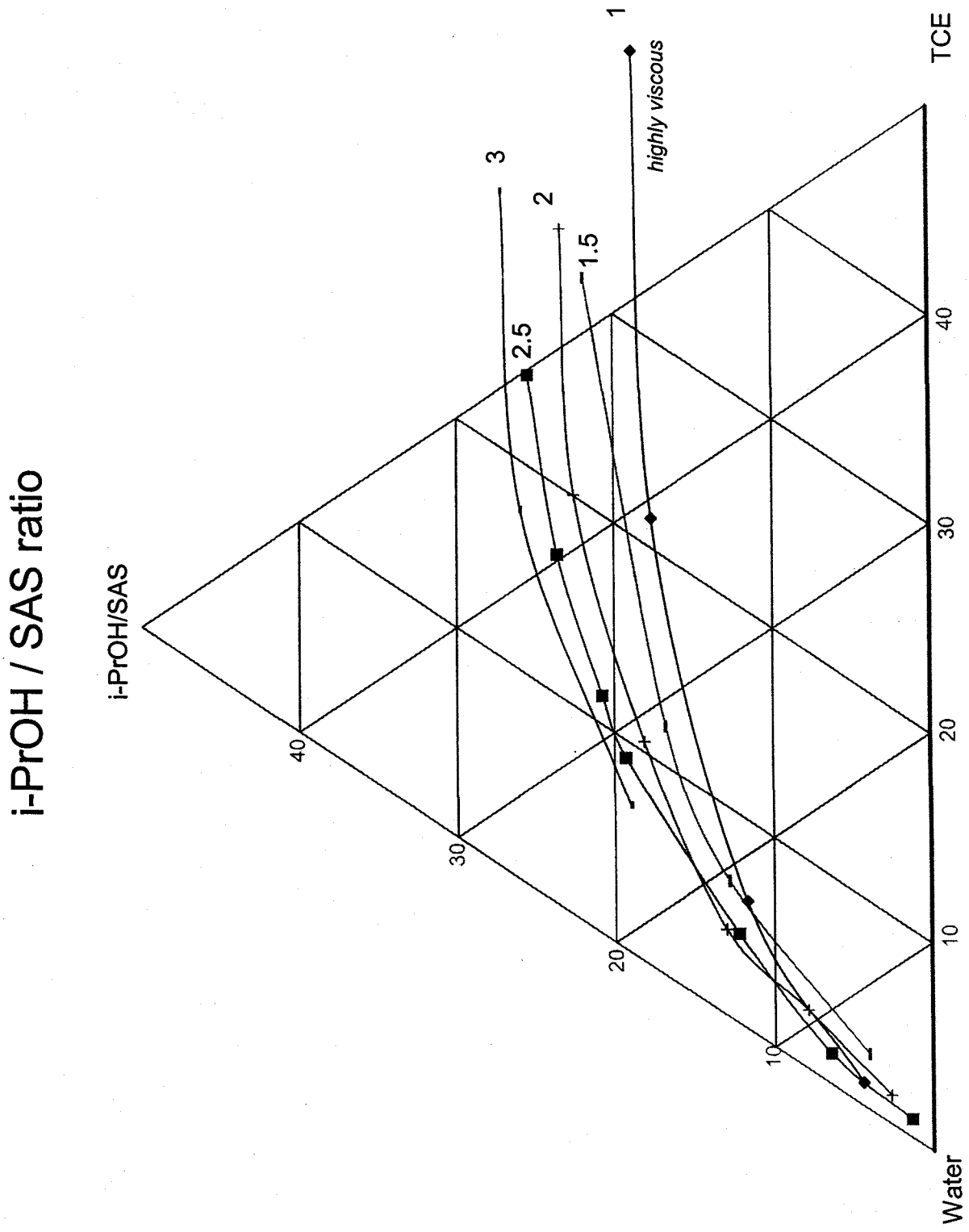
i-PrOH / SAS ratio
i-PrOH/SAS
40
30
20
10
3
2.5
2
1.5
1
highly viscous
TCE
40
30
20
10
Water

i-PrOH/SAS

ratio 1

% tce	% a.m.	% water
30,7330344	21,9033249	47,3636407
11,9395602	16,7734908	71,286949
6,52876211	12,7907609	80,6804769
2,65049096	4,00146888	93,3480402

ratio 1,5

% tce	% a.m.	% water
43,1690279	18,7612926	38,0696795
21,4130244	17,6606759	60,9262997
6,11601564	11,6939323	82,1900521
1,09537789	4,37764648	94,5269756

ratio 2

% tce	% a.m.	% water
32,1514808	27,1026473	40,7458719
17,552662	25,9151878	56,5321501
6,92908954	18,9598513	74,1110592

ratio 2,5

% tce	% a.m.	% water
24,357783	25,4170558	50,2251612
16,7046973	23,6102255	59,6850772
11,3766503	20,7706219	67,8527278
9,15224076	19,28936	71,5583992
4,30415208	12,1999359	83,495912
1,4692815	6,4429485	92,08777
0,87883131	1,3295468	97,7916219

ratio 3

% tce	% a.m.	% water
32,3748652	23,3248312	44,3003036
20,0484537	22,553348	57,3981983
10,5019349	18,1272046	71,3708605
4,12254964	12,9871627	82,8902876
2,82033357	7,89498403	89,2846824
1,37035102	2,6179	96,0118

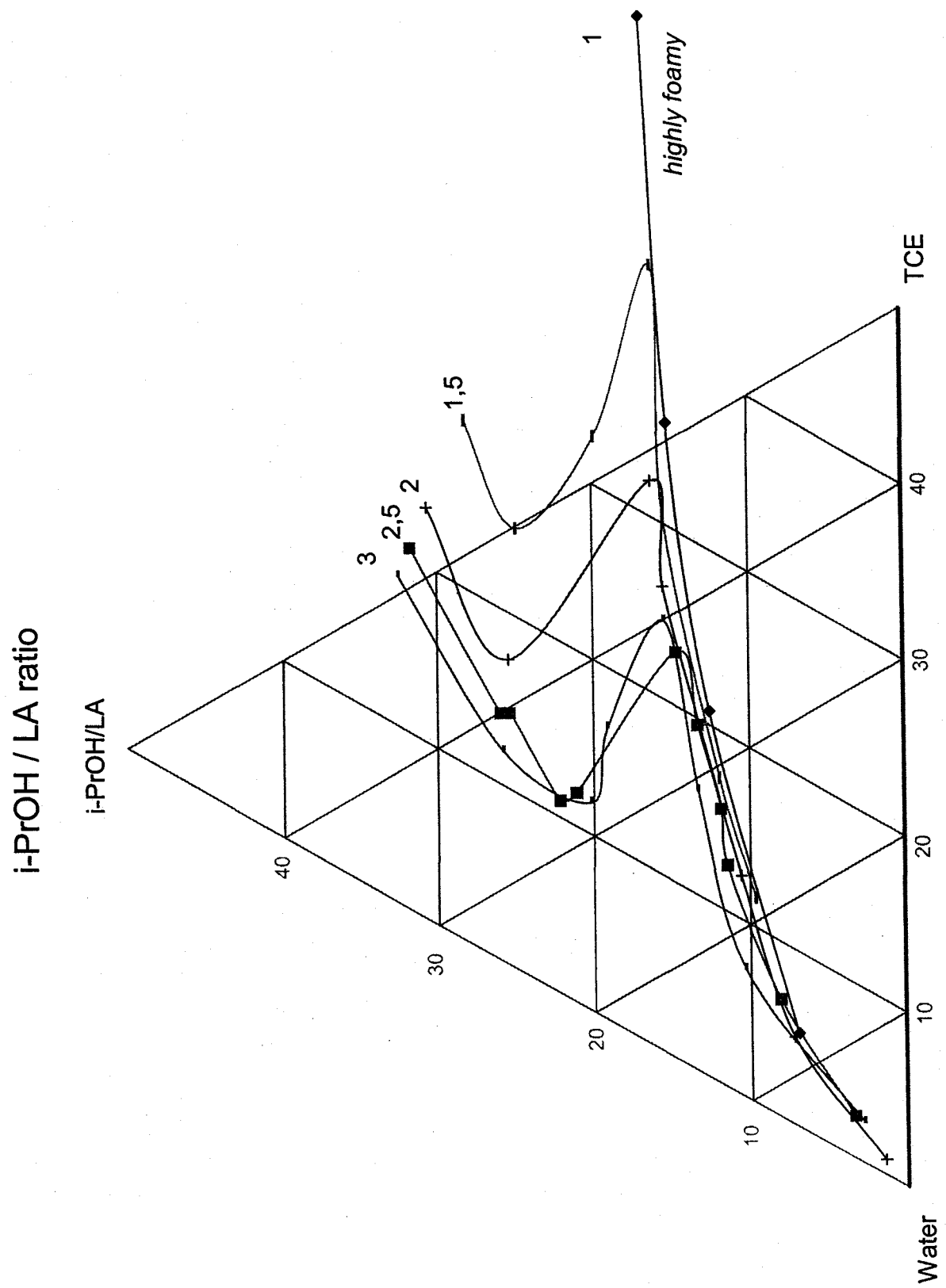
i-PrOH / LA ratio
i-PrOH/LA
40
30
20
10
Water
TCE
40
30
20
10
1
highly foamy
1,5
2
2,5
3

i-PrOH/LA

ratio 1

% tce	% a.m.	% water
58,0923804	16,762922	25,1446976
35,8195621	15,2395215	48,9409165
20,7773708	12,5653649	66,6572643
5,36612107	6,94363962	87,6902393

ratio 1,5

% tce	% a.m.	% water
29,5402951	28,1836704	42,2760345
25,0112069	24,8877879	50,1010052
32,7573053	19,8601025	47,3825922
44,2956097	16,203065	39,5013252
30,4757755	15,4742651	54,0499593
17,3340306	11,9505541	70,7154153
11,7031567	9,63481223	78,6620311

ratio 2

% tce	% a.m.	% water
23,3383725	30,6476826	46,0139449
17,3042188	25,4329578	57,2628233
32,0298089	16,2481673	51,7220239
26,4006487	15,4986663	58,1006849
19,6904982	13,2071	67,1024
12,4773414	10,5904928	76,9321658
5,01080736	7,20743949	87,7817532
0,87310433	1,40699619	97,7198995

ratio 2,5

% tce	% a.m.	% water
20,511583	31,7447415	47,7436755
14,0172255	25,9494879	60,0332866
14,3129245	25,3400733	60,3470021
10,9491295	22,1522332	66,8986373
11,9226946	21,1083315	66,9689739
23,072783	14,7012383	62,2259787
19,6270667	13,3358332	67,0371001
15,6235029	11,8869189	72,4895782
12,6339587	11,4897578	75,8762835
6,70361573	8,07971367	85,2166706
2,41963097	3,33119126	94,2491778

ratio 3

% tce	% a.m.	% water
18,5168892	32,5248703	48,9582405
11,9243221	25,7483807	62,3272972
11,840318	20,1586068	68,0010752
16,5869458	19,0803103	64,332744
24,4573733	15,4557211	60,0869056
15,9363054	13,3237907	70,7399038
7,28894015	10,3424831	82,3685767
2,34136922	2,71221767	94,9464131

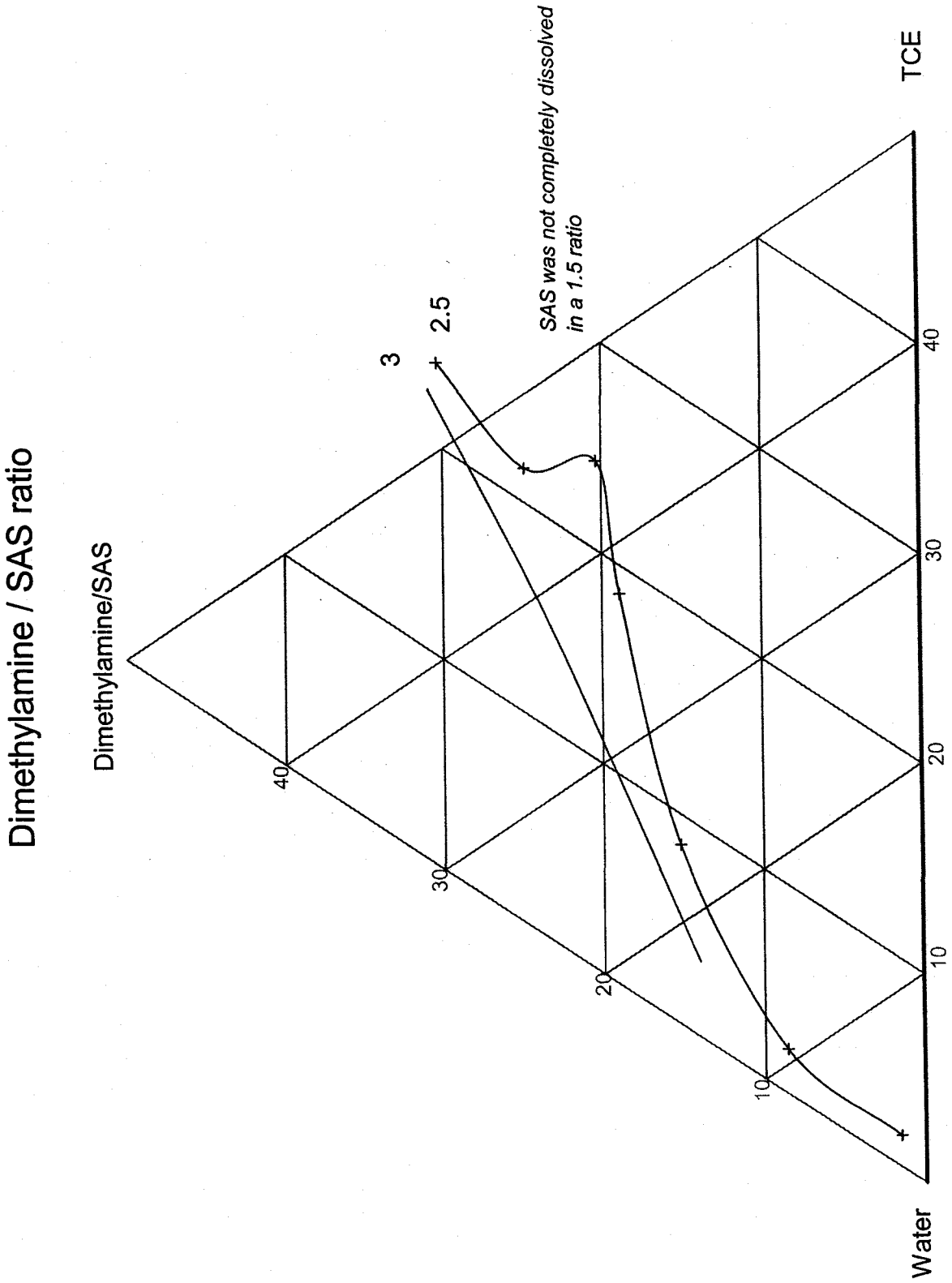
Dimethylamine / SAS ratio
Dimethylamine/SAS
40
30
20
10
3
2.5
SAS was not completely dissolved in a 1.5 ratio
TCE
40
30
20
10
Water

Dimethylamine/SAS

ratio 3

% tce	% a.m.	% water
23,8967154	30,3727363	45,7305483
21,616578	24,8679316	53,5154904
24,2165523	20,3363433	55,4471045
18,6315648	18,8955538	62,4728815
8,5397564	15,2038618	76,2563818
2,14120143	8,57739345	89,2814051
1,51876939	1,5007617	96,9804689

ratio 2,5

% tce	% a.m.	% water
22,3933975	30,9108167	46,6957857
14,6653455	23,0340977	62,3005568
3,59684568	14,0062382	82,3969162

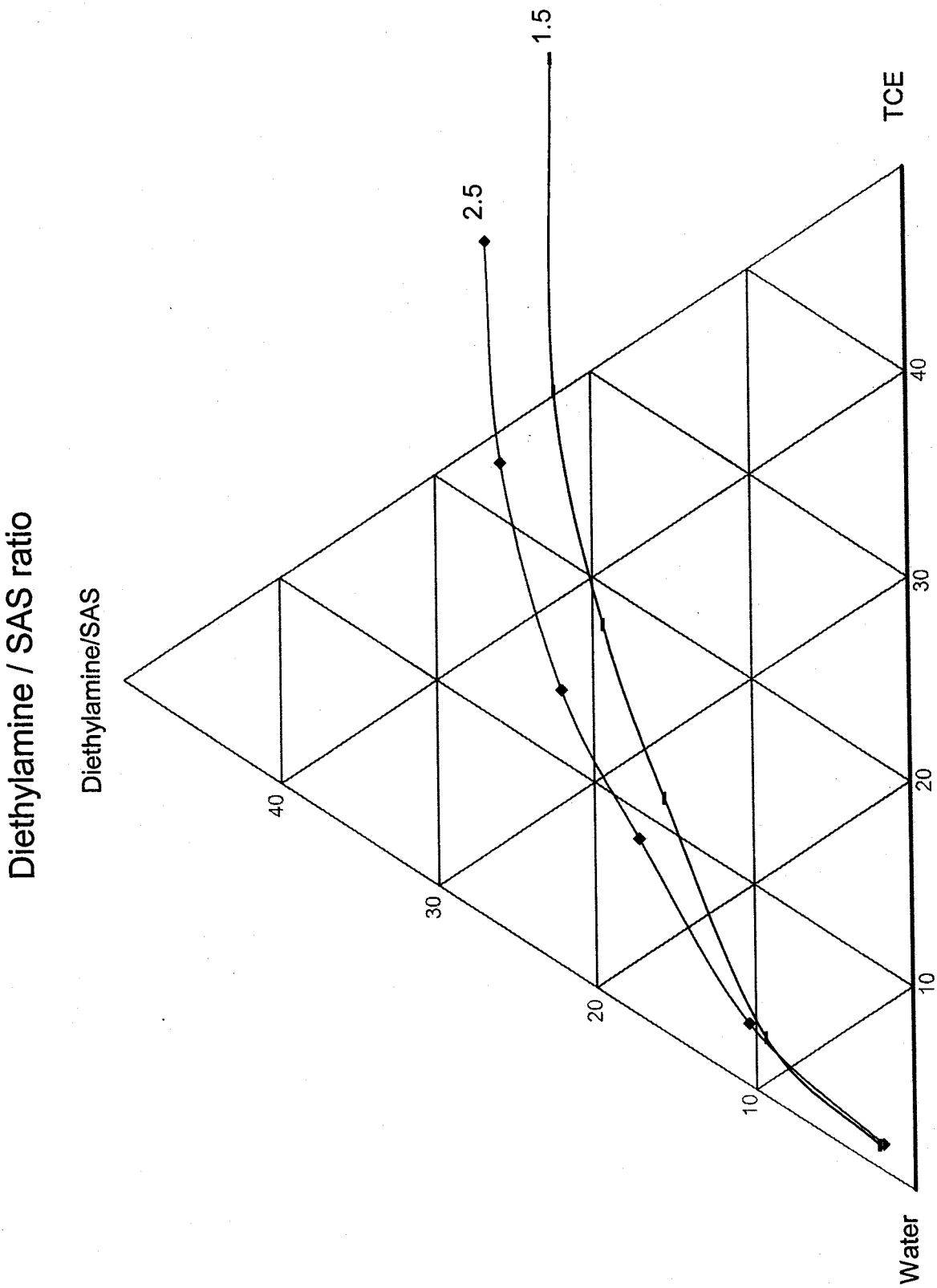
Diethylamine / SAS ratio
Diethylamine/SAS
2.5
1.5
TCE
Water
40
30
20
10
40
30
20
10

Diethylamine/SAS

ratio 2,5

% tce	% a.m.	% water
33,0296517	26,6696964	40,3006519
22,6523221	25,8056724	51,5420056
13,4470388	22,0430368	64,5099243
8,64837807	17,1987144	74,1529076
3,01781951	10,4078875	86,574293
1,26598327	1,98343968	96,7505771

ratio 1,5

% tce	% a.m.	% water
44,0459333	22,3760313	33,5780354
27,8676704	22,3296324	49,8026973
17,9842064	19,3715925	62,6442011
11,4091455	15,60026	72,9905945
2,84364214	9,38525443	87,7711034
1,11231232	2,22173554	96,6659521

APPENDICE C

Résultats complémentaires
(expérience de récupération du TCE)

C-1

Essai de traceur

APPENDIX C-1: Tracer Test

1. Experimental Data

Sample	Pore Volume	Flow rate	Position of tracer front		Position of tracer pulse center	Read out	Chloride concentration	C/C_0
		ml/min	(cm)	(m)	(cm)	mV	ppm	
Cl 1	0.09	4.9	4.492	0.045	-4.508	271.5	0.002	0.000
Cl 11	0.612	5.1	35.942	0.359	26.942	269.3	0.259	0.002
Cl 15	0.716	3.2	41.275	0.413	32.275	267.2	0.530	0.004
Cl 17	0.771	2.8	44.775	0.448	35.775	265.3	0.800	0.006
Cl 19	0.813	3	47.275	0.473	38.275	259	1.884	0.013
Cl 21	0.857	2.5	49.879	0.499	40.879	247.6	4.866	0.034
Cl 23	0.928	2.3	54.192	0.542	45.192	230.4	13.734	0.097
Cl 25	0.941	1.7	54.546	0.545	45.546	217.7	26.684	0.188
Cl 27	0.973	2.3	56.942	0.569	47.942	206.6	46.283	0.326
Cl 30	1.041	2	61.275	0.613	52.275	192.9	89.544	0.631
Cl 32	1.109	1.8	64.875	0.649	55.875	183.4	140.498	0.991
Cl 34	1.148	1.7	67.142	0.671	58.142	183.2	141.830	1.000
Cl 36	1.183	1.7	69.338	0.693	60.338	184.4	134.017	0.945
Cl 37	1.201	1.7	70.188	0.702	61.188	184.5	133.385	0.940
Cl 39	1.235	1.7	72.313	0.723	63.313	185.8	125.434	0.884
Cl 41	1.268	1.6	74.313	0.743	65.313	189.6	104.763	0.739
Cl 44	1.317	1.5	77.125	0.771	68.125	195.5	79.092	0.558
Cl 47	1.412	1.4	82.667	0.827	73.667	212.9	33.941	0.239
Cl 50	1.475	1.4	87.625	0.876	78.625	245.2	5.721	0.040
DV_05 1	1.586	1.4	129.333	1.293	120.333	255.4	2.661	0.019

2. Ogata-Banks equation (simplified version)

(Ogata, A. and Banks, R.B., 1961. A solution of the differential equation of longitudinal dispersion in a porous media, U.S. Geol. Surv. Prof. Pap., 411-A, 7 pp.)

Replacement of the product "vt" by the distance of transport "d" (in meters)
Parameter "a" used as representing dispersivity
Total dispersion is the product "a*d"
2 sources are superimposed in order to represent a tracer pulse

Parameters:

l	0.18	Tracer source width (m)
a	0.006	Dispersion factor

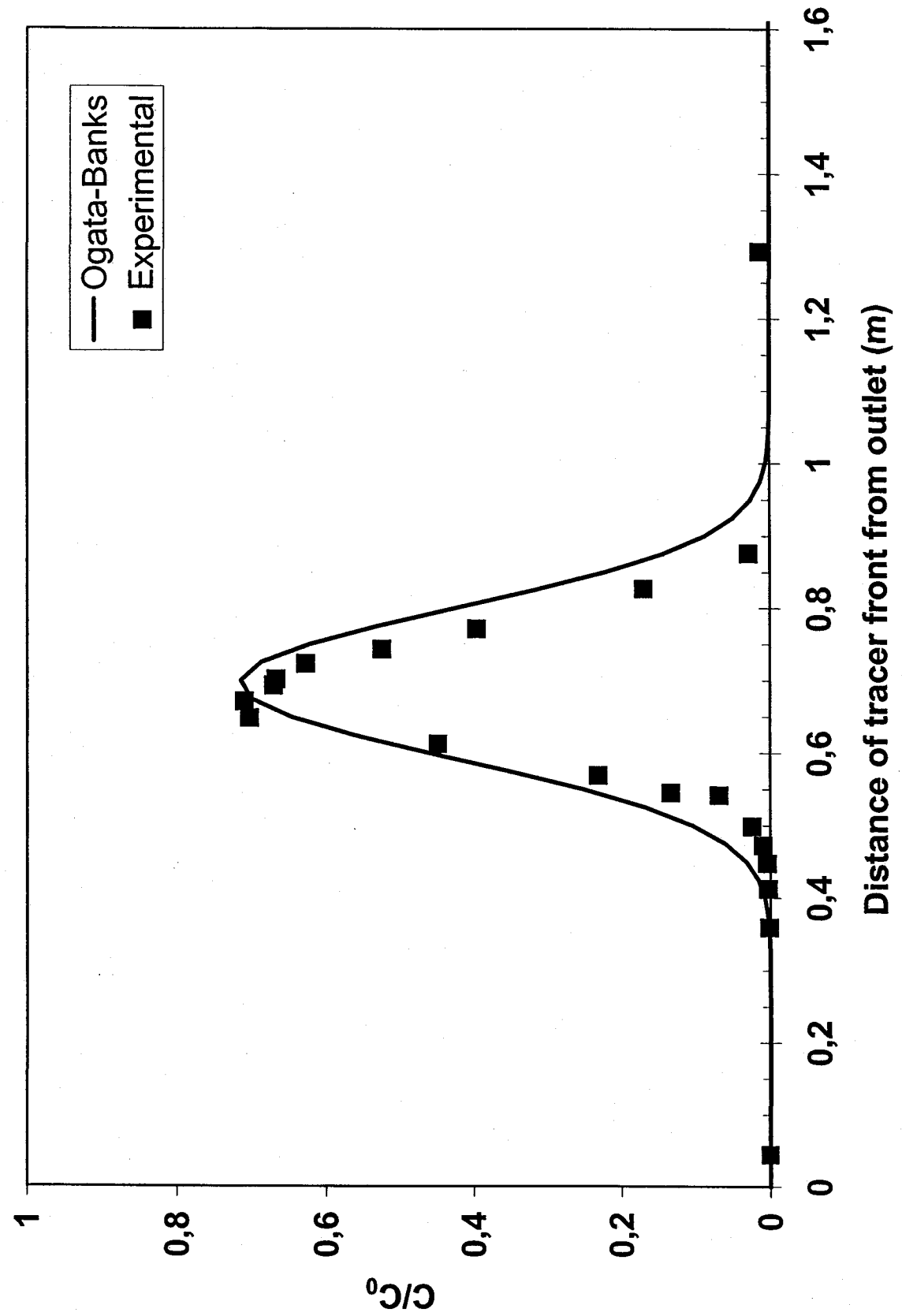
Ogata-Banks
Experimental
C/C0
Distance of tracer front from outlet (m)
0
0,2
0,4
0,6
0,8
1
1,2
1,4
1,6

C-2

Propriétés du système eau/W2722-SAS/TCE

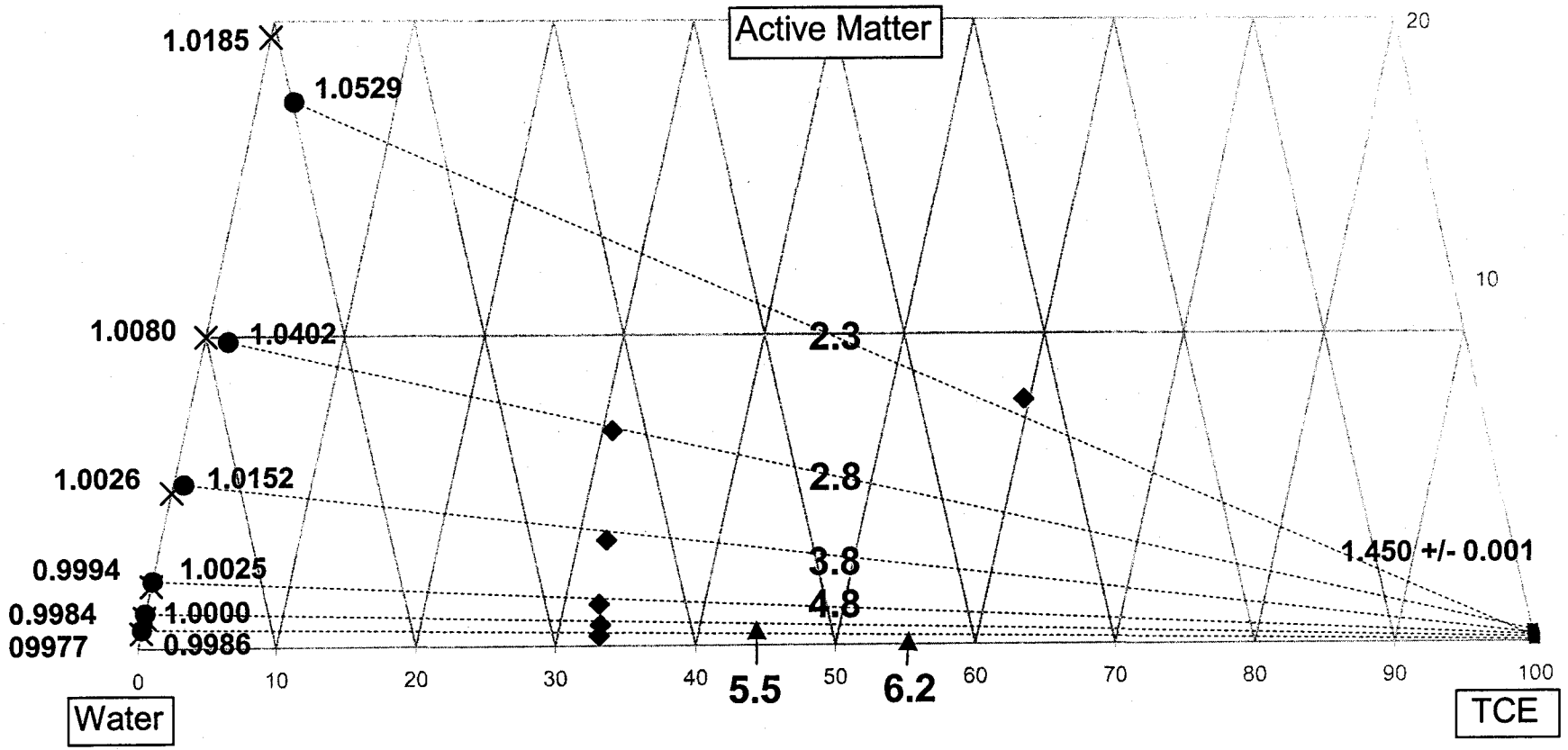

× Initial composition of washing solution	..... Tie-lines
● Aqueous phase composition	1.0185 Density in g/cm^3
■ Organic phase composition	2.3 Interfacial tension in mN/m
◆ Overall sample composition	

C-3

Résultats comparés de l'expérience

(a) Densité de l'effluent, concentration en TCE dans l'effluent et débit, en fonction du nombre de volume des pores circulés dans la chambre.

(b) Densité de l'effluent, concentration en TCE dans l'effluent et débit, en fonction du temps.

Tableau C-3.1 – Débit

Tableau C-3.2 – Concentration en TCE dans l'effluent

Tableau C-3.3 – Densité de l'effluent

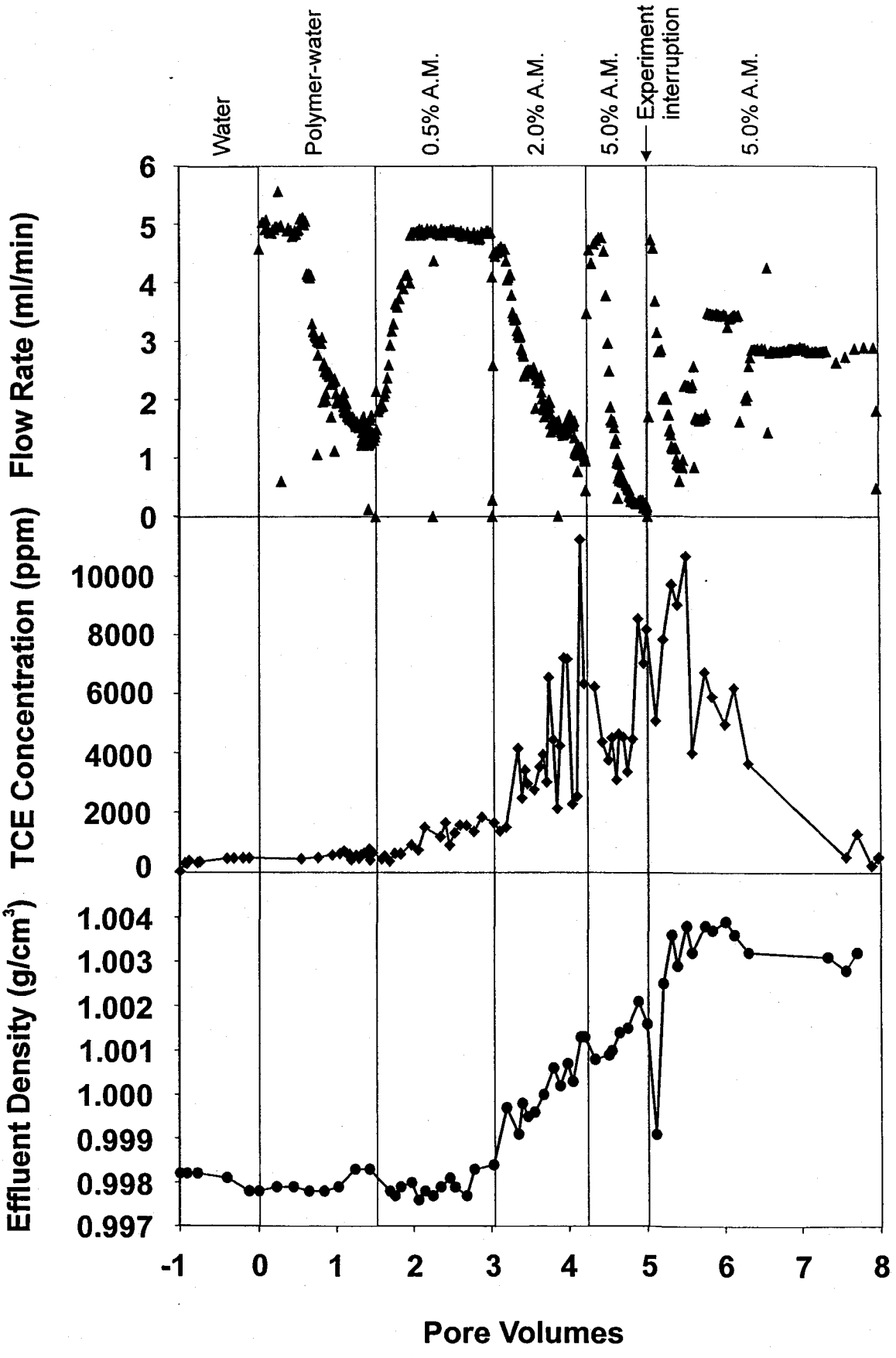
Water
Polymer-water
0.5% A.M.
2.0% A.M.
5.0% A.M.
Experiment interruption
5.0% A.M.
Flow Rate (ml/min)
TCE Concentration (ppm)
Effluent Density (g/cm3)
Pore Volumes

(A)

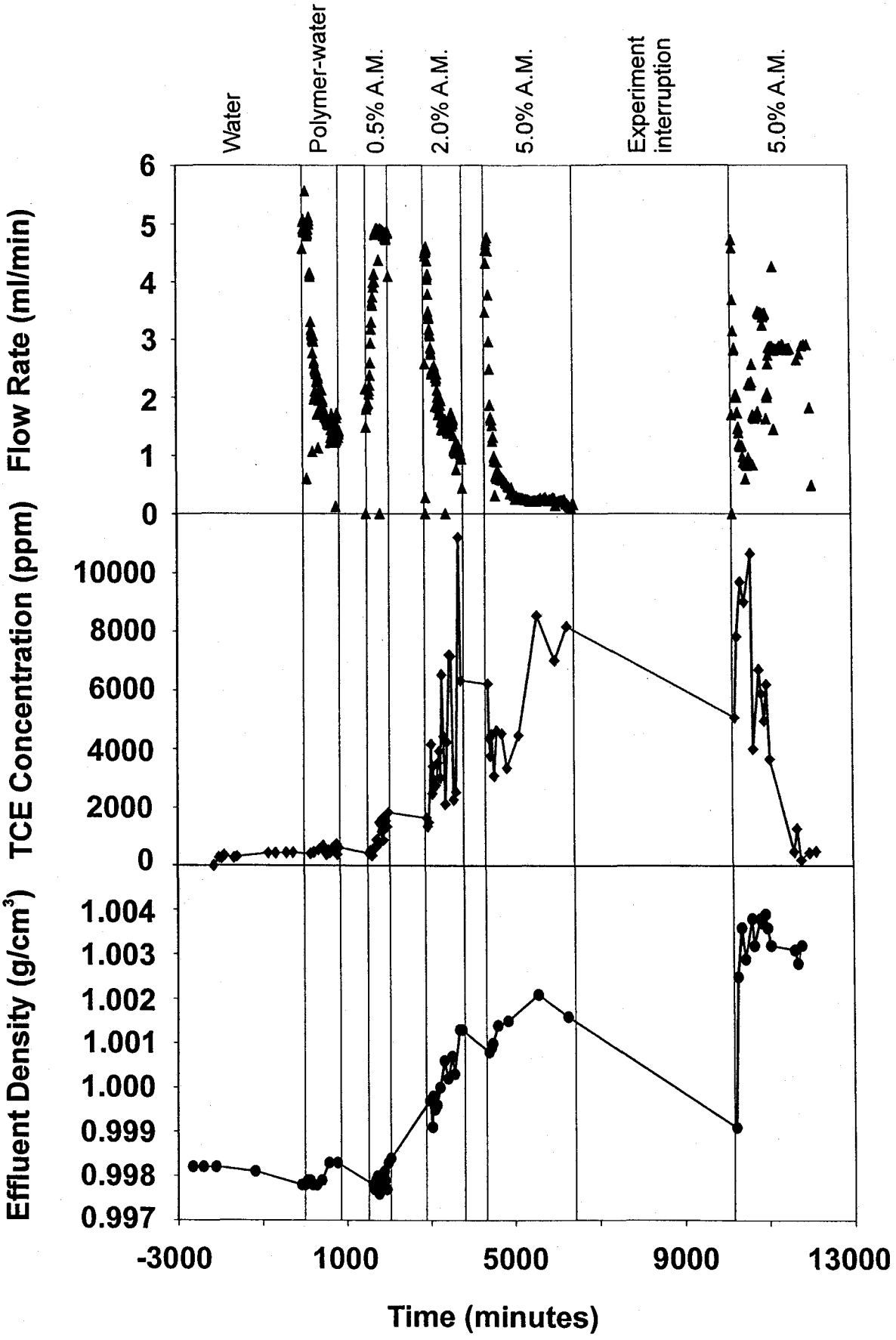
Water
Polymer-water
0.5% A.M.
2.0% A.M.
5.0% A.M.
Experiment interruption
5.0% A.M.
Flow Rate (ml/min)
TCE Concentration (ppm)
Effluent Density (g/cm3)
Time (minutes)
-3000
1000
5000
9000
13000

(B)

Table C-3.1 Flow Rate

Flush	Time		Pore Volume		Flow Rate
	This Flush min	Overall min	This Flush PV	Overall	ml/min
Preflush	0	0			
Preflush	2.5	2.5	0.01147582	0.01147582	4.57097033
Preflush	5	5			
Preflush	7.5	7.5	0.0387136	0.0387136	7.8989575
Preflush	10	10			
Preflush	12.5	12.5	0.05606559	0.05606559	5.03207698
Preflush	15	15			
Preflush	17.5	17.5	0.07341758	0.07341758	5.03207698
Preflush	20	20			
Preflush	22.5	22.5	0.09035478	0.09035478	4.91178829
Preflush	25	25			
Preflush	27.5	27.5	0.10784503	0.10784503	5.07217322
Preflush	30	30			
Preflush	32.5	32.5	0.12485137	0.12485137	4.93183641
Preflush	35	35			
Preflush	37.5	37.5	0.14165031	0.14165031	4.87169206
Preflush	40	40			
Preflush	42.5	42.5	0.15838011	0.15838011	4.85164395
Preflush	45	45			
Preflush	47.5	47.5	0.17510992	0.17510992	4.85164395
Preflush	50	50			
Preflush	52.5	52.5	0.19204712	0.19204712	4.91178829
Preflush	55	55			
Preflush	57.5	57.5	0.20898432	0.20898432	4.91178829
Preflush	60	60			
Preflush	62.5	62.5	0.22605978	0.22605978	4.95188452
Preflush	65	65			
Preflush	67.5	67.5	0.24313525	0.24313525	4.95188452
Preflush	70	70			
Preflush	72.5	72.5	0.26232613	0.26232613	5.56535686
Preflush	75	75			
Preflush	77.5	77.5	0.2794016	0.2794016	4.95188452
Preflush	80	80			
Preflush	82.5	82.5	0.29654619	0.29654619	4.97193264
Preflush	85	85			
Preflush	87.5	87.5	0.29862014	0.29862014	0.60144346
Preflush	90	90			
Preflush	92.5	92.5	0.29862014	0.29862014	-
Preflush	95	95			
Preflush	97.5	97.5	0.35641401	0.35641401	-
Preflush	100	100			
Preflush	102.5	102.5	0.37328208	0.37328208	4.89174018
Preflush	105	105			
Preflush	107.5	107.5	0.39028842	0.39028842	4.93183641
Preflush	110	110			
Preflush	112.5	112.5	0.40715649	0.40715649	4.89174018
Preflush	115	115			

Preflush	117.5	117.5	0.42402456	0.42402456	4.89174018
Preflush	120	120			
Preflush	122.5	122.5	0.44054697	0.44054697	4.7914996
Preflush	125	125			
Preflush	127.5	127.5	0.45713851	0.45713851	4.81154771
Preflush	130	130			
Preflush	132.5	132.5	0.47400658	0.47400658	4.89174018
Preflush	135	135			
Preflush	137.5	137.5	0.49066726	0.49066726	4.83159583
Preflush	140	140			
Preflush	142.5	142.5	0.50753533	0.50753533	4.89174018
Preflush	145	145			
Preflush	147.5	147.5	0.52447253	0.52447253	4.91178829
Preflush	150	150			
Preflush	152.5	152.5	0.54203191	0.54203191	5.09222133
Preflush	155	155			
Preflush	157.5	157.5	0.55931477	0.55931477	5.01202887
Preflush	160	160			
Preflush	162.5	162.5	0.57694328	0.57694328	5.11226945
Preflush	165	165			
Preflush	167.5	167.5	0.59415701	0.59415701	4.99198075
Preflush	170	170			
Preflush	172.5	172.5	0.61157813	0.61157813	5.0521251
Preflush	175	175			
Preflush	177.5	177.5	0.62588834	0.62588834	4.1499599
Preflush	180	180			
Preflush	182.5	182.5	0.64006028	0.64006028	4.10986367
Preflush	185	185			
Preflush	187.5	187.5	0.65437049	0.65437049	4.1499599
Preflush	190	190			
Preflush	192.5	192.5	0.6684733	0.6684733	4.08981556
Preflush	195	195			
Preflush	197.5	197.5	0.68271438	0.68271438	4.12991179
Preflush	200	200			
Preflush	202.5	202.5	0.69412106	0.69412106	3.30793905
Preflush	205	205			
Preflush	207.5	207.5	0.70504383	0.70504383	3.16760225
Preflush	210	210			
Preflush	212.5	212.5	0.7159666	0.7159666	3.16760225
Preflush	215	215			
Preflush	217.5	217.5	0.72668197	0.72668197	3.1074579
Preflush	220	220			
Preflush	222.5	222.5	0.73732821	0.73732821	3.08740978
Preflush	225	225			
Preflush	227.5	227.5	0.74790532	0.74790532	3.06736167
Preflush	230	230			
Preflush	232.5	232.5	0.75827503	0.75827503	3.00721732
Preflush	235	235			
Preflush	237.5	237.5	0.761939	0.761939	1.06255012
Preflush	240	240			
Preflush	242.5	242.5	0.77147914	0.77147914	2.76663994
Preflush	245	245			

Preflush	247.5	247.5	0.78177972	0.78177972	2.98716921
Preflush	250.05	250.05			
Preflush	252.55	252.55	0.7922877	0.7922877	3.01714213
Preflush	255.05	255.05			
Preflush	257.55	257.55	0.80265741	0.80265741	3.00721732
Preflush	260.05	260.05			
Preflush	262.55	262.55	0.81288886	0.81288886	2.96712109
Preflush	265.05	265.05			
Preflush	267.55	267.55	0.82346597	0.82346597	3.06736167
Preflush	270.05	270.05			
Preflush	272.55	272.55	0.83024085	0.83024085	1.96471532
Preflush	275.05	275.05			
Preflush	277.55	277.55	0.83915881	0.83915881	2.5862069
Preflush	280.05	280.05			
Preflush	282.55	282.55	0.84821503	0.84821503	2.62630313
Preflush	285.05	285.05			
Preflush	287.55	287.55	0.85678732	0.85678732	2.48596632
Preflush	290.05	290.05			
Preflush	292.55	292.55	0.8637696	0.8637696	2.02485966
Preflush	295.05	295.05			
Preflush	297.55	297.55	0.8710284	0.8710284	2.10505213
Preflush	300.05	300.05			
Preflush	302.55	302.55	0.87787241	0.87787241	1.98476343
Preflush	305.05	305.05			
Preflush	307.55	307.55	0.88630645	0.88630645	2.44587009
Preflush	310.05	310.05			
Preflush	312.55	312.55	0.89474048	0.89474048	2.44587009
Preflush	315.05	315.05			
Preflush	317.55	317.55	0.90317452	0.90317452	2.44587009
Preflush	320.05	320.05			
Preflush	322.55	322.55	0.91147029	0.91147029	2.40577386
Preflush	325.05	325.05			
Preflush	327.55	327.55	0.91997345	0.91997345	2.4659182
Preflush	330.05	330.05			
Preflush	332.55	332.55	0.92778531	0.92778531	2.26543705
Preflush	335.05	335.05			
Preflush	337.55	337.55	0.93566629	0.93566629	2.28548516
Preflush	340.05	340.05			
Preflush	342.55	342.55	0.94154246	0.94154246	1.70408982
Preflush	345.05	345.05			
Preflush	347.55	347.55	0.94942344	0.94942344	2.28548516
Preflush	350.05	350.05			
Preflush	352.55	352.55	0.9572353	0.9572353	2.26543705
Preflush	355.05	355.05			
Preflush	357.55	357.55	0.96518541	0.96518541	2.30553328
Preflush	360.05	360.05			
Preflush	362.55	362.55	0.97327379	0.97327379	2.34562951
Preflush	365.05	365.05			
Preflush	367.55	367.55	0.9814313	0.9814313	2.36567763
Preflush	370.05	370.05			
Preflush	372.55	372.55	0.98530266	0.98530266	1.12269447
Preflush	375.05	375.05			

Preflush	377.55	377.55	0.9933219	0.9933219	2.3255814
Preflush	380.05	380.05			
Preflush	382.55	382.55	1.0005807	1.0005807	2.10505213
Preflush	385.05	385.05			
Preflush	387.55	387.55	1.00728645	1.00728645	1.9446672
Preflush	390.05	390.05			
Preflush	392.55	392.55	1.01413046	1.01413046	1.98476343
Preflush	395.05	395.05			
Preflush	397.55	397.55	1.02090535	1.02090535	1.96471532
Preflush	400.05	400.05			
Preflush	402.55	402.55	1.02781849	1.02781849	2.00481155
Preflush	405.05	405.05			
Preflush	407.55	407.55	1.03452424	1.03452424	1.9446672
Preflush	410.05	410.05			
Preflush	412.55	412.55	1.04143738	1.04143738	2.00481155
Preflush	415.05	415.05			
Preflush	417.55	417.55	1.04828139	1.04828139	1.98476343
Preflush	420.05	420.05			
Preflush	422.55	422.55	1.05505627	1.05505627	1.96471532
Preflush	425.05	425.05			
Preflush	427.55	427.55	1.06183115	1.06183115	1.96471532
Preflush	430.05	430.05			
Preflush	432.55	432.55	1.06867517	1.06867517	1.98476343
Preflush	435.05	435.05			
Preflush	437.55	437.55	1.07551918	1.07551918	1.98476343
Preflush	440.05	440.05			
Preflush	442.55	442.55	1.08236319	1.08236319	1.98476343
Preflush	445.05	445.05			
Preflush	447.55	447.55	1.0892072	1.0892072	1.98476343
Preflush	450.05	450.05			
Preflush	452.55	452.55	1.09570556	1.09570556	1.88452285
Preflush	455.05	455.05			
Preflush	457.55	457.55	1.10303349	1.10303349	2.12510024
Preflush	460.05	460.05			
Preflush	462.55	462.55	1.10932445	1.10932445	1.82437851
Preflush	465.05	465.05			
Preflush	467.55	467.55	1.11547715	1.11547715	1.78428228
Preflush	470.05	470.05			
Preflush	472.55	472.55	1.12211376	1.12211376	1.92461909
Preflush	475.05	475.05			
Preflush	477.55	477.55	1.12888864	1.12888864	1.96471532
Preflush	480.05	480.05			
Preflush	482.55	482.55	1.13552526	1.13552526	1.92461909
Preflush	485.05	485.05			
Preflush	487.55	487.55	1.14181622	1.14181622	1.82437851
Preflush	490.05	490.05			
Preflush	492.55	492.55	1.14776152	1.14776152	1.72413793
Preflush	495.05	495.05			
Preflush	497.55	497.55	1.15370683	1.15370683	1.72413793
Preflush	500.117	500.117			
Preflush	502.617	502.617	1.15965213	1.15965213	1.70133998
Preflush	505.117	505.117			

Preflush	507.617	507.617	1.1655283	1.1655283	1.70408982
Preflush	510.117	510.117			
Preflush	512.617	512.617	1.17147361	1.17147361	1.72413793
Preflush	515.117	515.117			
Preflush	517.617	517.617	1.17721151	1.17721151	1.66399358
Preflush	520.117	520.117			
Preflush	522.617	522.617	1.18308769	1.18308769	1.70408982
Preflush	525.117	525.117			
Preflush	527.617	527.617	1.18889473	1.18889473	1.6840417
Preflush	530.117	530.117			
Preflush	532.617	532.617	1.19470177	1.19470177	1.6840417
Preflush	535.117	535.117			
Preflush	537.617	537.617	1.20057794	1.20057794	1.70408982
Preflush	540.117	540.117			
Preflush	542.617	542.617	1.20631585	1.20631585	1.66399358
Preflush	545.117	545.117			
Preflush	547.617	547.617	1.21219202	1.21219202	1.70408982
Preflush	550.117	550.117			
Preflush	552.617	552.617	1.2178608	1.2178608	1.64394547
Preflush	555.117	555.117			
Preflush	557.617	557.617	1.22359871	1.22359871	1.66399358
Preflush	560.117	560.117			
Preflush	562.617	562.617	1.22919835	1.22919835	1.62389735
Preflush	565.117	565.117			
Preflush	567.617	567.617	1.23493626	1.23493626	1.66399358
Preflush	570.117	570.117			
Preflush	572.617	572.617	1.24053591	1.24053591	1.62389735
Preflush	575.117	575.117			
Preflush	577.617	577.617	1.24606642	1.24606642	1.60384924
Preflush	580.117	580.117			
Preflush	582.617	582.617	1.2515278	1.2515278	1.58380112
Preflush	585.117	585.117			
Preflush	587.617	587.617	1.25685092	1.25685092	1.54370489
Preflush	590.117	590.117			
Preflush	592.617	592.617	1.26238144	1.26238144	1.60384924
Preflush	595.117	595.117			
Preflush	597.617	597.617	1.26784282	1.26784282	1.58380112
Preflush	600.117	600.117			
Preflush	602.617	602.617	1.27344247	1.27344247	1.62389735
Preflush	605.117	605.117			
Preflush	607.617	607.617	1.27890385	1.27890385	1.58380112
Preflush	610.117	610.117			
Preflush	612.617	612.617	1.28443437	1.28443437	1.60384924
Preflush	615.117	615.117			
Preflush	617.617	617.617	1.28982662	1.28982662	1.56375301
Preflush	620.117	620.117			
Preflush	622.617	622.617	1.29508061	1.29508061	1.52365678
Preflush	625.117	625.117			
Preflush	627.617	627.617	1.30040373	1.30040373	1.54370489
Preflush	630.117	630.117			
Preflush	632.617	632.617	1.30579598	1.30579598	1.56375301
Preflush	635.117	635.117			

Preflush	637.617	637.617	1.31125736	1.31125736	1.58380112
Preflush	640.117	640.117			
Preflush	642.617	642.617	1.31651135	1.31651135	1.52365678
Preflush	645.117	645.117			
Preflush	647.617	647.617	1.32197273	1.32197273	1.58380112
Preflush	650.117	650.117			
Preflush	652.617	652.617	1.32729585	1.32729585	1.54370489
Preflush	655.117	655.117			
Preflush	657.617	657.617	1.33151287	1.33151287	1.22293504
Preflush	660.117	660.117			
Preflush	662.617	662.617	1.33600642	1.33600642	1.30312751
Preflush	665.117	665.117			
Preflush	667.617	667.617	1.34049996	1.34049996	1.30312751
Preflush	670.117	670.117			
Preflush	672.617	672.617	1.34547742	1.34547742	1.44346431
Preflush	675.117	675.117			
Preflush	677.617	677.617	1.35107707	1.35107707	1.62389735
Preflush	680.117	680.117			
Preflush	682.617	682.617	1.35695324	1.35695324	1.70408982
Preflush	685.117	685.117			
Preflush	687.617	687.617	1.36269115	1.36269115	1.66399358
Preflush	690.117	690.117			
Preflush	692.617	692.617	1.36773774	1.36773774	1.46351243
Preflush	695.117	695.117			
Preflush	697.617	697.617	1.37250781	1.37250781	1.38331997
Preflush	700.117	700.117			
Preflush	702.617	702.617	1.37727788	1.37727788	1.38331997
Preflush	705.117	705.117			
Preflush	707.617	707.617	1.38184056	1.38184056	1.32317562
Preflush	710.117	710.117			
Preflush	712.617	712.617	1.38688715	1.38688715	1.46351243
Preflush	715.117	715.117			
Preflush	717.617	717.617	1.39207201	1.39207201	1.50360866
Preflush	720.117	720.117			
Preflush	722.617	722.617	1.39691121	1.39691121	1.40336808
Preflush	725.117	725.117			
Preflush	727.617	727.617	1.40202693	1.40202693	1.48356055
Preflush	730.117	730.117			
Preflush	732.617	732.617	1.4070044	1.4070044	1.44346431
Preflush	735.117	735.117			
Preflush	737.617	737.617	1.41191273	1.41191273	1.4234162
Preflush	740.117	740.117			
Preflush	742.617	742.617	1.41695932	1.41695932	1.46351243
Preflush	745.117	745.117			
Preflush	747.617	747.617	1.42186765	1.42186765	1.4234162
Preflush	770.4	770.4			
Preflush	772.9	772.9	1.42401073	1.42401073	0.12290701
Preflush	775.4	775.4			
Preflush	777.9	777.9	1.42822775	1.42822775	1.22293504
Preflush	780.4	780.4			
Preflush	782.9	782.9	1.43265216	1.43265216	1.28307939
Preflush	785.4	785.4			

Preflush	787.9	787.9	1.43693831	1.43693831	1.24298316
Preflush	790.4	790.4			
Preflush	792.9	792.9	1.44212316	1.44212316	1.50360866
Preflush	795.4	795.4			
Preflush	797.9	797.9	1.44799934	1.44799934	1.70408982
Preflush	800.4	800.4			
Preflush	802.9	802.9	1.45366811	1.45366811	1.64394547
Preflush	805.4	805.4			
Preflush	807.9	807.9	1.45961342	1.45961342	1.72413793
Preflush	810.4	810.4			
Preflush	812.9	812.9	1.46548959	1.46548959	1.70408982
Preflush	815.4	815.4			
Preflush	817.9	817.9	1.46984487	1.46984487	1.26303128
Preflush	820.4	820.4			
Preflush	822.9	822.9	1.47461494	1.47461494	1.38331997
Preflush	825.4	825.4			
Preflush	827.9	827.9	1.4795924	1.4795924	1.44346431
Preflush	830.4	830.4			
Preflush	832.9	832.9	1.48422421	1.48422421	1.34322374
Preflush	835.4	835.4			
Preflush	837.9	837.9	1.48878688	1.48878688	1.32317562
Preflush	840.4	840.4			
Preflush	842.9	842.9	1.49328042	1.49328042	1.30312751
Preflush	845.4	845.4			
Preflush	847.9	847.9	1.49777397	1.49777397	1.30312751
Preflush	850.4	850.4			
Preflush	852.9	852.9	1.50261317	1.50261317	1.40336808
Preflush	855.4	855.4			
Preflush	857.9	857.9	1.5075215	1.5075215	1.4234162
Preflush	860.4	860.4			
Preflush	862.9	862.9	1.51222244	1.51222244	1.36327185
Preflush	865.4	865.4			
Preflush	867.9	867.9	1.51713077	1.51713077	1.4234162
Preflush	870.4	870.4			
0.5% AM	0	1486.95	0	1.5171308	0
0.5% AM	5	1491.95	0.00740151	1.52453251	2.14643932
0.5% AM	10	1496.95			
0.5% AM	15	1501.95	0.01763912	1.53477012	1.48445336
0.5% AM	20	1506.95			
0.5% AM	25	1511.95	0.0300211	1.5471521	1.79538616
0.5% AM	30	1516.95			
0.5% AM	35	1521.95	0.04274894	1.55987994	1.84553661
0.5% AM	40	1526.95			
0.5% AM	45	1531.95	0.05568429	1.57281529	1.87562688
0.5% AM	50	1536.95			
0.5% AM	55	1541.95	0.06861965	1.58575065	1.87562688
0.5% AM	60	1546.95			
0.5% AM	65	1551.95	0.08162418	1.59875518	1.88565697
0.5% AM	70	1556.95			
0.5% AM	75	1561.95	0.09469789	1.61182889	1.89568706
0.5% AM	80	1566.95			
0.5% AM	85	1571.95	0.10887836	1.62600936	2.05616851

0.5% AM	90	1576.95			
0.5% AM	95	1581.95	0.12347387	1.64060487	2.11634905
0.5% AM	100	1586.95			
0.5% AM	105	1591.95	0.13869194	1.65582294	2.20661986
0.5% AM	110	1596.95			
0.5% AM	115	1601.95	0.15508595	1.67221695	2.37713139
0.5% AM	120	1606.95			
0.5% AM	125	1611.95	0.17300176	1.69013276	2.59779338
0.5% AM	130	1616.95			
0.5% AM	135	1621.95	0.19326946	1.71040046	2.93881645
0.5% AM	140	1626.95			
0.5% AM	145	1631.95	0.21519732	1.73232832	3.17953862
0.5% AM	150	1636.95			
0.5% AM	155	1641.95	0.23795525	1.75508625	3.2998997
0.5% AM	160	1646.95			
0.5% AM	165	1651.95	0.26306506	1.78019606	3.64092277
0.5% AM	170	1656.95			
0.5% AM	175	1661.95	0.287829	1.80496	3.59077232
0.5% AM	180	1666.95			
0.5% AM	185	1671.95	0.31356137	1.83069237	3.73119358
0.5% AM	190	1676.95			
0.5% AM	195	1681.95	0.34102307	1.85815407	3.98194584
0.5% AM	200	1686.95			
0.5% AM	205	1691.95	0.36793138	1.88506238	3.90170512
0.5% AM	210	1696.95			
0.5% AM	215	1701.95	0.3963615	1.9134925	4.1223671
0.5% AM	220	1706.95			
0.5% AM	225	1711.95	0.42486079	1.94199179	4.13239719
0.5% AM	230	1716.95			
0.5% AM	234.81	1721.76	0.45190745	1.96903845	3.99772201
0.5% AM	237.31	1724.26	0.46020821	1.97733921	4.81444333
0.5% AM	239.81	1726.76			
0.5% AM	242.31	1729.26	0.47694809	1.99407909	4.85456369
0.5% AM	244.81	1731.76			
0.5% AM	247.31	1734.26	0.49368796	2.01081896	4.85456369
0.5% AM	249.81	1736.76			
0.5% AM	252.31	1739.26	0.51042784	2.02755884	4.85456369
0.5% AM	254.81	1741.76			
0.5% AM	257.31	1744.26	0.52716771	2.04429871	4.85456369
0.5% AM	259.81	1746.76			
0.5% AM	262.31	1749.26	0.54397676	2.06110776	4.87462387
0.5% AM	264.81	1751.76			
0.5% AM	267.31	1754.26	0.56071663	2.07784763	4.85456369
0.5% AM	269.81	1756.76			
0.5% AM	272.31	1759.26	0.57766403	2.09479503	4.91474423
0.5% AM	274.81	1761.76			
0.5% AM	277.31	1764.26	0.59426556	2.11139656	4.81444333
0.5% AM	279.81	1766.76			
0.5% AM	282.31	1769.26	0.61114378	2.12827478	4.89468405
0.5% AM	284.81	1771.76			
0.5% AM	287.31	1774.26	0.62781448	2.14494548	4.83450351
0.5% AM	289.81	1776.76			

0.5% AM	292.31	1779.26	0.64455435	2.16168535	4.85456369
0.5% AM	294.81	1781.76			
0.5% AM	297.31	1784.26	0.66129423	2.17842523	4.85456369
0.5% AM	299.81	1786.76			
0.5% AM	302.31	1789.26	0.67824162	2.19537262	4.91474423
0.5% AM	304.81	1791.76			
0.5% AM	307.31	1794.26	0.6949815	2.2121125	4.85456369
0.5% AM	309.81	1796.76			
0.5% AM	312.31	1799.26	0.71179054	2.22892154	4.87462387
0.5% AM	314.81	1801.76			
0.5% AM	317.31	1804.26	0.72866876	2.24579976	4.89468405
0.5% AM	319.81	1806.76			
0.5% AM	322.31	1809.26	0.74547781	2.26260881	4.87462387
0.5% AM	324.81	1811.76			
0.5% AM	327.31	1814.26	0.74547781	2.26260881	0
0.5% AM	329.81	1816.76			
0.5% AM	332.31	1819.26	0.76055753	2.27768853	4.37311936
0.5% AM	334.81	1821.76			
0.5% AM	337.31	1824.26	0.77743576	2.29456676	4.89468405
0.5% AM	339.81	1826.76			
0.5% AM	342.31	1829.26	0.7942448	2.3113758	4.87462387
0.5% AM	344.81	1831.76			
0.5% AM	347.31	1834.26	0.81091551	2.32804651	4.83450351
0.5% AM	349.81	1836.76			
0.5% AM	352.31	1839.26	0.82758621	2.34471721	4.83450351
0.5% AM	354.81	1841.76			
0.5% AM	357.31	1844.26	0.84418774	2.36131874	4.81444333
0.5% AM	359.81	1846.76			
0.5% AM	362.31	1849.26	0.86113513	2.37826613	4.91474423
0.5% AM	364.81	1851.76			
0.5% AM	367.31	1854.26	0.87773666	2.39486766	4.81444333
0.5% AM	369.81	1856.76			
0.5% AM	372.31	1859.26	0.89454571	2.41167671	4.87462387
0.5% AM	374.81	1861.76			
0.5% AM	377.31	1864.26	0.91128558	2.42841658	4.85456369
0.5% AM	379.81	1866.76			
0.5% AM	382.31	1869.26	0.92809463	2.44522563	4.87462387
0.5% AM	384.81	1871.76			
0.5% AM	387.31	1874.26	0.94490368	2.46203468	4.87462387
0.5% AM	389.81	1876.76			
0.5% AM	392.31	1879.26	0.96171272	2.47884372	4.87462387
0.5% AM	394.81	1881.76			
0.5% AM	397.31	1884.26	0.97859095	2.49572195	4.89468405
0.5% AM	399.81	1886.76			
0.5% AM	402.31	1889.26	0.99533082	2.51246182	4.85456369
0.5% AM	404.81	1891.76			
0.5% AM	407.31	1894.26	1.01220904	2.52934004	4.89468405
0.5% AM	409.81	1896.76			
0.5% AM	412.31	1899.26	1.02894892	2.54607992	4.85456369
0.5% AM	414.81	1901.76			
0.5% AM	417.31	1904.26	1.04568879	2.56281979	4.85456369
0.5% AM	419.81	1906.76			

0.5% AM	422.31	1909.26	1.06242867	2.57955967	4.85456369
0.5% AM	424.81	1911.76			
0.5% AM	427.31	1914.26	1.07916854	2.59629954	4.85456369
0.5% AM	429.81	1916.76			
0.5% AM	432.31	1919.26	1.09577007	2.61290107	4.81444333
0.5% AM	434.81	1921.76			
0.5% AM	437.31	1924.26	1.11257912	2.62971012	4.87462387
0.5% AM	439.81	1926.76			
0.5% AM	442.31	1929.26	1.12911147	2.64624247	4.79438315
0.5% AM	444.81	1931.76			
0.5% AM	447.31	1934.26	1.14578217	2.66291317	4.83450351
0.5% AM	449.81	1936.76			
0.5% AM	452.31	1939.26	1.16231453	2.67944553	4.79438315
0.5% AM	454.81	1941.76			
0.5% AM	457.31	1944.26	1.17884689	2.69597789	4.79438315
0.5% AM	459.81	1946.76			
0.5% AM	462.31	1949.26	1.19558676	2.71271776	4.85456369
0.5% AM	464.81	1951.76			
0.5% AM	467.31	1954.26	1.21211912	2.72925012	4.79438315
0.5% AM	469.81	1956.76			
0.5% AM	472.31	1959.26	1.22865147	2.74578247	4.79438315
0.5% AM	474.81	1961.76			
0.5% AM	477.31	1964.26	1.24518383	2.76231483	4.79438315
0.5% AM	479.81	1966.76			
0.5% AM	482.31	1969.26	1.26157784	2.77870884	4.75426279
0.5% AM	484.86	1971.81			
0.5% AM	487.36	1974.31	1.27845606	2.79558706	4.84622183
0.5% AM	489.86	1976.81			
0.5% AM	492.36	1979.31	1.29491924	2.81205024	4.77432297
0.5% AM	494.86	1981.81			
0.5% AM	497.36	1984.31	1.3114516	2.8285826	4.79438315
0.5% AM	499.86	1986.81			
0.5% AM	502.36	1989.31	1.32805312	2.84518412	4.81444333
0.5% AM	504.86	1991.81			
0.5% AM	507.36	1994.31	1.34437796	2.86150896	4.73420261
0.5% AM	509.86	1996.81			
0.5% AM	512.36	1999.31	1.36077197	2.87790297	4.75426279
0.5% AM	514.86	2001.81			
0.5% AM	517.36	2004.31	1.37751185	2.89464285	4.85456369
0.5% AM	519.86	2006.81			
0.5% AM	522.36	2009.31	1.39418255	2.91131355	4.83450351
0.5% AM	524.86	2011.81			
0.5% AM	527.36	2014.31	1.41085325	2.92798425	4.83450351
0.5% AM	529.86	2016.81			
0.5% AM	532.36	2019.31	1.42752395	2.94465495	4.83450351
0.5% AM	534.86	2021.81			
0.5% AM	537.36	2024.31	1.444333	2.961464	4.87462387
0.5% AM	539.86	2026.81			
0.5% AM	542.36	2029.31	1.46114205	2.97827305	4.87462387
0.5% AM	544.86	2031.81			
0.5% AM	547.36	2034.31	1.47781275	2.99494375	4.83450351
0.5% AM	549.86	2036.81			

0.5% AM	552.36	2039.31	1.49455262	3.01168362	4.85456369
0.5% AM	554.86	2041.81			
0.5% AM	557.36	2044.31	1.50866392	3.02579492	4.09227683
0.5% AM	559.86	2046.81			
2% A.M.	0	2910.667	0	3.025795	0
2% A.M.	2.5	2913.167	0.0004831	3.0262781	0.28019614
2% A.M.	5	2915.667			
2% A.M.	7.5	2918.167	0.00938588	3.03518088	2.58180727
2% A.M.	10	2920.667			
2% A.M.	12.5	2923.167	0.02491399	3.05070899	2.89002302
2% A.M.	15	2925.667			
2% A.M.	17.5	2928.167	0.04023506	3.06603006	4.44311018
2% A.M.	20	2930.667			
2% A.M.	22.5	2933.167	0.05583219	3.08162719	3.59807421
2% A.M.	25	2935.667			
2% A.M.	27.5	2938.167	0.0713603	3.0971553	4.50315221
2% A.M.	30	2940.667			
2% A.M.	32.5	2943.167	0.08709545	3.11289045	4.56319424
2% A.M.	35	2945.667			
2% A.M.	37.5	2948.167	0.10269257	3.12848757	4.52316622
2% A.M.	40	2950.667			
2% A.M.	42.5	2953.167	0.11856575	3.14436075	4.60322226
2% A.M.	45	2955.667			
2% A.M.	47.5	2958.167	0.13416288	3.15995788	4.52316622
2% A.M.	50	2960.667			
2% A.M.	52.5	2963.167	0.14989803	3.17569303	4.56319424
2% A.M.	55	2965.667			
2% A.M.	57.5	2968.167	0.16563318	3.19142818	4.56319424
2% A.M.	60	2970.667			
2% A.M.	62.5	2973.167	0.1806782	3.2064732	4.36305414
2% A.M.	65	2975.667			
2% A.M.	67.5	2978.167	0.19461899	3.22041399	4.04282998
2% A.M.	70	2980.667			
2% A.M.	72.5	2983.167	0.20869781	3.23449281	4.082858
2% A.M.	75	2985.667			
2% A.M.	77.5	2988.167	0.22291466	3.24870966	4.12288602
2% A.M.	80	2990.667			
2% A.M.	82.5	2993.167	0.23713151	3.26292651	4.12288602
2% A.M.	85	2995.667			
2% A.M.	87.5	2998.167	0.25017512	3.27597012	3.78264785
2% A.M.	90	3000.667			
2% A.M.	92.5	3003.167	0.26218353	3.28797853	3.48243771
2% A.M.	95	3005.667			
2% A.M.	97.5	3008.167	0.27398489	3.29977989	3.42239568
2% A.M.	100	3010.667			
2% A.M.	102.5	3013.167	0.28557922	3.31137422	3.36235365
2% A.M.	105	3015.667			
2% A.M.	107.5	3018.167	0.29717354	3.32296854	3.36235365
2% A.M.	110	3020.667			
2% A.M.	112.5	3023.167	0.30883688	3.33463188	3.38236766
2% A.M.	115	3025.667			
2% A.M.	117.5	3028.167	0.31981007	3.34560507	3.18222756

2% A.M.	120	3030.667			
2% A.M.	122.5	3033.167	0.33050722	3.35630222	3.10217152
2% A.M.	125	3035.667			
2% A.M.	127.5	3038.167	0.3414114	3.3672064	3.16221355
2% A.M.	130	3040.667			
2% A.M.	132.5	3043.167	0.35197052	3.37776552	3.0621435
2% A.M.	135	3045.667			
2% A.M.	137.5	3048.167	0.36259865	3.38839365	3.08215751
2% A.M.	140	3050.667			
2% A.M.	142.5	3053.167	0.37246762	3.39826262	2.8620034
2% A.M.	145	3055.667			
2% A.M.	147.5	3058.167	0.38226759	3.40806259	2.84198939
2% A.M.	150	3060.667			
2% A.M.	152.5	3063.167	0.39186051	3.41765551	2.78194736
2% A.M.	155	3065.667			
2% A.M.	157.5	3068.167	0.4013154	3.4271104	2.74191934
2% A.M.	160	3070.667			
2% A.M.	162.5	3073.167	0.40959706	3.43539206	2.40168118
2% A.M.	165	3075.667			
2% A.M.	167.5	3078.167	0.41801675	3.44381175	2.4417092
2% A.M.	170	3080.667			
2% A.M.	172.5	3083.167	0.42643644	3.45223144	2.4417092
2% A.M.	175	3085.667			
2% A.M.	177.5	3088.167	0.43499415	3.46078915	2.48173722
2% A.M.	180	3090.667			
2% A.M.	182.5	3093.167	0.44341384	3.46920884	2.4417092
2% A.M.	185	3095.667			
2% A.M.	187.5	3098.167	0.45183352	3.47762852	2.4417092
2% A.M.	190	3100.667			
2% A.M.	192.5	3103.167	0.46046025	3.48625525	2.50175123
2% A.M.	195	3105.667			
2% A.M.	197.5	3108.167	0.46887994	3.49467494	2.4417092
2% A.M.	200	3110.667			
2% A.M.	202.5	3113.167	0.47736864	3.50316364	2.46172321
2% A.M.	205	3115.667			
2% A.M.	207.5	3118.167	0.48599537	3.51179037	2.50175123
2% A.M.	210	3120.667			
2% A.M.	212.5	3123.167	0.49441506	3.52021006	2.4417092
2% A.M.	215	3125.667			
2% A.M.	217.5	3128.167	0.50297277	3.52876777	2.48173722
2% A.M.	220	3130.667			
2% A.M.	222.5	3133.167	0.5115995	3.5373945	2.50175123
2% A.M.	225	3135.667			
2% A.M.	227.5	3138.167	0.52015721	3.54595221	2.48173722
2% A.M.	230	3140.667			
2% A.M.	232.5	3143.167	0.52892197	3.55471697	2.54177925
2% A.M.	235	3145.667			
2% A.M.	237.5	3148.167	0.5375487	3.5633437	2.50175123
2% A.M.	240	3150.667			
2% A.M.	242.5	3153.167	0.54617543	3.57197043	2.50175123
2% A.M.	245	3155.667			
2% A.M.	247.5	3158.167	0.5525247	3.5783197	1.8412889

2% A.M.	250.05	3160.717			
2% A.M.	252.55	3163.217	0.56094439	3.58673939	2.41753386
2% A.M.	255.05	3165.717			
2% A.M.	257.55	3168.217	0.569019	3.594814	2.34163915
2% A.M.	260.05	3170.717			
2% A.M.	262.55	3173.217	0.57716263	3.60295763	2.36165316
2% A.M.	265.05	3175.717			
2% A.M.	267.55	3178.217	0.58523725	3.61103225	2.34163915
2% A.M.	270.05	3180.717			
2% A.M.	272.55	3183.217	0.59331187	3.61910687	2.34163915
2% A.M.	275.05	3185.717			
2% A.M.	277.55	3188.217	0.60117945	3.62697445	2.28159712
2% A.M.	280.05	3190.717			
2% A.M.	282.55	3193.217	0.60925406	3.63504906	2.34163915
2% A.M.	285.05	3195.717			
2% A.M.	287.55	3198.217	0.61725967	3.64305467	2.32162514
2% A.M.	290.05	3200.717			
2% A.M.	292.55	3203.217	0.62554133	3.65133633	2.40168118
2% A.M.	295.05	3205.717			
2% A.M.	297.55	3208.217	0.63285679	3.65865179	2.12148504
2% A.M.	300.05	3210.717			
2% A.M.	302.55	3213.217	0.63975818	3.66555318	2.00140098
2% A.M.	305.05	3215.717			
2% A.M.	307.55	3218.217	0.64624548	3.67204048	1.88131692
2% A.M.	310.05	3220.717			
2% A.M.	312.55	3223.217	0.65259475	3.67838975	1.8412889
2% A.M.	315.05	3225.717			
2% A.M.	317.55	3228.217	0.65887501	3.68467001	1.82127489
2% A.M.	320.05	3230.717			
2% A.M.	322.55	3233.217	0.66536231	3.69115731	1.88131692
2% A.M.	325.05	3235.717			
2% A.M.	327.55	3238.217	0.67122848	3.69702348	1.70119083
2% A.M.	330.05	3240.717			
2% A.M.	332.55	3243.217	0.67785381	3.70364881	1.92134494
2% A.M.	335.05	3245.717			
2% A.M.	337.55	3248.217	0.68420308	3.70999808	1.8412889
2% A.M.	340.05	3250.717			
2% A.M.	342.55	3253.217	0.69062137	3.71641637	1.86130291
2% A.M.	345.05	3255.717			
2% A.M.	347.55	3258.217	0.69703965	3.72283465	1.86130291
2% A.M.	350.05	3260.717			
2% A.M.	352.55	3263.217	0.70345794	3.72925294	1.86130291
2% A.M.	355.05	3265.717			
2% A.M.	357.55	3268.217	0.70960017	3.73539517	1.78124687
2% A.M.	360.05	3270.717			
2% A.M.	362.55	3273.217	0.71608747	3.74188247	1.88131692
2% A.M.	365.05	3275.717			
2% A.M.	367.55	3278.217	0.72250575	3.74830075	1.86130291
2% A.M.	370.05	3280.717			
2% A.M.	372.55	3283.217	0.72933812	3.75513312	1.98138697
2% A.M.	375.05	3285.717			
2% A.M.	377.55	3288.217	0.73575641	3.76155141	1.86130291

2% A.M.	380.05	3290.717			
2% A.M.	382.55	3293.217	0.74245075	3.76824575	1.94135895
2% A.M.	385.05	3295.717			
2% A.M.	387.55	3298.217	0.74845495	3.77424995	1.74121885
2% A.M.	390.05	3300.717			
2% A.M.	392.55	3303.217	0.75390705	3.77970205	1.58110677
2% A.M.	395.05	3305.717			
2% A.M.	397.55	3308.217	0.75887604	3.78467104	1.44100871
2% A.M.	400.05	3310.717			
2% A.M.	402.55	3313.217	0.76439715	3.79019215	1.60112078
2% A.M.	405.05	3315.717			
2% A.M.	407.55	3318.217	0.76998727	3.79578227	1.62113479
2% A.M.	410.05	3320.717			
2% A.M.	412.55	3323.217	0.77550837	3.80130337	1.60112078
2% A.M.	415.05	3325.717			
2% A.M.	417.55	3328.217	0.78096047	3.80675547	1.58110677
2% A.M.	420.05	3330.717			
2% A.M.	422.55	3333.217	0.78655059	3.81234559	1.62113479
2% A.M.	425.05	3335.717			
2% A.M.	427.55	3338.217	0.79193366	3.81772866	1.56109276
2% A.M.	430.05	3340.717			
2% A.M.	432.55	3343.217	0.79752378	3.82331878	1.62113479
2% A.M.	435.05	3345.717			
2% A.M.	437.55	3348.217	0.80290686	3.82870186	1.56109276
2% A.M.	440.05	3350.717			
2% A.M.	442.55	3353.217	0.80835895	3.83415395	1.58110677
2% A.M.	445.05	3355.717			
2% A.M.	447.55	3358.217	0.81381105	3.83960605	1.58110677
2% A.M.	450.05	3360.717			
2% A.M.	452.55	3363.217	0.81919413	3.84498913	1.56109276
2% A.M.	455.05	3365.717			
2% A.M.	457.55	3368.217	0.82471523	3.85051023	1.60112078
2% A.M.	460.05	3370.717			
2% A.M.	462.55	3373.217	0.82989127	3.85568627	1.50105074
2% A.M.	465.05	3375.717			
2% A.M.	467.55	3378.217	0.83534336	3.86113836	1.58110677
2% A.M.	470.05	3380.717			
2% A.M.	472.55	3383.217	0.84065743	3.86645243	1.54107876
2% A.M.	475.05	3385.717			
2% A.M.	477.55	3388.217	0.84610952	3.87190452	1.58110677
2% A.M.	480.05	3390.717			
2% A.M.	482.55	3393.217	0.84610952	3.87190452	
2% A.M.	485.05	3395.717			
2% A.M.	487.55	3398.217	0.85169964	3.87749464	1.62113479
2% A.M.	490.05	3400.717			
2% A.M.	492.55	3403.217	0.8570137	3.8828087	1.54107876
2% A.M.	495.05	3405.717			
2% A.M.	497.55	3408.217	0.86212073	3.88791573	1.48103673
2% A.M.	500.116667	3410.78367			
2% A.M.	502.6167	3413.2837	0.86736578	3.89316078	1.50104086
2% A.M.	505.116733	3415.78373			
2% A.M.	507.616766	3418.28377	0.8724728	3.8982678	1.48101718

2% A.M.	510.116799	3420.7838			
2% A.M.	512.616832	3423.28383	0.87764884	3.90344384	1.50103092
2% A.M.	515.116865	3425.78387			
2% A.M.	517.616898	3428.2839	0.88282487	3.90861987	1.50103092
2% A.M.	520.116931	3430.78393			
2% A.M.	522.616964	3433.28396	0.8879319	3.9137269	1.48101718
2% A.M.	525.116997	3435.784			
2% A.M.	527.61703	3438.28403	0.89290089	3.91869589	1.44098969
2% A.M.	530.117063	3440.78406			
2% A.M.	532.617096	3443.2841	0.89800792	3.92380292	1.48101718
2% A.M.	535.117129	3445.78413			
2% A.M.	537.617162	3448.28416	0.9029079	3.9287029	1.42097594
2% A.M.	540.117195	3450.7842			
2% A.M.	542.617228	3453.28423	0.90801492	3.93380992	1.48101718
2% A.M.	545.117261	3455.78426			
2% A.M.	547.617294	3458.28429	0.91277687	3.93857187	1.38094845
2% A.M.	550.117327	3460.78433			
2% A.M.	552.61736	3463.28436	0.91767686	3.94347186	1.42097594
2% A.M.	555.117393	3465.78439			
2% A.M.	557.617426	3468.28443	0.92250782	3.94830282	1.40096219
2% A.M.	560.117459	3470.78446			
2% A.M.	562.617492	3473.28449	0.92733879	3.95313379	1.40096219
2% A.M.	565.117525	3475.78453			
2% A.M.	567.617558	3478.28456	0.93265286	3.95844786	1.54105841
2% A.M.	570.117591	3480.78459			
2% A.M.	572.617624	3483.28462	0.93769087	3.96348587	1.46100343
2% A.M.	575.117657	3485.78466			
2% A.M.	577.61769	3488.28469	0.94272888	3.96852388	1.46100343
2% A.M.	580.117723	3490.78472			
2% A.M.	582.617756	3493.28476	0.94790491	3.97369991	1.50103092
2% A.M.	585.117789	3495.78479			
2% A.M.	587.617822	3498.28482	0.95308095	3.97887595	1.50103092
2% A.M.	590.117855	3500.78486			
2% A.M.	592.617888	3503.28489	0.95811896	3.98391396	1.46100343
2% A.M.	595.117921	3505.78492			
2% A.M.	597.617954	3508.28495	0.96322598	3.98902098	1.48101718
2% A.M.	600.117987	3510.78499			
2% A.M.	602.61802	3513.28502	0.96833301	3.99412801	1.48101718
2% A.M.	605.118053	3515.78505			
2% A.M.	607.618086	3518.28509	0.97323299	3.99902799	1.42097594
2% A.M.	610.118119	3520.78512			
2% A.M.	612.618152	3523.28515	0.97820198	4.00399698	1.44098969
2% A.M.	615.118185	3525.78519			
2% A.M.	617.618218	3528.28522	0.98344703	4.00924203	1.52104467
2% A.M.	620.118251	3530.78525			
2% A.M.	622.618284	3533.28528	0.98938222	4.01517722	1.72118212
2% A.M.	625.118317	3535.78532			
2% A.M.	627.61835	3538.28535	0.99531741	4.02111241	1.72118212
2% A.M.	630.118383	3540.78538			
2% A.M.	632.618416	3543.28542	1.00111457	4.02690957	1.68115463
2% A.M.	635.118449	3545.78545			
2% A.M.	637.618482	3548.28548	1.00698075	4.03277575	1.70116838

2% A.M.	640.118515	3550.78552			
2% A.M.	642.618548	3553.28555	1.01215679	4.03795179	1.50103092
2% A.M.	645.118581	3555.78558			
2% A.M.	647.618614	3558.28561	1.01747085	4.04326585	1.54105841
2% A.M.	650.118647	3560.78565			
2% A.M.	652.61868	3563.28568	1.02278491	4.04857991	1.54105841
2% A.M.	655.118713	3565.78571			
2% A.M.	657.618746	3568.28575	1.02816799	4.05396299	1.56107216
2% A.M.	660.118779	3570.78578			
2% A.M.	662.618812	3573.28581	1.03355107	4.05934607	1.56107216
2% A.M.	665.118845	3575.78585			
2% A.M.	667.618878	3578.28588	1.03900316	4.06479816	1.5810859
2% A.M.	670.118911	3580.78591			
2% A.M.	672.618944	3583.28594	1.04431723	4.07011223	1.54105841
2% A.M.	675.118977	3585.78598			
2% A.M.	677.61901	3588.28601	1.04983834	4.07563334	1.60109965
2% A.M.	680.119043	3590.78604			
2% A.M.	682.619076	3593.28608	1.05542846	4.08122346	1.6211134
2% A.M.	685.119109	3595.78611			
2% A.M.	687.619142	3598.28614	1.06005238	4.08584738	1.34092096
2% A.M.	690.119175	3600.78618			
2% A.M.	692.619208	3603.28621	1.06377913	4.08957413	1.08074226
2% A.M.	695.119241	3605.78624			
2% A.M.	697.619274	3608.28627	1.0676439	4.0934389	1.12076976
2% A.M.	700.119307	3610.78631			
2% A.M.	702.61934	3613.28634	1.07137065	4.09716565	1.08074226
2% A.M.	705.119373	3615.78637			
2% A.M.	707.619406	3618.28641	1.07516641	4.10096141	1.10075601
2% A.M.	710.119439	3620.78644			
2% A.M.	712.619472	3623.28647	1.07889316	4.10468816	1.08074226
2% A.M.	715.119505	3625.78651			
2% A.M.	717.619538	3628.28654	1.08282694	4.10862194	1.1407835
2% A.M.	720.119571	3630.78657			
2% A.M.	722.619604	3633.2866	1.08648468	4.11227968	1.06072852
2% A.M.	725.119637	3635.78664			
2% A.M.	727.61967	3638.28667	1.09028044	4.11607544	1.10075601
2% A.M.	730.119703	3640.7867			
2% A.M.	732.619736	3643.28674	1.09386916	4.11966416	1.04071477
2% A.M.	735.119769	3645.78677			
2% A.M.	737.619802	3648.2868	1.09766492	4.12345992	1.10075601
2% A.M.	740.119835	3650.78684			
2% A.M.	742.619868	3653.28687	1.10028744	4.12608244	0.76052233
2% A.M.	745.119901	3655.7869			
2% A.M.	747.619934	3658.28693	1.10449729	4.13029229	1.22083848
2% A.M.	750.18333	3660.85033			
2% A.M.	752.6833	3663.3503	1.10850009	4.13429509	1.14628546
2% A.M.	755.18327	3665.85027			
2% A.M.	757.68324	3668.35024	1.11250289	4.13829789	1.1608265
2% A.M.	760.18321	3670.85021			
2% A.M.	762.68318	3673.35018	1.11643668	4.14223168	1.14081225
2% A.M.	765.18315	3675.85015			
2% A.M.	767.68312	3678.35012	1.12043948	4.14623448	1.1608265

2% A.M.	770.18309	3680.85009			
2% A.M.	772.68306	3683.35006	1.12423524	4.15003024	1.10078375
2% A.M.	775.18303	3685.85003			
2% A.M.	777.683	3688.35	1.128031	4.153826	1.10078375
2% A.M.	780.18297	3690.84997			
2% A.M.	782.68294	3693.34994	1.13175775	4.15755275	1.0807695
2% A.M.	785.18291	3695.84991			
2% A.M.	787.68288	3698.34988	1.13541548	4.16121048	1.06075525
2% A.M.	790.18285	3700.84985			
2% A.M.	792.68282	3703.34982	1.1394873	4.1652823	1.18084075
2% A.M.	795.18279	3705.84979			
2% A.M.	797.68276	3708.34976	1.1434901	4.1692851	1.1608265
2% A.M.	800.18273	3710.84973			
2% A.M.	802.6827	3713.3497	1.14756191	4.17335691	1.18084075
2% A.M.	805.18267	3715.84967			
2% A.M.	807.68264	3718.34964	1.1514957	4.1772907	1.14081225
2% A.M.	810.18261	3720.84961			
2% A.M.	812.68258	3723.34958	1.1554985	4.1812935	1.1608265
2% A.M.	815.18255	3725.84955			
2% A.M.	817.68252	3728.34952	1.15936328	4.18515828	1.120798
2% A.M.	820.18249	3730.84949			
2% A.M.	822.68246	3733.34946	1.16322805	4.18902305	1.120798
2% A.M.	825.18243	3735.84943			
2% A.M.	827.6824	3738.3494	1.16702381	4.19281881	1.10078375
2% A.M.	830.18237	3740.84937			
2% A.M.	832.68234	3743.34934	1.17081957	4.19661457	1.10078375
2% A.M.	835.18231	3745.84931			
2% A.M.	837.68228	3748.34928	1.17440829	4.20020329	1.040741
2% A.M.	840.18225	3750.84925			
2% A.M.	842.68222	3753.34922	1.17813504	4.20393004	1.0807695
2% A.M.	845.18219	3755.84919			
2% A.M.	847.68216	3758.34916	1.18165474	4.20744974	1.02072675
2% A.M.	850.18213	3760.84913			
2% A.M.	852.6821	3763.3491	1.18517445	4.21096945	1.02072675
2% A.M.	855.18207	3765.84907			
2% A.M.	857.68204	3768.34904	1.18848711	4.21428211	0.960684
2% A.M.	860.18201	3770.84901			
2% A.M.	862.68198	3773.34898	1.19186879	4.21766379	0.98069825
2% A.M.	865.18195	3775.84895			
2% A.M.	867.68192	3778.34892	1.19511244	4.22090744	0.94066975
2% A.M.	870.18189	3780.84889			
2% A.M.	872.68186	3783.34886	1.19835609	4.22415109	0.94066975
2% A.M.	875.18183	3785.84883			
2% A.M.	877.6818	3788.3488	1.19987439	4.22566939	0.4403135
5% A.M.	0	4351.81667	0	4.225669	
5% A.M.	5	4356.81667	0.01196769	4.23763669	3.4706293
5% A.M.	10	4361.81667			
5% A.M.	15	4366.81667	0.04333128	4.26900028	4.54772115
5% A.M.	20	4371.81667			
5% A.M.	25	4376.81667	0.07311294	4.29878194	4.31834048
5% A.M.	30	4381.81667			
5% A.M.	35	4386.81667	0.10516433	4.33083333	4.64745188

5% A.M.	40	4391.81667			
5% A.M.	45	4396.81667	0.1376284	4.3632974	4.70729032
5% A.M.	50	4401.81667			
5% A.M.	55	4406.81667	0.17043637	4.39610537	4.75715568
5% A.M.	60	4411.81667			
5% A.M.	65	4416.81667	0.20324434	4.42891334	4.75715568
5% A.M.	70	4421.81667			
5% A.M.	75	4426.81667	0.23447038	4.46013938	4.52777501
5% A.M.	80	4431.81667			
5% A.M.	85	4436.81667	0.26046915	4.48613815	3.76982148
5% A.M.	90	4441.81667			
5% A.M.	95	4446.81667	0.28089675	4.50656575	2.96200259
5% A.M.	100	4451.81667			
5% A.M.	105	4456.81667	0.29802292	4.52369192	2.4832951
5% A.M.	110	4461.81667			
5% A.M.	115	4466.81667	0.31088475	4.53655375	1.8649646
5% A.M.	120	4471.81667			
5% A.M.	125	4476.81667	0.32223342	4.54790242	1.645557
5% A.M.	130	4481.81667			
5% A.M.	135	4486.81667	0.33330697	4.55897597	1.60566471
5% A.M.	140	4491.81667			
5% A.M.	145	4496.81667	0.3444493	4.5701183	1.61563778
5% A.M.	150	4501.81667			
5% A.M.	155	4506.81667	0.35552285	4.58119185	1.60566471
5% A.M.	160	4511.81667			
5% A.M.	165	4516.81667	0.36597738	4.59164638	1.51590705
5% A.M.	170	4521.81667			
5% A.M.	175	4526.81667	0.37457485	4.60024385	1.24663409
5% A.M.	180	4531.81667			
5% A.M.	185	4536.81667	0.38358501	4.60925401	1.30647252
5% A.M.	190	4541.81667			
5% A.M.	195	4546.81667	0.39259517	4.61826417	1.30647252
5% A.M.	200	4551.81667			
5% A.M.	205	4556.81667	0.39885413	4.62452313	0.90754962
5% A.M.	210	4561.81667			
5% A.M.	215	4566.81667	0.40559455	4.63126355	0.97736112
5% A.M.	220	4571.81667			
5% A.M.	225	4576.81667	0.40772672	4.63339572	0.30916525
5% A.M.	230	4581.81667			
5% A.M.	235	4586.81667	0.41219741	4.63786641	0.64824973
5% A.M.	240	4591.81667			
5% A.M.	245	4596.81667	0.41838759	4.64405659	0.89757654
5% A.M.	250	4601.81667			
5% A.M.	255	4606.81667	0.42306462	4.64873362	0.67816894
5% A.M.	260	4611.81667			
5% A.M.	265	4616.81667	0.42726019	4.65292919	0.60835743
5% A.M.	270	4621.81667			
5% A.M.	275	4626.81667	0.43338159	4.65905059	0.88760347
5% A.M.	280	4631.81667			
5% A.M.	285	4636.81667	0.43854008	4.66420908	0.74798045
5% A.M.	290	4641.81667			
5% A.M.	295	4646.81667	0.44362979	4.66929879	0.73800738

5% A.M.	300	4651.81667			
5% A.M.	305	4656.81667	0.44837559	4.67404459	0.68814202
5% A.M.	310	4661.81667			
5% A.M.	315	4666.81667	0.45263994	4.67830894	0.61833051
5% A.M.	320	4671.81667			
5% A.M.	325	4676.81667	0.45683551	4.68250451	0.60835743
5% A.M.	330	4681.81667			
5% A.M.	335	4686.81667	0.46089352	4.68656252	0.58841129
5% A.M.	340	4691.81667			
5% A.M.	345	4696.81667	0.46522665	4.69089565	0.62830358
5% A.M.	350	4701.81667			
5% A.M.	355	4706.81667	0.46955977	4.69522877	0.62830358
5% A.M.	360	4711.81667			
5% A.M.	365	4716.81667	0.4738929	4.6995619	0.62830358
5% A.M.	370	4721.81667			
5% A.M.	375	4726.81667	0.47808847	4.70375747	0.60835743
5% A.M.	380	4731.81667			
5% A.M.	385	4736.81667	0.4820777	4.7077467	0.57843822
5% A.M.	390	4741.81667			
5% A.M.	395	4746.81667	0.48627327	4.71194227	0.60835743
5% A.M.	400	4751.81667			
5% A.M.	405	4756.81667	0.49033128	4.71600028	0.58841129
5% A.M.	417.6333	4769.44997			
5% A.M.	432.6333	4784.44997	0.50133605	4.72700505	0.57745243
5% A.M.	447.6333	4799.44997			
5% A.M.	462.6333	4814.44997	0.51254716	4.73821616	0.54187028
5% A.M.	477.6333	4829.44997			
5% A.M.	492.6333	4844.44997	0.52327681	4.74894581	0.51859978
5% A.M.	507.6333	4859.44997			
5% A.M.	522.6333	4874.44997	0.5331811	4.7588501	0.47870749
5% A.M.	537.6333	4889.44997			
5% A.M.	552.6333	4904.44997	0.54260393	4.76827293	0.45543699
5% A.M.	567.6333	4919.44997			
5% A.M.	582.6333	4934.44997	0.54968826	4.77535726	0.34240883
5% A.M.	597.6333	4949.44997			
5% A.M.	612.6333	4964.44997	0.55897353	4.78464253	0.44878827
5% A.M.	627.6333	4979.44997			
5% A.M.	642.6333	4994.44997	0.56695199	4.79262099	0.38562548
5% A.M.	657.6333	5009.44997			
5% A.M.	672.6333	5024.44997	0.57348607	4.79915507	0.31581397
5% A.M.	687.6333	5039.44997			
5% A.M.	702.6333	5054.44997	0.57871334	4.80438234	0.25265118
5% A.M.	717.6333	5069.44997			
5% A.M.	732.6333	5084.44997	0.5849723	4.8106413	0.30251654
5% A.M.	747.6333	5099.44997			
5% A.M.	762.6333	5114.44997	0.59068102	4.81635002	0.27592168
5% A.M.	777.6333	5129.44997			
5% A.M.	792.6333	5144.44997	0.59632097	4.82198997	0.27259732
5% A.M.	807.6333	5159.44997			
5% A.M.	822.6333	5174.44997	0.60182335	4.82749235	0.26594861
5% A.M.	837.6333	5189.44997			
5% A.M.	852.6333	5204.44997	0.60725696	4.83292596	0.26262425

5% A.M.	867.6333	5219.44997			
5% A.M.	882.6333	5234.44997	0.61262178	4.83829078	0.25929989
5% A.M.	897.6333	5249.44997			
5% A.M.	912.6333	5264.44997	0.61764271	4.84331171	0.2426781
5% A.M.	927.6333	5279.44997			
5% A.M.	942.6333	5294.44997	0.62266364	4.84833264	0.2426781
5% A.M.	957.6333	5309.44997			
5% A.M.	972.6333	5324.44997	0.62768456	4.85335356	0.2426781
5% A.M.	987.6333	5339.44997			
5% A.M.	1002.6333	5354.44997	0.63256793	4.85823693	0.23602939
5% A.M.	1017.6333	5369.44997			
5% A.M.	1032.6333	5384.44997	0.63717618	4.86284518	0.22273196
5% A.M.	1047.6333	5399.44997			
5% A.M.	1062.6333	5414.44997	0.64164686	4.86731586	0.21608324
5% A.M.	1077.6333	5429.44997			
5% A.M.	1092.6333	5444.44997	0.64604877	4.87171777	0.21275888
5% A.M.	1107.6333	5459.44997			
5% A.M.	1122.6333	5474.44997	0.65051946	4.87618846	0.21608324
5% A.M.	1137.6333	5489.44997			
5% A.M.	1152.6333	5504.44997	0.65512771	4.88079671	0.22273196
5% A.M.	1167.6333	5519.44997			
5% A.M.	1182.6333	5534.44997	0.65973595	4.88540495	0.22273196
5% A.M.	1197.6333	5549.44997			
5% A.M.	1212.6333	5564.44997	0.66420664	4.88987564	0.21608324
5% A.M.	1227.6333	5579.44997			
5% A.M.	1242.6333	5594.44997	0.66895245	4.89462145	0.22938067
5% A.M.	1257.6333	5609.44997			
5% A.M.	1272.6333	5624.44997	0.6739046	4.8995736	0.23935374
5% A.M.	1287.6333	5639.44997			
5% A.M.	1302.6333	5654.44997	0.67926942	4.90493842	0.25929989
5% A.M.	1317.6333	5669.44997			
5% A.M.	1332.6333	5684.44997	0.68415279	4.90982179	0.23602939
5% A.M.	1347.6333	5699.44997			
5% A.M.	1362.6333	5714.44997	0.68917371	4.91484271	0.2426781
5% A.M.	1377.6333	5729.44997			
5% A.M.	1392.6333	5744.44997	0.69460732	4.92027632	0.26262425
5% A.M.	1407.6333	5759.44997			
5% A.M.	1422.6333	5774.44997	0.70024726	4.92591626	0.27259732
5% A.M.	1437.6333	5789.44997			
5% A.M.	1452.6333	5804.44997	0.70540575	4.93107475	0.24932682
5% A.M.	1467.6333	5819.44997			
5% A.M.	1482.6333	5834.44997	0.70994522	4.93561422	0.2194076
5% A.M.	1497.6333	5849.44997			
5% A.M.	1512.6333	5864.44997	0.71489736	4.94056636	0.23935374
5% A.M.	1527.6333	5879.44997			
5% A.M.	1542.6333	5894.44997	0.71978073	4.94544973	0.23602939
5% A.M.	1557.6333	5909.44997			
5% A.M.	1572.6333	5924.44997	0.725008	4.950677	0.25265118
5% A.M.	1587.6333	5939.44997			
5% A.M.	1602.6333	5954.44997	0.73057916	4.95624816	0.26927296
5% A.M.	1617.6333	5969.44997			
5% A.M.	1632.6333	5984.44997	0.73587521	4.96154421	0.25597553

5% A.M.	1647.6333	5999.44997			
5% A.M.	1662.6333	6014.44997	0.73883274	4.96450174	0.14294738
5% A.M.	1677.6333	6029.44997			
5% A.M.	1692.6333	6044.44997	0.74302831	4.96869731	0.20278581
5% A.M.	1707.6333	6059.44997			
5% A.M.	1722.6333	6074.44997	0.74736143	4.97303043	0.20943453
5% A.M.	1737.6333	6089.44997			
5% A.M.	1752.6333	6104.44997	0.75183212	4.97750112	0.21608324
5% A.M.	1767.6333	6119.44997			
5% A.M.	1782.6333	6134.44997	0.75637159	4.98204059	0.2194076
5% A.M.	1797.6333	6149.44997			
5% A.M.	1812.6333	6164.44997	0.76097984	4.98664884	0.22273196
5% A.M.	1827.6333	6179.44997			
5% A.M.	1842.6333	6194.44997	0.76565686	4.99132586	0.22605631
5% A.M.	1857.6333	6209.44997			
5% A.M.	1872.6333	6224.44997	0.77047145	4.99614045	0.23270503
5% A.M.	1887.6333	6239.44997			
5% A.M.	1902.6333	6254.44997	0.77391044	4.99957944	0.16621788
5% A.M.	1917.7	6269.51667			
5% A.M.	1932.7	6284.51667	0.77748699	5.00315599	0.17248311
5% A.M.	1947.7	6299.51667			
5% A.M.	1962.7	6314.51667	0.78044452	5.00611352	0.14294738
5% A.M.	1977.7	6329.51667			
5% A.M.	1992.7	6344.51667	0.78285182	5.00852082	0.11635251
5% A.M.	2007.7	6359.51667			
5% A.M.	2022.7	6374.51667	0.78512155	5.01079055	0.1097038
5% A.M.	2037.7	6389.51667			
5% A.M.	2052.7	6404.51667	0.78842298	5.01409198	0.15956916
5% A.M.	2067.7	6419.51667			
5% A.M.	2082.7	6434.51667	0.79165563	5.01732463	0.15624481
5% A.M.	2097.7	6449.51667			
5% A.M.	5827.75	10179.5667	0.79165563	5.01732463	0
5% A.M.	5832.75	10184.5667			
5% A.M.	5837.75	10189.5667	0.8033482	5.0290172	1.69542236
5% A.M.	5842.75	10194.5667			
5% A.M.	5847.75	10199.5667	0.83588105	5.06155005	4.71726339
5% A.M.	5852.75	10204.5667			
5% A.M.	5857.75	10209.5667	0.86745099	5.09311999	4.57764037
5% A.M.	5862.75	10214.5667			
5% A.M.	5867.75	10219.5667	0.89283074	5.11849974	3.68006383
5% A.M.	5872.75	10224.5667			
5% A.M.	5877.75	10229.5667	0.91449638	5.14016538	3.1415179
5% A.M.	5882.75	10234.5667			
5% A.M.	5887.75	10239.5667	0.93389228	5.15956128	2.8124065
5% A.M.	5892.75	10244.5667			
5% A.M.	5897.75	10249.5667	0.95328819	5.17895719	2.8124065
5% A.M.	5902.75	10254.5667			
5% A.M.	5907.75	10259.5667	0.97289044	5.19855944	2.84232572
5% A.M.	5912.75	10264.5667			
5% A.M.	5917.75	10269.5667	0.98671518	5.21238418	2.00458761
5% A.M.	5922.75	10274.5667			
5% A.M.	5927.75	10279.5667	1.0006087	5.2262777	2.01456069

5% A.M.	5932.75	10284.5667			
5% A.M.	5937.75	10289.5667	1.01463978	5.24030878	2.03450683
5% A.M.	5942.75	10294.5667			
5% A.M.	5947.75	10299.5667	1.02867086	5.25433986	2.03450683
5% A.M.	5952.75	10304.5667			
5% A.M.	5957.75	10309.5667	1.04242683	5.26809583	1.99461454
5% A.M.	5962.75	10314.5667			
5% A.M.	5967.75	10319.5667	1.05432573	5.27999473	1.72534158
5% A.M.	5972.75	10324.5667			
5% A.M.	5977.75	10329.5667	1.06622464	5.29189364	1.72534158
5% A.M.	5982.75	10334.5667			
5% A.M.	5987.75	10339.5667	1.07626649	5.30193549	1.45606861
5% A.M.	5992.75	10344.5667			
5% A.M.	5997.75	10349.5667	1.08644591	5.31211491	1.47601476
5% A.M.	6002.75	10354.5667			
5% A.M.	6007.75	10359.5667	1.0960063	5.3216753	1.38625711
5% A.M.	6012.75	10364.5667			
5% A.M.	6017.75	10369.5667	1.1041911	5.3298601	1.18679565
5% A.M.	6022.75	10374.5667			
5% A.M.	6027.75	10379.5667	1.11216956	5.33783856	1.15687643
5% A.M.	6032.75	10384.5667			
5% A.M.	6037.75	10389.5667	1.12014801	5.34581701	1.15687643
5% A.M.	6042.75	10394.5667			
5% A.M.	6047.75	10399.5667	1.12812647	5.35379547	1.15687643
5% A.M.	6052.75	10404.5667			
5% A.M.	6057.75	10409.5667	1.13610493	5.36177393	1.15687643
5% A.M.	6062.75	10414.5667			
5% A.M.	6067.75	10419.5667	1.14401461	5.36968361	1.14690336
5% A.M.	6072.75	10424.5667			
5% A.M.	6077.75	10429.5667	1.15206185	5.37773085	1.16684951
5% A.M.	6082.75	10434.5667			
5% A.M.	6087.75	10439.5667	1.1600403	5.3857093	1.15687643
5% A.M.	6092.75	10444.5667			
5% A.M.	6097.75	10449.5667	1.16678073	5.39244973	0.97736112
5% A.M.	6102.75	10454.5667			
5% A.M.	6107.75	10459.5667	1.17290213	5.39857113	0.88760347
5% A.M.	6112.75	10464.5667			
5% A.M.	6117.75	10469.5667	1.17902353	5.40469253	0.88760347
5% A.M.	6122.75	10474.5667			
5% A.M.	6127.75	10479.5667	1.18507616	5.41074516	0.8776304
5% A.M.	6132.75	10484.5667			
5% A.M.	6137.75	10489.5667	1.19112878	5.41679778	0.8776304
5% A.M.	6142.75	10494.5667			
5% A.M.	6147.75	10499.5667	1.19711262	5.42278162	0.86765733
5% A.M.	6152.75	10504.5667			
5% A.M.	6157.75	10509.5667	1.20123941	5.42690841	0.59838436
5% A.M.	6162.75	10514.5667			
5% A.M.	6167.75	10519.5667	1.2070857	5.4327547	0.84771118
5% A.M.	6172.75	10524.5667			
5% A.M.	6177.75	10529.5667	1.2128632	5.4385322	0.83773811
5% A.M.	6182.75	10534.5667			
5% A.M.	6187.75	10539.5667	1.2186407	5.4443097	0.83773811

5% A.M.	6192.75	10544.5667			
5% A.M.	6197.75	10549.5667	1.22434943	5.45001843	0.82776503
5% A.M.	6202.75	10554.5667			
5% A.M.	6207.75	10559.5667	1.23005815	5.45572715	0.82776503
5% A.M.	6212.75	10564.5667			
5% A.M.	6217.75	10569.5667	1.23576688	5.46143588	0.82776503
5% A.M.	6222.75	10574.5667			
5% A.M.	6227.75	10579.5667	1.24161316	5.46728216	0.84771118
5% A.M.	6232.75	10584.5667			
5% A.M.	6237.75	10589.5667	1.24821602	5.47388502	0.95741498
5% A.M.	6242.75	10594.5667			
5% A.M.	6247.75	10599.5667	1.26355392	5.48922292	2.22399521
5% A.M.	6252.75	10604.5667			
5% A.M.	6257.75	10609.5667	1.2789606	5.5046296	2.23396829
5% A.M.	6262.75	10614.5667			
5% A.M.	6267.75	10619.5667	1.2942985	5.5199675	2.22399521
5% A.M.	6272.75	10624.5667			
5% A.M.	6277.75	10629.5667	1.3096364	5.5353054	2.22399521
5% A.M.	6282.75	10634.5667			
5% A.M.	6287.75	10639.5667	1.32497429	5.55064329	2.22399521
5% A.M.	6292.75	10644.5667			
5% A.M.	6297.75	10649.5667	1.34017463	5.56584363	2.20404907
5% A.M.	6302.75	10654.5667			
5% A.M.	6307.75	10659.5667	1.35544375	5.58111275	2.21402214
5% A.M.	6312.75	10664.5667			
5% A.M.	6317.75	10669.5667	1.37098799	5.59665699	2.25391443
5% A.M.	6322.75	10674.5667			
5% A.M.	6327.8167	10679.6334	1.38880196	5.61447096	2.5659112
5% A.M.	6332.8167	10684.6334			
5% A.M.	6337.8167	10689.6334	1.39457946	5.62024846	0.83773811
5% A.M.	6342.8167	10694.6334			
5% A.M.	6347.8167	10699.6334	1.40620325	5.63187225	1.68544929
5% A.M.	6352.8167	10704.6334			
5% A.M.	6357.8167	10709.6334	1.41768948	5.64335848	1.66550314
5% A.M.	6362.8167	10714.6334			
5% A.M.	6367.8167	10719.6334	1.42910693	5.65477593	1.65553007
5% A.M.	6372.8167	10724.6334			
5% A.M.	6377.8167	10729.6334	1.44052438	5.66619338	1.65553007
5% A.M.	6382.8167	10734.6334			
5% A.M.	6387.8167	10739.6334	1.45194183	5.67761083	1.65553007
5% A.M.	6392.8167	10744.6334			
5% A.M.	6397.8167	10749.6334	1.46322172	5.68889072	1.63558392
5% A.M.	6402.8167	10754.6334			
5% A.M.	6407.8167	10759.6334	1.47463916	5.70030816	1.65553007
5% A.M.	6412.8167	10764.6334			
5% A.M.	6417.8167	10769.6334	1.48619417	5.71186317	1.67547621
5% A.M.	6422.8167	10774.6334			
5% A.M.	6427.8167	10779.6334	1.4976804	5.7233494	1.66550314
5% A.M.	6432.8167	10784.6334			
5% A.M.	6437.8167	10789.6334	1.50916663	5.73483563	1.66550314
5% A.M.	6442.8167	10794.6334			
5% A.M.	6447.8167	10799.6334	1.52072164	5.74639064	1.67547621

5% A.M.	6452.8167	10804.6334			
5% A.M.	6457.8167	10809.6334	1.53241421	5.75808321	1.69542236
5% A.M.	6462.8167	10814.6334			
5% A.M.	6467.8167	10819.6334	1.54445067	5.77011967	1.74528772
5% A.M.	6472.8167	10824.6334			
5% A.M.	6477.8167	10829.6334	1.56845483	5.79412383	3.48060237
5% A.M.	6482.8167	10834.6334			
5% A.M.	6487.8167	10839.6334	1.59232142	5.81799042	3.46065623
5% A.M.	6492.8167	10844.6334			
5% A.M.	6497.8167	10849.6334	1.61618802	5.84185702	3.46065623
5% A.M.	6502.8167	10854.6334			
5% A.M.	6507.8167	10859.6334	1.63998583	5.86565483	3.45068316
5% A.M.	6512.8167	10864.6334			
5% A.M.	6517.8167	10869.6334	1.66371487	5.88938387	3.44071008
5% A.M.	6522.8167	10874.6334			
5% A.M.	6527.8167	10879.6334	1.68758146	5.91325046	3.46065623
5% A.M.	6532.8167	10884.6334			
5% A.M.	6537.8167	10889.6334	1.71137928	5.93704828	3.45068316
5% A.M.	6542.8167	10894.6334			
5% A.M.	6547.8167	10899.6334	1.73503953	5.96070853	3.43073701
5% A.M.	6552.8167	10904.6334			
5% A.M.	6557.8167	10909.6334	1.75869979	5.98436879	3.43073701
5% A.M.	6562.8167	10914.6334			
5% A.M.	6567.8167	10919.6334	1.7824976	6.0081666	3.45068316
5% A.M.	6572.8167	10924.6334			
5% A.M.	6577.8167	10929.6334	1.80615786	6.03182686	3.43073701
5% A.M.	6582.8167	10934.6334			
5% A.M.	6587.8167	10939.6334	1.8285113	6.0541803	3.24124863
5% A.M.	6592.8167	10944.6334			
5% A.M.	6597.8167	10949.6334	1.85182765	6.07749665	3.38087165
5% A.M.	6602.8167	10954.6334			
5% A.M.	6607.8167	10959.6334	1.87528157	6.10095057	3.40081779
5% A.M.	6612.8167	10964.6334			
5% A.M.	6617.8167	10969.6334	1.89894182	6.12461082	3.43073701
5% A.M.	6622.8167	10974.6334			
5% A.M.	6627.8167	10979.6334	1.92267086	6.14833986	3.44071008
5% A.M.	6632.8167	10984.6334			
5% A.M.	6637.8167	10989.6334	1.94626233	6.17193133	3.42076394
5% A.M.	6642.8167	10994.6334			
5% A.M.	6647.8167	10999.6334	1.96999137	6.19566037	3.44071008
5% A.M.	6652.8167	11004.6334			
5% A.M.	6657.8167	11009.6334	1.98120248	6.20687148	1.62561085
5% A.M.	6662.8167	11014.6334			
5% A.M.	6667.8167	11019.6334	2.04083457	6.26650357	8.64665403
5% A.M.	6672.8167	11024.6334			
5% A.M.	6677.8167	11029.6334	2.05486566	6.28053466	2.03450683
5% A.M.	6682.8167	11034.6334			
5% A.M.	6687.8167	11039.6334	2.06862162	6.29429062	1.99461454
5% A.M.	6692.8167	11044.6334			
5% A.M.	6697.8167	11049.6334	2.08285904	6.30852804	2.06442605
5% A.M.	6702.8167	11054.6334			
5% A.M.	6707.8167	11059.6334	2.10060423	6.32627323	2.57305276

5% A.M.	6712.8167	11064.6334			
5% A.M.	6717.8167	11069.6334	2.11938112	6.34505012	2.72264885
5% A.M.	6722.8167	11074.6334			
5% A.M.	6727.8167	11079.6334	2.13905215	6.36472115	2.85229879
5% A.M.	6732.8167	11084.6334			
5% A.M.	6737.8167	11089.6334	2.15872317	6.38439217	2.85229879
5% A.M.	6742.8167	11094.6334			
5% A.M.	6747.8167	11099.6334	2.17846298	6.40413198	2.86227187
5% A.M.	6752.8167	11104.6334			
5% A.M.	6757.8167	11109.6334	2.198134	6.423803	2.85229879
5% A.M.	6762.8167	11114.6334			
5% A.M.	6767.8167	11119.6334	2.21794259	6.44361159	2.87224494
5% A.M.	6772.8167	11124.6334			
5% A.M.	6777.8167	11129.6334	2.23754484	6.46321384	2.84232572
5% A.M.	6782.8167	11134.6334			
5% A.M.	6787.8167	11139.6334	2.25721586	6.48288486	2.85229879
5% A.M.	6792.8167	11144.6334			
5% A.M.	6797.8167	11149.6334	2.27702445	6.50269345	2.87224494
5% A.M.	6802.8167	11154.6334			
5% A.M.	6807.8167	11159.6334	2.29662669	6.52229569	2.84232572
5% A.M.	6812.8167	11164.6334			
5% A.M.	6817.8167	11169.6334	2.3163665	6.5420355	2.86227187
5% A.M.	6822.8167	11174.6334			
5% A.M.	6827.883	11179.6997	2.34587304	6.57154204	4.25026891
5% A.M.	6832.933	11184.7497			
5% A.M.	6837.983	11189.7997	2.35591489	6.58158389	1.44165209
5% A.M.	6843.033	11194.8497			
5% A.M.	6848.083	11199.8997	2.37544836	6.60111736	2.80430955
5% A.M.	6853.133	11204.9497			
5% A.M.	6858.183	11209.9997	2.39518816	6.62085716	2.83393254
5% A.M.	6863.233	11215.0497			
5% A.M.	6868.283	11220.0997	2.41485919	6.64052819	2.82405821
5% A.M.	6873.333	11225.1497			
5% A.M.	6878.383	11230.1997	2.43453022	6.66019922	2.82405821
5% A.M.	6883.433	11235.2497			
5% A.M.	6888.483	11240.2997	2.45413246	6.67980146	2.81418388
5% A.M.	6893.533	11245.3497			
5% A.M.	6898.583	11250.3997	2.47380349	6.69947249	2.82405821
5% A.M.	6903.633	11255.4497			
5% A.M.	6908.683	11260.4997	2.49340574	6.71907474	2.81418388
5% A.M.	6913.733	11265.5497			
5% A.M.	6918.783	11270.5997	2.51307676	6.73874576	2.82405821
5% A.M.	6923.833	11275.6497			
5% A.M.	6928.883	11280.6997	2.53274779	6.75841679	2.82405821
5% A.M.	6933.933	11285.7497			
5% A.M.	6938.983	11290.7997	2.55248759	6.77815659	2.83393254
5% A.M.	6944.033	11295.8497			
5% A.M.	6949.083	11300.8997	2.57229618	6.79796518	2.84380687
5% A.M.	6954.133	11305.9497			
5% A.M.	6959.183	11310.9997	2.59196721	6.81763621	2.82405821
5% A.M.	6964.233	11316.0497			
5% A.M.	6969.283	11321.0997	2.61177579	6.83744479	2.84380687

5% A.M.	6974.333	11326.1497			
5% A.M.	6979.383	11331.1997	2.63179072	6.85745972	2.87342986
5% A.M.	6984.433	11336.2497			
5% A.M.	6989.483	11341.2997	2.65180564	6.87747464	2.87342986
5% A.M.	6994.533	11346.3497			
5% A.M.	6999.583	11351.3997	2.67182057	6.89748957	2.87342986
5% A.M.	7004.633	11356.4497			
5% A.M.	7009.683	11361.4997	2.69176671	6.91743571	2.86355553
5% A.M.	7014.733	11366.5497			
5% A.M.	7019.783	11371.5997	2.71164408	6.93731308	2.8536812
5% A.M.	7024.833	11376.6497			
5% A.M.	7029.883	11381.6997	2.731659	6.957328	2.87342986
5% A.M.	7034.933	11386.7497			
5% A.M.	7039.983	11391.7997	2.75167393	6.97734293	2.87342986
5% A.M.	7045.033	11396.8497			
5% A.M.	7050.083	11401.8997	2.77189519	6.99756419	2.90305285
5% A.M.	7055.133	11406.9497			
5% A.M.	7060.183	11411.9997	2.7919789	7.0176479	2.88330419
5% A.M.	7065.233	11417.0497			
5% A.M.	7070.283	11422.0997	2.8120626	7.0377316	2.88330419
5% A.M.	7075.333	11427.1497			
5% A.M.	7080.383	11432.1997	2.83214631	7.05781531	2.88330419
5% A.M.	7085.433	11437.2497			
5% A.M.	7090.483	11442.2997	2.85195489	7.07762389	2.84380687
5% A.M.	7095.533	11447.3497			
5% A.M.	7100.583	11452.3997	2.87183226	7.09750126	2.8536812
5% A.M.	7105.633	11457.4497			
5% A.M.	7110.683	11462.4997	2.89150329	7.11717229	2.82405821
5% A.M.	7115.733	11467.5497			
5% A.M.	7120.783	11472.5997	2.91110553	7.13677453	2.81418388
5% A.M.	7125.833	11477.6497			
5% A.M.	7130.883	11482.6997	2.93077656	7.15644556	2.82405821
5% A.M.	7135.933	11487.7497			
5% A.M.	7140.983	11492.7997	2.9503788	7.1760478	2.81418388
5% A.M.	7146.033	11497.8497			
5% A.M.	7151.083	11502.8997	2.97011861	7.19578761	2.83393254
5% A.M.	7156.133	11507.9497			
5% A.M.	7161.183	11512.9997	2.98978964	7.21545864	2.82405821
5% A.M.	7166.233	11518.0497			
5% A.M.	7171.283	11523.0997	3.00939188	7.23506088	2.81418388
5% A.M.	7176.333	11528.1497			
5% A.M.	7181.383	11533.1997	3.02906291	7.25473191	2.82405821
5% A.M.	7186.433	11538.2497			
5% A.M.	7191.483	11543.2997	3.04873394	7.27440294	2.82405821
5% A.M.	7196.533	11548.3497			
5% A.M.	7201.583	11553.3997	3.06847374	7.29414274	2.83393254
5% A.M.	7206.633	11558.4497			
5% A.M.	7211.683	11563.4997	3.08821355	7.31388255	2.83393254
5% A.M.	7216.733	11568.5497			
5% A.M.	7221.783	11573.5997	3.10795335	7.33362235	2.83393254
5% A.M.	7226.833	11578.6497			
5% A.M.	7329.69967	11681.5163			

5% A.M.	7334.7	11686.5167	3.13780379	7.36347279	
5% A.M.	7389.7	11741.5167	3.23705306	7.46272206	2.64284958
5% A.M.	7449.7	11801.5167	3.35535434	7.58102334	2.74302861
5% A.M.	7509.7	11861.5167	3.47544389	7.70111289	2.88055583
5% A.M.	7569.7	11921.5167	3.595671	7.82134	2.90382634
5% A.M.	7629.7	11981.5167	3.71562299	7.94129199	2.90216416
5% A.M.	7689.7	12041.5167	3.74581733	7.97148633	1.81426814
5% A.M.	7719.7	12071.5167	3.74588611	7.97155511	0.48757244

Table C-3.2 TCE Concentration in Effluent

Sample ID	Cumulative Time min	Pore Volume	TCE Concentration mg/kg	Cumulative TCE Mass mg
GC 1	-2160	-1	0	-
GC 2	-2034	-0.9416667	283.4804891	-
GC 3	-1974	-0.9138889	264.5119246	-
GC 4	-1914	-0.8861111	357.8603784	-
GC 5	-1674	-0.775	282.9574567	-
GC 6	-1614	-0.7472222	318.1850153	-
GC 7	-870	-0.4027778	438.378763	-
GC 8	-690	-0.3194444	438.3788	-
GC 9	-270	-0.125	455.2625335	-
GC 10	-435	0	455.2625	2156
GC 11	152	0.542	422.8910924	2288.44949
GC 12	230	0.758	471.8748983	2414.34571
GC 13	340	0.942	557.793543	2494.41698
GC 18	412	1.041	605.6369791	2536.56931
GC 19	445	1.089	691.7794353	2556.63091
GC 20	460	1.109	655.175944	2575.63102
GC 21	475	1.129	610.2463572	2608.37073
GC 22	505	1.166	576.8428037	2622.58991
GC 23	523	1.183	397.4549079	2642.76074
GC 24	550	1.218	484.4979474	2666.64649
GC 25	580	1.252	538.0192403	2691.61059
GC 26	610	1.284	448.6402959	2713.07802
GC 27	640	1.317	555.1295863	2745.27554
GC 28	680	1.357	615.3700345	2763.12127
GC 29	700	1.377	632.3054449	2790.62656
GC 30	730	1.407	675.1154738	2807.26815
GC 31	762	1.424	760.4013711	2817.19139
GC 32	780	1.433	390.748646	2840.4214
GC 33	820	1.474	631.8827705	2942.67267
GC 34	1535	1.5856	426.7174461	2967.66978
GC 49	1565	1.626	516.7476711	3015.62396
GC 35	1610	1.69	356.1589213	3049.19194
GC 36	1640	1.755	602.6830794	3115.60761
GC 37	1670	1.831	596.2191996	3234.91108
GC 38	1715	1.969	898.5760096	3354.78112
GC 39	1750	2.061	724.513696	3443.02688
GC 40	1775	2.145	1493.103542	3876.02691
GC 41	1840	2.345	1172.674725	3989.95226
GC 42	1859	2.412	1638.093105	4108.71401
GC 43	1875	2.462	893.3382006	4195.50182
GC 44	1895	2.529	1287.564807	4320.58874
GC 45	1915	2.596	1563.945077	4508.80953
GC 46	1938	2.679	1561.86585	4735.28008
GC 47	1970	2.779	1343.179763	4928.09353
GC 48	2000	2.878	1837.368439	5346.37046
GC 50	2915	3.035	1644.660056	5532.38151

GC 51	2940	3.113	1356.446866	5687.7625
GC 52	2967	3.192	1488.545421	6020.15469
GC 53	3027	3.346	4154.925275	6333.43606
GC 54	3050	3.398	2479.386612	6470.05026
GC 55	3071	3.436	3407.433336	6633.09594
GC 56	3091	3.469	2961.159524	7002.35254
GC 57	3140	3.555	2760.741877	7290.57399
GC 58	3185	3.627	3537.067368	7521.36763
GC 59	3215	3.672	3935.256981	7778.14315
GC 60	3250	3.717	3022.792594	7918.40073
GC 61	3275	3.749	6532.318345	8420.40939
GC 62	3320	3.802	4443.147103	8736.09499
GC 63	3365	3.851	2125.230819	8850.11363
GC 64	3405	3.888	4238.191617	9163.5279
GC 65	3455	3.939	7213.434233	9634.20448
GC 66	3500	3.984	7162.989308	10309.3162
GC 67	3560	4.049	2276.676148	10494.1823
GC 69	3620	4.105	2540.719898	10659.9643
GC 70	3680	4.15	11206.79747	11423.7075
GC 71	3740	4.197	6342.474773	12656.0504
GC 72	4385	4.331	6220.568437	13539.9932
GC 73	4415	4.429	4359.312722	14033.0314
GC 74	4445	4.507	3768.390574	14257.0623
GC 75	4475	4.548	4503.556984	14661.932
GC 76	4535	4.61	3088.54868	14814.1975
GC 77	4595	4.644	4623.209428	15189.6021
GC 78	4710	4.7	4520.030399	15510.7502
GC 79	4835	4.749	3355.168957	15841.5699
GC 80	5114	4.817	4465.87306	16314.2826
GC 81	5555	4.89	8538.678745	17205.7206
GC 82	5975	4.962	7019.112505	17592.4737
GC 83	6260	5	8170.795506	19002.3445
GC 84	10215	5.119	5074.409211	19693.9865
GC 85	10265	5.213	7829.954872	20931.5108
GC 86	10355	5.322	9696.249689	21929.7397
GC 87	10445	5.393	9015.086182	23393.7897
GC 88	10605	5.505	10662.3184	24568.7772
GC 89	10655	5.581	3995.994401	25530.6131
GC 90	10795	5.747	6713.70151	26455.4255
GC 91	10845	5.842	5893.697329	27874.0384
GC 92	10915	6.008	4969.706722	28717.1492
GC 93	10965	6.125	6195.032105	30369.9837
GC 94	11045	6.309	3651.369331	34978.0837
GC 95	11610	7.566	485.9336326	35078.1375
GC 96	11681	7.708	1272.293608	35424.9647
GC 97	11775	7.896	203.3725209	35448.5559
GC 98	11971	7.976	450.0170245	35451.8185
GC 99	12131	7.981	500.2009803	35451.8185

Table C-3.3 - Density of Effluent

Sample ID	Cumulative Time min	Pore Volume	Density g/cm3
DV1	-2665	-1	998.2
DV4	-2415	-0.914	998.2
DV6	-2115	-0.775	998.2
DV8	-1195	-0.403	998.1
DV10	-71	-0.125	997.8
zero	0	0	997.8
CI3	63	0.226	997.9
CI6	120	0.441	997.9
CI12	180	0.64	997.8
CI20	275	0.839	997.8
CI29	395	1.021	997.9
CI39	565	1.235	998.3
CI48	762	1.423	998.3
DV_05 3	1610	1.69	997.8
DV_05 4	1640	1.755	997.7
DV_05 5	1670	1.831	997.9
DV_05 6	1715	1.969	998
DV_05 7	1750	2.061	997.6
DV_05 8	1775	2.145	997.8
DV_05 9	1805	2.246	997.7
DV_05 10	1840	2.345	997.9
DV_05 12	1875	2.462	998.1
DV_05 13	1895	2.529	997.9
DV_05 15	1938	2.679	997.7
DV_05 16	1970	2.779	998.3
DV_05 18	2030	3.026	998.4
DV_2 2	2967	3.194	999.7
DV_2 3	3027	3.346	999.1
DV_2 4	3050	3.398	999.8
DV_2 6	3091	3.469	999.5
DV_2 7	3140	3.555	999.6
DV_2 9	3215	3.672	1000
DV_2 12	3320	3.801	1000.6
DV_2 14	3405	3.888	1000.2
DV_2 16	3500	3.984	1000.7
DV_2 17	3560	4.049	1000.3
DV_2 19	3680	4.15	1001.3
DV_2 20	3740	4.2	1001.3
DV_5 1	4385	4.331	1000.8
DV_5 3	4445	4.507	1000.9
DV_5 4	4475	4.548	1001
DV_5 6	4595	4.644	1001.4
DV_5 8	4835	4.749	1001.5
DV_5 10	5555	4.89	1002.1
DV_5 11	6256	5	1001.6
DV_5' 1	10215	5.118	999.1
DV_5' 2	10265	5.212	1002.5

DV_5' 3	10355	5.322	1003.6
DV_5' 4	10445	5.392	1002.9
DV_5' 5	10605	5.505	1003.8
DV_5' 6	10655	5.581	1003.2
DV_5' 7	10795	5.746	1003.8
DV_5' 8	10845	5.842	1003.7
DV_5' 9	10915	6.008	1003.9
DV_5' 10	10965	6.125	1003.6
DV_5' 11	11045	6.309	1003.2
DV_5' 12	11610	7.334	1003.1
DV_5' 13	11681	7.566	1002.8
DV_5' 14	11775	7.708	1003.2